



Fakultät für Medizin

Institut für Virologie



Generation, Characterization and Application of a Novel BAC System for MVA Mutagenesis to Investigate the Function of Vaccinia Virus Immune Modulatory Gene *N1L*

Lianpan Dai

Vollständiger Abdruck der von der Fakultät für Medizin der Technischen Universität München zur Erlangung des akademischen Grades eines

Doctor of Philosophy (Ph.D.)

genehmigten Dissertation.

Vorsitzende: Univ.-Prof. Dr. Agnes Görlach

Betreuer: Univ.-Prof. Dr. Ingo Drexler

Prüfer der Dissertation:

1. apl. Prof. Dr. Volker Bruß

2. apl. Prof. Dr. Heiko Adler,
Ludwig-Maximilians-Universität München

Die Dissertation wurde am 10.02.2014 bei der Fakultät für Medizin der Technischen Universität München eingereicht und durch die Fakultät für Medizin am 02.04.2014 angenommen.

Abbreviation list

aa	amino acid
APC	Antigen Presenting Cell
APS	Ammoniumperoxidsulfate
BAC	Bacterial Artificial chromosome
BFA	Brefeldin A
BMDC	Bone-Marrow derived Dendritic Cell
BMΦ	Bone Marrow derived Macrophage
bp	Basepair
BSA	Bovine Serum Albumin
CAM	Chlorophenicol
CD	Cluster of Differentiation
cDC	conventional Dendritic Cell
CEF	Chicken Embryo Fibroblast
CPE	Cytopathic Effect
CTL	Cytotoxic T Lymphocyte
CVA	Chorioallantosis Vaccinia virus Ankara
del	deletion
DMSO	Dimethylsulfoxide
EMA	Ethidium Monoazide Bromide
FACS	Fluorescence Activated Cell Sorting
FBS	Fetal Bovine Serum
FPV	Fowlpox Virus
FSC	FSC Forward Scatter
GFP	Green Fluorescent Protein
GM-CSF	Granulocyte Macrophage Colony-Stimulating Factor
hpi	hours post infection
HRP	horseradish peroxidase
i.p.	Intraperitoneal
ICS	Intracellular Cytokine Stain
IFN	Interferon
IFNAR	Interferon Alpha Receptor
IFN-I	Type I Interferon
IL	Interleukin
IRF	Interferon regulatory factor
ISGs	Interferon Stimulated Genes
Kana	Kanamycin
MCS	Multiply Cloning Sites
M-CSF	Macrophage Colony-Stimulating Factor
MDA5	Melanoma Differentiation-associated Gene 5
MFI	Mean Fluorescent Intensity
MHC	Major Histocompatibility Complex
MOI	Multiplicity of Infection
mRNA	Message RNA
MVA	Modified Vaccinia virus Ankara
NF-κB	Nuclear Factor κ B
ORFs	Open Reading Frame (s)
OVA	Chicken Ovalbumin

PARP	Poly (ADP-ribose) polymerase
PB	Pacific Blue
PBS	Phosphate Buffered Saline
PCR	Polymerase Chain Reaction
pDC	plasmacytoid Dendritic Cell
PE	Phycoerythrin
PFA	Paraformaldehyde
pMHC	peptide-MHC complex
PRRs	Pattern Recognition Receptor
Rec	Recombinant
RFV	Rabbit Fibroma Virus
RIG-I	Retinoic acid-Inducible Gene I
SDS	Sodiumdodecylsulfate
SEM	Standard Error of the Mean
SSC	Sideward Scatter
STAT	Signal Transducers and Activators of Transcription
STS	Staurosporine
TCID₅₀	Tissue Culture Infection does 50
TE	Tris EDTA-Buffer
Th	T helper
TLR	Toll-Like Receptors
Tris	Trishydroxymethylaminomethane
VV	Vaccinia Virus
WB	Western blot
WT	wildtype

Abstract

Recombinant Modified Vaccinia Virus Ankara (recMVA) engineered to express foreign genes has been employed as viral vector vaccine against infectious diseases and cancer. Strength and temporal expression of MVA-delivered antigens (Ag) play a vital role in modulating the antigen-specific immune response. We introduced the bacterial artificial chromosomes (BAC) system to rapidly generate recombinant MVA by the *en passant* technology. The transgene was targeted into MVA naturally occurring deletion VI region. Fluorescent reporter gene mCherry driven by different promoters was explored as a model to monitor and characterize the transgene expression. The promoters were activated at distinct times of the virus life cycle or operated with different strength. The BAC cassette can be spontaneously deleted when BAC self-excisable recMVA was grown in eukaryotic cells. The generated recMVAs had normal viral growth kinetics and similar genomic stability compared with MVA wild type, regardless of the presence or absence of the BAC cassette. Moreover, quantitative analysis of gene transcription and protein synthesis of mCherry showed that these recMVAs had the desired vaccinia virus (VV) promoter-specific kinetics of their transgene expression. The evaluation of this MVA BAC system indicated its applicability as gene delivery vector and vaccine.

Subsequently, this well-established platform was successfully applied to create a series of mutational recMVAs to investigate the gene function of VV *N1L*. *N1* is a vaccinia virulence factor that can inhibit TBK-1 and IRF3 activation. We found *N1L* knock-in MVA can significantly suppress the type I IFN expression in dendritic cells (DCs). Mice vaccinated with MVA-OVA-*N1L* dramatically impaired the MVA-vector antigen and OVA-specific T cell priming. This impairment caused by *N1* was highly dependent on type I IFN signalling. During boost vaccinations, proliferation of IFN γ producing T cells were unaffected in the context of MVA-OVA-*N1L* immunization, however, IL-2 producing T cell expansion was dramatically reduced. Moreover Ag-specific T cells standing higher in the immunodominance hierarchy were more sensitive to the inhibitory effect. A possible explanation for this phenomenon is that *N1* retards the co-stimulation exerted by infected APC by weakening the IFN-I production. This leads to the impaired T cell priming and the poor proliferation of IL-2 producing T cells in the recall. This is the first demonstration of the immune modulatory function of *N1* in adaptive immunity. Our findings give important new insights into the design and optimization of poxviral vectors as vaccines.

Contents

1.	Introduction.....	7
1.1.	The viral vaccine vector MVA.....	7
1.2.	Genetic engineering of MVA.....	8
1.3.	The BAC-based method using <i>en passant</i> mutagenesis.....	9
1.4.	Pathogen-induced innate immune response by IFN-I production.....	11
1.5.	Virus induced T cell priming and memory.....	13
1.6.	Virus induced type I interferon impacts on T cell immunity.....	14
1.7.	VV encoded immune modulator viral protein N1.....	15
1.8.	Aim of the thesis.....	18
2.	Materials.....	20
2.1.	Chemicals.....	20
2.2.	Buffers and solutions.....	20
2.3.	Cell Culture Media.....	21
2.4.	Biochemicals.....	22
2.5.	Enzymes.....	22
2.6.	Kits.....	22
2.7.	Synthetic Oligonucleotides.....	23
2.8.	Plasmids.....	24
2.9.	Synthetic Peptides.....	24
2.10.	Antibodies.....	25
2.11.	Fluorescent Dyes.....	25
2.12.	Bacteria.....	25
2.13.	Cell lines.....	26
2.14.	Mice.....	26
2.15.	Viruses.....	26
2.16.	Consumables.....	27
2.17.	Laboratory Instrument.....	27
2.18.	Software.....	28
3.	Methods.....	29
3.1.	Molecular biology.....	29
3.1.1.	Generation of electrocompetent bacteria.....	29
3.1.2.	Generation of competent <i>E. coli</i> bacteria.....	29
3.1.3.	Generation of electrocompetent GS1783 <i>E. coli</i>	29
3.1.4.	Transformation.....	30
3.1.5.	DNA isolation from bacteria.....	30
3.1.6.	Polymerase chain reaction (PCR).....	31
3.1.7.	Dephosphorylation and Ligation.....	34
3.1.8.	Generation of recombinant MVA_BAC genomes in GS1783 <i>E. coli</i>	34
3.2.	Cell biology.....	39
3.2.1.	Adherent eukaryotic cell culture.....	39
3.2.2.	Cryo-preservation of cell lines.....	39
3.2.3.	Recovery of cell culture.....	39
3.2.4.	Primary chicken embryo fibroblast (CEF) culture.....	40
3.2.5.	Preparation of bone marrow-derived dendritic cells (BMDC) and bone marrow-derived macrophages (BM Φ).....	40
3.2.6.	Antigen specific CD4+ T cell re-stimulation and culture.....	41
3.2.7.	CD4+ T cell re-activation assay.....	41
3.2.8.	Annexin staining.....	42
3.3.	Virology methods.....	42
3.3.1.	MVA_BAC rescue.....	42
3.3.2.	Subcloning of BAC-excised recMVA.....	43
3.3.3.	Virus amplification and crude stock preparation.....	43
3.3.4.	RecMVA purification.....	44
3.3.5.	Virus titration and growth kinetic analysis by TCID ₅₀	44
3.4.	Biochemistry methods.....	44

3.4.1.	Quantitative real time PCR assay	44
3.4.2.	Fluorescent protein quantification by FACS	45
3.4.3.	Western blot	45
3.5.	Immunologic methods.....	46
3.5.1.	Immunizations	46
3.5.2.	Preparation of splenocytes	47
3.5.3.	Intracellular Cytokine Staining (ICS)	47
3.5.4.	Statistics	48
4.	Results	49
4.1.	Construction of VV-specific promoter transfer plasmids targeting MVA deletion VI	49
4.2.	Insertion of the transgene cassette in MVA deletion VI by Red Recombination...52	
4.3.	Generation of recombinant viruses by MVA_BAC recombineering.....54	
4.4.	Growth kinetics of BAC-derived recMVAs	57
4.5.	VV promoter-specific gene transcription kinetics.....59	
4.6.	VV promoter-specific kinetics of target protein synthesis.....62	
4.7.	Construction and generation of MVA-N1L and related recombinant or revertant viruses using the two-step red-mediated recombination system	64
4.8.	MVA-N1L and related recMVA show comparable growth kinetics.....66	
4.9.	Western blot analysis of N1 and OVA synthesis upon recMVA infection.....67	
4.10.	N1 impairs MVA-induced T cell priming	68
4.11.	Interference with IFN-I signalling inhibits T cell priming after MVA-OVA-N1L vaccination	74
4.12.	MVA-OVA-N1L inhibits IL-2 secretion in secondary T cell responses	78
4.13.	Vaccinia N1 has a marginal effect on antigen-specific CD4+ T cell reactivation <i>in vitro</i>	85
4.14.	MVA-N1L can not block STS- or infection-induced apoptosis	90
5.	Discussion	93
5.1.	BAC-MVA mutagenesis platform for vector vaccine development and gene delivery	93
5.2.	The versatile usage of VV promoters for antigen expression in recMVA	94
5.3.	The benefit of the BAC- recombinant MVA system to investigate viral gene function	95
5.4.	Other applications of the BAC-recombinant MVA system to generate recMVA ...96	
5.4.1.	Vaccinia virus N1 inhibits MVA- induced IFN β production.....96	
5.4.2.	N1 is not an anti-apoptotic protein	98
5.4.3.	Immune modulatory role of N1 in MVA-induced T cell responses	99
5.4.4.	Role of N1L in NF- κ B activation in the context of MVA infection	103
5.4.5.	Implication for MVA vector vaccine optimization	103
6.	Final conclusion	104
7.	Reference	106
8.	Appendix.....	117
8.1.	Generation of recMVA expressing non-secreted OVA	120
8.2.	Generation of recMVA expressing fusion protein B5-OVA	120
9.	Acknowledgement	121

1. Introduction

0.1. The viral vaccine vector MVA

Viruses have evolved highly efficient strategies to infect host cells and to use the cellular machinery for the synthesis of virally encoded proteins. During the course of infection, however, the innate and adaptive immune system will be evoked. Hence, viral vectors are naturally gifted and preferred vehicles for heterologous gene delivery for inducing immune responses in experimental and clinical research (Brave *et al.*, 2007).

Modified vaccinia virus Ankara (MVA) was derived from parental chorioallantosis vaccinia virus Ankara (CVA) by more than 570 serially passages on chicken embryo fibroblast (CEF) cells (Blanchard *et al.*, 1998; Carroll and Moss, 1997), a process to mimic the evolution of other Orthopoxviruses to be restricted to a narrow host range. During the passaging, large genomic deletions, truncations, gene fragmentations and mutations were acquired. A broad spectrum of cellular host range was lost in vaccinia virus (VV), which thereby led to the inability of MVA to grow in most mammalian cells. MVA lost ~15% of its parental genome (ca.30 kb) including the 24 kb of six major deletion regions from CVA (Meisinger-Henschel *et al.*, 2007; Meisinger-Henschel *et al.*, 2010). There are several distinctive advantages of engineering MVA to express recombinant antigens and to use it as antigen delivery system: 1) the large packaging capacity for recombinant DNA, theoretically up to 50 kb. This makes it capable to express large or multiple antigens in one viral vector (Prieur *et al.*, 2004; Robinson *et al.*, 2007; Sutter and Staib, 2003). 2) Controllable virus-specific gene expression. MVA encoded genes are expressed under the control of VV specific promoters, which make it convenient to regulate the antigen expression in terms of desired strength and timing (Moss, 1996). 3) Lack of persistence or genomic integration in the host. The poxvirus encoded genes are transcribed in the cytoplasm of the host cell and hence exempt the risk of host genomic integration of the viral DNA (Stickl *et al.*, 1974). 4) High immunogenicity targeting both innate and adaptive immunity (Frenz *et al.*, 2010; Sutter and Staib, 2003; Waibler *et al.*, 2009), 5) Safe clinical records. As the 3rd generation of smallpox vaccine, MVA has been safely administered to more than 100,000 humans, including immunocompromised or elderly patients and those with atopic skin diseases (Earl *et al.*, 2004; Mayr *et al.*,

1978; Stittelaar *et al.*, 2005), 6) Ease of vector and vaccine production as it can be generated under conditions of bio-safety level 1 for large scale production (Drexler *et al.*, 2004).

MVA expressing recombinant antigens have been extensively evaluated as safe vaccine candidates in clinical trials. Here are some examples: HIV-1 Nef antigen or multiantigen for HIV infection (Cosma *et al.*, 2003; Mwau *et al.*, 2004), *p.falciparum* ME-Trap antigen for malaria (McConkey *et al.*, 2003; Moorthy *et al.*, 2003), 85A antigen for Mycobacterium tuberculosis (McShane *et al.*, 2004), HPV E2 antigen for cervical cancer (Corona Gutierrez *et al.*, 2002), MUC 1 for prostate cancer (Rochlitz *et al.*, 2003), Her2 antigen for breast cancer (Bavarian Nordic Corps.), tyrosinase antigen for melanoma (Di Nicola *et al.*, 2003; Di Nicola *et al.*, 2004) or 5T4 antigen for Renal cancer (Mulryan *et al.*, 2002). Veterinary vaccine development includes recombinant MVA vaccine trails carried out in pigs (Nam *et al.*, 2002), cattles (Taracha *et al.*, 2003), horse (Breathnach *et al.*, 2006) and dogs (Ramos *et al.*, 2008). In summary, MVA has been characterized as an excellent live vector for vaccine development.

1.2. Genetic engineering of MVA

To generate recombinant MVA for target antigen expression or genome mutagenesis, genetic engineering of MVA is usually carried out by homologous recombination between the viral genome and the transfer DNA vector (Drexler *et al.*, 2004; Staib *et al.*, 2004; Staib *et al.*, 2003). The non-essential regions of the viral genome were usually exploited for antigen insertion. There were several methods established to generate recMVA. Here some of the commonly used methods are summarized as follows:

- 1) **LacZ/gpt selection/screen system** (Scheiflinger *et al.*, 1998). Genes of interest are linked with selecting marker cassette of the *E.coli gpt* gene (guanine phosphoribosyltransferase) and *lacZ* (beta-galactosidase). The first step is to transiently select the homologous recombinants by gpt selection pressure and screen by β -galactosidase staining. The second step is to purify plaques without selection pressure. Then the marker flanked by the repeats is lost, yielding the recMVA containing only the gene of interest. Besides, *LacZ* has been recently substituted with *GFP* for an easier detection of recMVA.

2) **Rescue of D4R-defective MVA.** The MVA open reading frame D4R encodes the gene for Uracil-DNA-glycosylase (*UNG*). *UNG* is an essential gene for vaccinia that is required to eliminate uracil from DNA molecules in DNA replication and prevent mutagenesis. Therefore the MVA- Δ D4R can be propagated in an avian complementing cell line. The recMVA is rescued in the wild-type cell line by the help of rescue plasmids containing the *D4R* gene and the genes of interest (Ricci *et al.*, 2011).

3) **Host range selection.** VV *K1L* is the host range factor for MVA to allow for growth in RK13 cells. The *K1L* gene is transiently introduced into the MVA genome by a transfer plasmid in which *K1L* was flanked by MVA homologous sequences. The recMVA could be isolated in RK13 cells. The *K1L* marker is again lost from the viral genome by recombination of repeats flanking the marker in a MVA permissive cell line (e.g. BHK-21). Another method is utilizing the *E3L* deletion MVA virus (MVA- Δ E3L). *E3L* is a host range factor for MVA to allow for growth in CEF cells. MVA- Δ E3L could not resist to the type I interferon secreted by CEFs, therefore is unable to grow in CEFs. Re-insertion of the *E3L* gene together with the gene of interest enables the isolation of recMVA (Galindo *et al.*, 2001).

4) **MVA-BAC based recMVA generation.** MVA genome is inserted in a bacterial artificial chromosome (BAC), which thereby allows for homologous recombination into the viral genome in *E.coli*. Helper virus is required for the rescue of viral progeny from the BAC (Cottingham *et al.*, 2008; Cottingham and Gilbert, 2010). This method will be discussed in section 1.3 in detail.

0.3. The BAC-based method using *en passant* mutagenesis

Bacterial artificial chromosomes (BAC) are capable to accommodate large DNA sequences up to 300 kb in *E.coli*. Therefore, it has been used for maintaining and cloning of eukaryotic genomes and large DNA or RNA viral genomes. Based on the BAC, Tischer, B.K devised the so-call *en passant* mutagenesis to manipulate the virus genome (Tischer *et al.*, 2006). In this system, the viral genome is maintained in the *E.coli* with the BAC mini F region. The Red Recombination system of the λ phage is integrated into the *E.coli* genomic DNA. The Red system consists of three pivotal genes expressing Gam, Exo and Beta proteins (Zagursky and Hays, 1983). The free ends of linearized double stranded DNA are the functional substrates for the

recombination. Initially, the degradation of free DNA ends caused by the *E.coli* endogenous RecB/C/D is blocked by the Gam protein. Next, the Exo protein possessing 5' to 3' exonuclease activity will

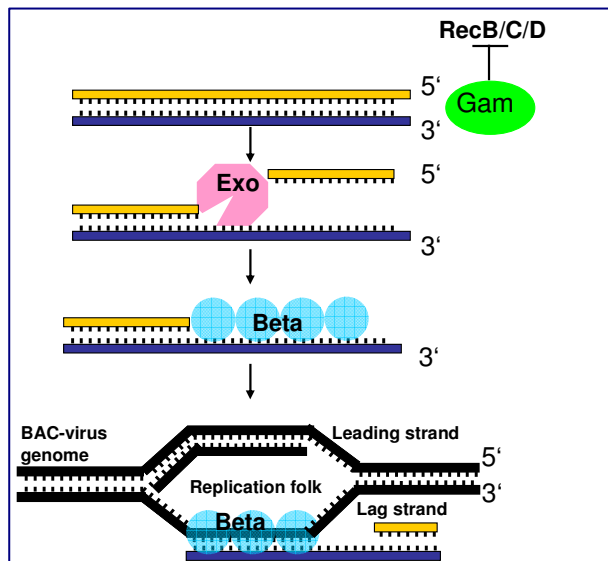


Figure.1.1. Schematic presentation of λ Red Recombination. A ds DNA end is substrate for the Red Recombination system. Gam protects the degradation of linear DNA by bacterial RecB/C/D. Exo forms a toroidal homotrimeric molecule and exert 5' to 3' exonuclease activity. Beta binds to the resulting ssDNA and anneals it to complementary sequences.

produce a 3' single strand extension, which would be immediately bound with Beta protein. When viral genome is replicating in the *E.coli*, the Beta protein will induce annealing of the single strand ends to homologous sequences of the lag strands from the replicating viral DNA (Fig.1.1). Usually, for the convenience of recombinant selection, a marker gene is included in the transfer cassette. In order to delete the unwanted marker gene out of the recombinant virus, an 18 bp *I-SceI* homing endonuclease recognition site is designed to be adjacent to the marker gene. The marker gene can be removed by the *en passant* recombination of the sequence repeats that flank the marker gene. In this system, an artificial GS1783 *E.coli* (derived from DH10B) harbouring the BAC-virus genome is used to perform the genome manipulation. The Red recombinase genes and *I-SceI* endonuclease gene are inserted into the *E.coli* chromosome, under the control of promoters inducible by heat and arabinose, respectively. The recombinant viruses are positively selected by antibiotic pressure for the marker (e.g. *aphA1* gene). The markerless recombinant viruses after 2nd homologous Red Recombination are negatively selected for the marker gene (Fig.1.2).

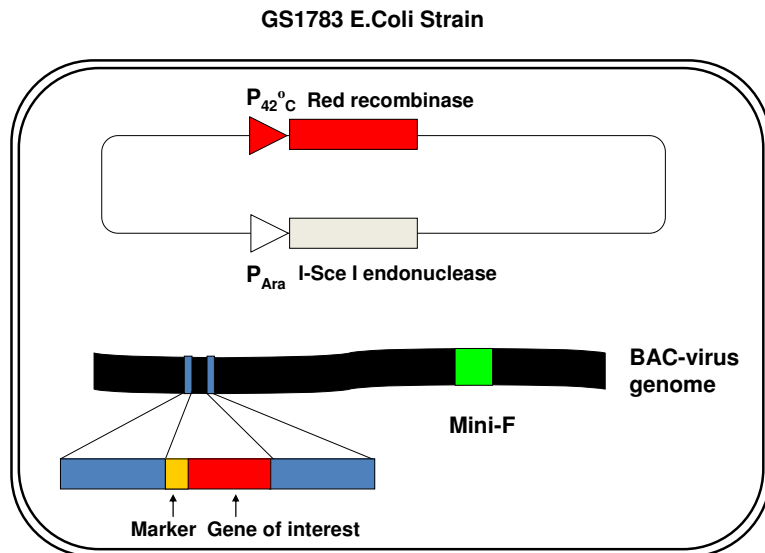


Figure.1.2. Schematic demonstration of GS1783 *E.coli* system for BAC-DNA recombination (Tischer *et al.*, 2010). The Red recombinase cassette is under the control of a heat-inducible promoter. The gene encoding *I-Sce I* endonuclease is driven by an arabinose-inducible promoter. Viral DNA harboured in the cytoplasm of the *E.coli* is engineered to carry a BAC Mini-F region which enables its replication in bacteria.

To rescue recombinant progeny virus from the recombinant BAC genome, a helper virus is used to provide early transcriptional products that activate the life cycle of recombinant virus in a permissive cell line.

0.4. Pathogen-induced innate immune response by IFN-I production

As described above, viral vector vaccines are naturally preferred vehicles to induce innate and adaptive immunity. Nevertheless, little is known about the mechanisms that account for their high immunogenicity. Generally, the virus infection is usually first sensed by the innate immune system, which is able to elicit the production of type I interferon and proinflammatory cytokines. Besides, type I IFNs can impact adaptive immunity by enhancing priming of T helper and cytotoxic T cells, therefore influencing antigen specific T cell responses (Perdiguero and Esteban, 2009). Type I interferons mainly consist of $IFN\alpha$ and $IFN\beta$. $IFN\alpha$ is variably made out of several closely related proteins encoded by 14 genes, while $IFN\beta$ is just encoded by a single gene. Interferons are considered as antiviral proteins and entail three major functions: 1) Interfering with the viral replication in uninfected cells which is achieved by activating an endoribonuclease that degrades viral RNA or the serine-threonine

kinase PKR to phosphorylate eIF2 to block viral replication. 2) Upregulating the expression of MHC and co-stimulatory molecules in antigen presenting cells (APCs), which renders infected cells more susceptible to be killed by CTL. 3) Activating NK cells, which subsequently selectively kill virus-infected cells (Murphy, 2007). There are two signalling cascades known to regulate type I interferon production. One is the virus-induced IFN-producing signal and the other is the IFN receptor-modulated secondary signal (Honda *et al.*, 2006; van Boxel-Dezaire *et al.*, 2006). The virus-induced signal is usually elicited through the triggering of host pattern recognition receptor (PRRs) by viral pathogen-associated molecular patterns (PAMPs). A series of transcription factors are then activated, such as IFN regulatory factors (IRFs), activating transcription factor 2 (ATF2)/c-Jun and nuclear factor κ B (NF- κ B). These factors are then bound to the promoter region of *IFNA* and *IFNB* genes (Perdiguero and Esteban, 2009). IRF3 and IRF7 have been demonstrated as the pivotal regulators for the IFN gene activation (Lin *et al.*, 1998; Wathelet *et al.*, 1998).

The immune system has several ways to detect MVA infections. The first one is recognition of viral PAMPs from outside of the cell by host Toll-like receptors (TLRs). TLR2-TLR6 and TLR4 are localized on the plasma membrane, and they could recognize the VV / MVA glycoproteins on virions and therefore activate the type I IFN genes and pro-inflammatory cytokine gene expression through MyD88 and TRIF signalling (Barbalat *et al.*, 2009; Delaloye *et al.*, 2009). The second way is to recognize double-stranded RNA (dsRNA) from VV/MVA by TLR3 present in the host cell's endosomes. VV/MVA produces dsRNA during transcription of viral early, intermediate or late genes (Condit and Niles, 2002; Willis *et al.*, 2011). Since the transcripts from viral genes are heterogeneous at their 3' ends, the complementary RNAs could form dsRNAs by transcribed products from the same genomic region on opposite strands. TLR3 usually recognizes dsRNA in conventional DCs and then activates TRIF dependent signalling pathways. As a result, the expression of IFN I and pro-inflammatory cytokines are elicited. The third way is to recognize single-stranded RNA (ssRNA) via TLR7/8. After detection, MyD88 dependent signalling pathways will be activated which induce expression of IFN I and NF- κ B (Alexopoulou *et al.*, 2001). Moreover, another strategy is the recognition of viral RNA by retinoic acid-inducible gene I (RIG-I)-like receptors (RLRs). In this pathway, RIG-I and melanoma differentiation-associated gene 5 (MDA5) are involved for the sensing. At last, viral cytosolic DNA sensing pathways are involved in the induction of type I IFN.

Recently, DNA-dependent activator of IFN regulatory factors (DAI) has been identified as a candidate cytosolic DNA sensor (DLM-1/ZBP1). This pathway relies on the kinase TBK 1 and IKKi when activated by unmethylated DNA, and is independent of TLR or helicase RIG-I pathways. IRF3 is then phosphorylated and activates the promoter of IFN β (Ishii *et al.*, 2006). After the type I IFN expression, all of produced IFN-I molecules mediate their function via binding to the ubiquitous IFNAR (IFN- α receptor). The IFNAR consists of two subunits: IFNAR1 and IFNAR2. The signalling transduction after IFNAR activation promotes phosphorylation of the signal transducers and activators of transcription (STAT) and subsequently triggers the expression of interferon-stimulate genes (ISGs). Besides, the pro-inflammatory cytokine induction leads to the release of a variety of cytokines and chemokines which will cause an inflammatory response.

0.5. Virus induced T cell priming and memory

When the virus infection overwhelms the innate defense system, usually an adaptive immune response is induced. It is usually initiated at the sites of infection in peripheral tissues where antigen presenting cells (APCs) meet the pathogens. DC, macrophages and B cells are 3 major classes of APCs. They take up the virus, process the viral antigens and then present the epitopes to the cell surface by MHC I or MHC II. Meanwhile, TLR sensing of the pathogen and signalling can stimulate pro-inflammatory responses which up-regulate chemokine receptors on the cell surface. This process will lead to the migration of infected APCs towards the draining lymph nodes and peripheral lymphoid tissues. Moreover, sensing by pDCs usually induces the secretion of a panel of cytokines such as IFN- α and IFN- β , which subsequently promote the expression of co-stimulatory molecules on the DC surface such as CD80/CD86. This process is termed DC maturation. At the peripheral lymphoid organs, the mature DCs (mDCs) encounter naïve CD4 $^+$ or CD8 $^+$ T cells which are trapped in the cortex, and activate the pMHC-matched T cells. This process is named naïve T cell priming. A successful T cell priming is usually determined by 3 signals, which are as following: Signal 1: antigen specific interaction between peptide-MHC (pMHC) on DCs and TCR on T cells; Signal 2: co-stimulation through the binding of CD80/CD86 on DCs with CD28 on T cells; Signal 3: cytokines secreted for T cell differentiation, such as IL-12, TGF- β or IL-4. After priming, naïve T cells are subsequently switched to effector T cells and maximize the population by

clonal expansion on 7-8 days post-infection. The activation of T cells changes the expression of cytokines and modulates several cell-surface molecules such as CD62L. On one hand, effector CD8⁺ T cells exert functions as cytotoxic T lymphocytes (CTLs). They protect the host from further infection through the killing of infected cells by secretion of perforin and granzymes or expression of fas ligand. On the other hand, two subtypes of effector CD4⁺ T cells (T helper, Th) which are differentiated from naïve precursors will consolidate the immune response. The presence of cytokines IL-12 and IFN γ favor the differentiation of CD4⁺ T cells to Th1 which mainly produce IFN γ and IL-2, whereas IL-4 is responsible for the differentiation of CD4⁺ cells to Th2 which will generate IL-4 and IL-5. Th1 cells play a critical role in cellular immune responses. Secreted IL-2 maintains survival and proliferation of Th1 cells by signal transduction through their cognate IL-2 receptors. The expression of IL-2 is highly dependent on the co-stimulation of activated T cells through CD28 signalling (Carreno *et al.*, 2000). In addition, IFN γ secretion has profound anti-viral effects, such as activation of macrophages and B cells. Th2 cells are important for the humoral immune responses, which can drive the differentiation and class switch of B cells, Effector T cells change their expression profiles of surface molecules and egress from the lymphoid nodes into the sites of infection through blood circulation. After 4-5 days of rapid proliferation, activated T cells induced by IL-2 will be further differentiated into specialized effector T cells such as T helper or CTL. Meanwhile T cell memory is also forming. After 7-8 days of proliferation, the populations of antigen-specific effector T cells endure a contraction to a level of 100-1000 fold reduction, but subsequently may persist for many years. These long-lived T cells are designated as memory T cells. These memory T cells have distinctive activation requirements compared with naïve T cells. Upon encounter with the same antigen, they react more quickly and switch to the effector T cells with less dependency for co-stimulation (Murphy, 2007).

0.6. Virus induced type I interferon impacts on T cell immunity

How the innate immune system interacts with the adaptive immune system is a global research hotspot. Type I interferons play a role for both immunostimulation and immunoregulation upon virus infection. They modulate the quantity and quality of T cell responses on both sides, antigen presenting cells (APCs) and T cells (Welsh *et al.*, 2012) e.g. mature APCs by up-regulating MHC and induce costimulatory

molecules on the T cell surface (Montoya *et al.*, 2002). As a result, the initiation of T cell responses is affected. Furthermore, by binding to the IFNAR on CD8+ T cells, type I IFN can directly influence the virus-induced expansion of antigen-specific T cells (Quigley *et al.*, 2008). Nevertheless, in the memory stage, CD8+ T cells express moderately higher levels of IFNAR than naïve T cells. Consequently ~ 50-80% of the memory CD8+ T cells endure an IFN I-induced apoptosis (Bahl *et al.*, 2010; McNally *et al.*, 2001). Recently, some reports elucidate the immunosuppressive role of type I interferons in LCMV persistent infection model which revealed another aspect of type IFN-I's function (Teijaro *et al.*, 2013; Wilson *et al.*, 2013).

MVA is competent to induce the production of type I interferon *in vivo* and *in vitro* (Waibler *et al.*, 2009). It has been shown that, compared with its parental virus VV CVA, the higher capability for CD8+ T cell activation during MVA infection is fairly dependent on IFNAR signalling (Delaloye *et al.*, 2009; Frenz *et al.*, 2010; Waibler *et al.*, 2009). However, more investigations are required to gain closer insight into the underlying mechanisms.

0.7. VV encoded immune modulator viral protein N1

Like other viruses, vaccinia virus has evolved sophisticated strategies to evade the host immune system by subverting key elements of the host antiviral immunity (Perdiguero and Esteban, 2009; Sadler and Williams, 2008). Vaccinia virus encodes several immune modulators that antagonize the antiviral function of type I IFNs. However during its attenuation, MVA has acquired deletions and truncations of several immune modulator genes interfering with the innate immune response such as *A52R*, *B18R*, *K1L*, *M2L* and *N1L* (Table.1.1). The respective viral proteins are involved in different steps of IFN-I inhibition.

	1	10	20	30	40	50	60	70
CVA	MRTLLIRYILWRNDNDQTYYNDDFKKLMLLDELVDDGDVCTLIKNMRMTLSDGPLLDRLNQPVNNIEDAK							
MVA	MRTLLIRYILWRNDNDQTYYNDDFKKLMLLDELVDDGDVCTLIKNMRMTLSDGPLLDRLNQPVNNIEDAK							
consensus	MRTLLIRYILWRNDNDQTYYNDDFKKLMLLDELVDDGDVCTLIKNMRMTLSDGPLLDRLNQPVNNIEDAK							
	80	90	100	110				
CVA	RMIAISAKVARDIGERSEIRWEESEFTILFRMIE TYFDDLMIDL YG EK							
MVA	RMIAISAKVARDIGERSEIRYRENSSRIQIMLTGSI...PYENYAS.							
consensus	RMIAISAKVARDIGERSEIR..E.....M.....Y...							

Fig.1.3. Protein sequence alignment of the N1 in CVA and its ortholog in MVA. Residues highlighted in red are conserved. The sequence alignment was generated with Clustal X (Thompson *et al.*, 1997) and ESPript (Gouet *et al.*, 2003).

VV N1 protein is a cytosolic virulence factor and made up of 117 amino acids. It has a protein size of approx. 13-14 kD. The *N1L* gene is highly conserved in all orthopoxviruses, including most of the vaccinia virus strains such as CVA (GI:160857909), Copenhagen (GI:335349), Lister (GI:88854057), Acambis3000 (GI:38348895), Western-reserve (GI:17933361). Nevertheless, the *N1L* orthologue is fragmented and truncated at the C-terminal end in the MVA genome in a region covering 27 aa (Fig.1.3). Some previous reports have shown its polyfunctionality as a virulence factor in various aspects. N1 could inhibit NF- κ B via suppressing the IL-1 α , TRAF6, IKK- α or IKK- β mediated signalling (DiPerna *et al.*, 2004; Graham *et al.*, 2008). It can lower IRF3 phosphorylation and, therefore, likely suppress IFN β activation (DiPerna *et al.*, 2004). *In vivo* experiments have shown that VV induces a stronger natural killer cell (NK) response in the presence of N1 (Jacobs *et al.*, 2008). Since N1 has a Bcl-2 like structure, it has been reported as a viral anti-apoptotic protein for STS-induced cell death in both, transfection and infection models (Cooray *et al.*, 2007; Maluquer de Motes *et al.*, 2011). However, the inhibitory function of N1 for apoptosis is contradictory as indicated by a recent report (Postigo and Way, 2012). Therefore, its anti-apoptotic role is still controversial. In addition, deletion of *N1L* from the VV genome leads to an attenuated phenotype (virulence) via intranasal infection and intradermal injection *in vivo* (Mathew *et al.*, 2008). The NF- κ B inhibitory function rather than the anti-apoptotic function contributes to N1-mediated virulence (Maluquer de Motes *et al.*, 2011). Recently developed N1 antagonists control virus growth in cell culture, suggesting a promising antiviral drug target (Cheltsov *et al.*, 2010).

Table.1.1 VV/MVA-encoded immune modulators for the interferon system

Protein / Gene	Function	Presumably intact		References
		ORFs		
		VV (CVA)	MVA	
A46/A46R	Sequesters adaptor proteins MyD88, TRIF, MAL, and TRAM; Interferes with	√	√	(Bowie <i>et al.</i> , 2000) (Stack <i>et al.</i> , 2005)

	downstream activation of MAPKs, NF-κB, and IRFs			
A52/A52R	Inhibits TLR-induced NF-κB activation	√	Δ	(Harte <i>et al.</i> , 2003) (Keating <i>et al.</i> , 2007)
B14/B14R	Inhibits NF-κB via prevention of phosphorylation and degradation of I κB	√	√	(Chen <i>et al.</i> , 2008)
B18/B18R	Inhibits the binding of IFN-α to IFN-α receptor as a secreted viral IFN-α decoy receptor	√	20 nt deletion, frame shifted, truncated and premature protein	(Waibler <i>et al.</i> , 2009)
C6/C6L	Inhibits PRR-induced activation of IRF3 and IRF7	√	√	(Unterholzner <i>et al.</i> , 2011)
E3/E3L	1) Sequesters viral dsRNA with a dsRNA binding domain 2) Inhibits DAI from interacting with cytosolic viral DNA 3) Suppresses the IRF3/7 activation 4) Inhibits the function of ISG15 5) Inhibits activation of PKR	√	√	1) (Chang <i>et al.</i> , 1992) 2) (Wang <i>et al.</i> , 2008) 3) (Smith <i>et al.</i> , 2001) 4) (Guerra <i>et al.</i> , 2008) 5) (Romano <i>et al.</i> , 1998)
H1 /H1L	Inhibits the type I IFN induced response by dephosphorylating STAT1	√	√	(Koksal and Cingolani, 2011)
K1/K1L	Suppresses NF-κB activation; Prevents early stage of viral dsRNA synthesis	√	Δ	(Willis <i>et al.</i> , 2011) (Shisler and Jin, 2004)
K3/K3L	Inhibits viral dsRNA induced PKR activation and eIF2α phosphorylation,	√	√	(Beattie <i>et al.</i> , 1991) (Willis <i>et al.</i> , 2011)
K7/K7R	Suppresses IFNβ induction by inhibiting TBK1/Ikkε mediated IRF activation	√	√	(Schroder <i>et al.</i> , 2008)
M2/M2L	Suppresses induction of NF-κB activation through ERK pathway	√	Δ	(Gedey <i>et al.</i> , 2006) (Hinthong <i>et al.</i> , 2008)
N1/N1L	Inhibits IRF3 and NF- κB activation by blocking the cytosolic TBK-1 and IKK complex	√	23 aa different; frameshift and truncated at the C terminus	(DiPerna <i>et al.</i> , 2004)
N2/N2L	Inhibits nuclear IRF3 downstream of TBK-1	√	5 aa truncation, 4 aa mutation	(Ferguson <i>et al.</i> , 2013)

√, Gene presented as the full-length ORF

Δ, Gene deleted in the viral genome

0.8. Aim of the thesis

MVA is an attenuated derivative from its ancestor strain vaccinia virus CVA. It has been exploited as a safe and efficient vaccine vector for infectious diseases and cancer. Genetic engineering of the MVA genome is the primary method to express foreign antigen(s) in recombinant MVA or to optimize the virus as a viral vector. Therefore, the first goal of the present thesis was to set up a reliable and efficient system to rapidly manipulate the MVA genome. Based on this system, we aimed to generate a series of recombinant MVA, by which model antigens could be expressed with distinct kinetics and amounts as desired. Based on that, the second goal of this thesis was to use the system as tool to investigate biologically relevant questions and generate genetic insertion mutants of wt and recMVA to dissect the role of the VV immunomodulator gene *N1L* in MVA-induced innate and adaptive immunity.

1) First of all, we will introduce the BAC-based *en passant* method to generate recombinant MVA. Our aim is to avoid the tedious and time-consuming procedures when using traditional methods for generating these recMVA. Therefore, the new system allows us to quickly generate insertions, mutations or deletions in the MVA genome and consequently will enable us to establish a versatile construction platform to perform faster investigations based on these recMVA. The reporter gene *mCherry* will be used to conveniently monitor recombinant gene expression. Viral growth, stability as well as gene transcription and translation profiles will be evaluated for the different constructs.

2) Subsequently, we will apply the efficient MVA mutagenesis system to investigate the gene function of viral immunomodulators. During the course of attenuation from CVA to MVA, 15% of the viral genome has been deleted and mutated including six large deletions and other mutations affecting 124 viral ORFs (Cottingham and Carroll, 2013; Meisinger-Henschel *et al.*, 2007). Especially, the loss of viral immunomodulators in MVA fairly changes the host immune response against the infection. Here, we will focus on the recently identified VV virulence factor N1, which is fragmented in the MVA genome. Mutagenized MVA viruses (wt and rec) will be generated by the BAC *en passant* method to insert (MVA-N1L) and delete *N1L* functional C terminal sequences (MVA- Δ N1L). Subsequently, immunologic methods will be used to investigate how the N1 protein interacts with the host during

MVA infection, with a special focus on the interplay between innate and adaptive immunity. The knowledge gained from these studies will shed light to the strategy that VV employs to subvert the host innate and adaptive immune system. This research will be of importance for the optimization of MVA viral vectors and their use in vaccination strategies.

2. Materials

2.1. Chemicals

CHEMICAL	MANUFACTURER
Agarose	Gibco/BRL
Ammoniumperoxidsulfat (APS)	Sigma
Brefeldin A	Sigma
DMSO	Merck
DTT	Serva
Ethidiumbromide	Serva
Glycerol	Roth
L(+)-arabinose	Sigma
Ponceau S	Sigma
Reti-Phenol/Chloroform/Isoamylalcohol	Roth
TEMED	Bio-Rad
Triton X-100	Sigma
Trypan blue	Biochrom KG
Tween 20	Sigma
β -mercaptoethanol	Sigma

2.2. Buffers and solutions

NAME	COMPOSITION
Tricine loading buffer (10x)	12.1 % Tris base (w/v) 17.9% Tricine (w/v) 10 % SDSI (w/v)
WB running buffer PH8.45 (2x)	3M Tris HCL 37 % Glycerol (v/v) 12 % SDS(w/v) 0.1 % Coomassie Blue (w/v) 0.1 % Phenol Rot (w/v)
16% WB separating gel	16% PAA (v/v) 2M Tris PH8.8 20% SDS (wv) 0.2% TEMED (v/v) 1.2% APS (v/v)
Compact Gel	PAA30 0.5 % yeast extract (w/v) 0.5 % NaCl (w/v) 0.1 % glucose (w/v)

FACS buffer pH7.4	1 % BSA (w/v) 0.02 % NaN ₃ from 20% stock (w/v) in 1x PBS
LB agar	1.5 % Agar in LB-Medium
LB medium pH 7.0	1 % casein extract (w/v) 0.5 % yeast extract (w/v) 0.5 % NaCl (w/v) 0.1 % glucose (w/v)
Paraformaldehyd (PFA)	2% Paraformaldehyde (w/v) in PBS buffer
PBS buffer pH 7.4	0.14 M NaCl 2.7 mM KCl 3.2 mM Na ₂ HPO ₄ 1.5 mM KH ₂ PO ₄
RIPA buffer pH7.4	50 mM Tris-HCl 1% NP-40 (v/v) 0.25% Na-deoxycholate (w/v) 150 mM NaCl 1 mM EDTA
SDS-PAGE runing buffer pH 8.3 (10x)	25 mM Tris 192 mM Glycine 0.1 % SDS (w/v)
Sucrose 36 % pH 9.0	36% sucrose (w/v) in 10 mM Tris
TAC lysis buffer	90% NH ₄ Cl from 0.16 M stock 10% Tris pH 7.65 from 0.17 M stock
TAE buffer pH 8.0	40 mM Tris/HCl 1 mM EDTA 20 mM sodium acetate
TE buffer pH 8.0	10 mM Tris/HCl 0.1 mM EDTA
TEN buffer pH 7.4 (10x)	100 mM Tris 10 mM EDTA 1 M NaCl
Tris buffer pH 9.0 (1 mM)	-
Tris buffer pH 9.0 (10 mM)	-
WB strip buffer pH 6.8	100 mM 2-Mercaptoethanol 2 % SDS (w/v) 62.5 mM Tris/HCl
WB transfer buffer anode pH 8.3	25 mM Tris-Base 192 mM Glycin 20 % Methanol (v/v)

2.3. Cell Culture Media

NAME	COMPOSITION
Freezing Medium	90 % FBS 10 % DMSO
RPMI 10%/2%/1%	RPMI 1640 supplemented with: 1-10% FBS 1% Pen-Strep
M2 medium	RPMI 1640 supplemented with: 10% FBS 1% Pen-StrepRPMI 50µM β-Mercaptoethanol

DMEM 10%	DMEM supplemented with: 10% FBS 1% Pen-StrepRPMI
----------	--------------------------------------------------------

2.4. Biochemicals

NAME	MANUFACTURER
1 kb DNA Ladder	Fermentas
Kanamycine	Sigma
Chloramphenicol	Sigma
Staurosprine (STS)	Sigma
Pen-Strep	Gibco
RPMI 1640	Gibco
Non-essential Amino Acid (NEAA)	Gibco
OptiMEM	Gibco
DMEM	Gibco
Phenylmethylsulfonyl fluoride (PMSF)	Sigma
Broad Range Protein ladder	Spectra

2.5. Enzymes

NAME	MANUFACTURER
Alkaline Phosphatase Klenow-Enzyme	Roche
Proteinase K	Sigma
Restriction enzymes	NEB BioLabs
RNAse	Fermentas
T4-DNA-Ligase	Roche
Trypsin	Gibco

2.6. Kits

NAME	MANUFACTURER
BD Cytotfix/Cytoperm Kit	BD Pharmingen
QIAGEN Plasmid Maxi Kit	QIAGEN
QIAquick Gel Extraction Kit	QIAGEN
QIAquick PCR purification Kit	QIAGEN
Lipofectamin2000	Invitrogen

X-tremHP	Roche
PCR-Master-Mix	Roche
RNeasy Mini Kit	Qiagen
QuantiTect Reverse Transcription kit	Qiagen
FastStart SYBR Green Master	Roche

2.7. Synthetic Oligonucleotides

PRIMERS	SEQUENCE 5' -> 3' (Manufacturer)
HindPacPL fw	GGTCTAAGCTTGGGTAA (Eurofins MWG Operon)
HindPacPL rw	TGCCCAAGCTTAATTAAC (Eurofins MWG Operon)
MVAExpEPfw	GTTGATATCTAGGGATAACAGGGTAATCGATTTA (Eurofins MWG Operon)
MVAExpEPrw	TTGGATCCGTTTAAACGCGGCCGATCTCCCAATTCATGCTATAAGACGCATGAAGGCTGAACG CCAGTGTACAACCAATTAACC (Eurofins MWG Operon)
PK1L primer fw	GGGGGTTTAAACCCATGATTAAGATTGGTCTTTCG (Eurofins MWG Operon)
PK1L primer rv	GGGGGAGCTCTTAAGAGATCTAGCGCTGTACATTTAAATGGATCCGTCTGAAACGAGACGCT AATTAGTG (Eurofins MWG Operon)
PG8 primer fw	GGGGGTTTAAACTTAACTTTAAATAATTTACAAAAATTTAAAGGATCCATTTAAATGTACAGCGC TAGATCTCTTAAGAGCTCCCCC (Eurofins MWG Operon)
PG8 primer rv	GGGGGAGCTCTTAAGAGATCTAGCGCTGTACATTTAAATGGATCCCTTTAAATTTTGTAATTA TTTAAAGTTAAGTTTAAACCCCC (Eurofins MWG Operon)
PH5 primer fw	GGGGGTTTAAACTGCAGGTCAGCTTAAAAATTG (Eurofins MWG Operon)
PH5 primer rv	GGGGGAGCTCTTAAGAGATCTAGCGCTGTACATTTAAATGGATCCGATCCTCTAGAGTCAACC TTATTTATG (Eurofins MWG Operon)
P1	CCACGCACGTATCTAAAG (Eurofins MWG Operon)
P2	CTCCTTCATTACAGAAACGGC (Eurofins MWG Operon)
P3	GATGCTATACTCGTTTATATTAG (Eurofins MWG Operon)
P4	GGCGTCCATATGAGTAAC (Eurofins MWG Operon)
fwd_OVA_toP7.5	GGGGGGATCC ATGGGCTCCATCGGTGCAG (Eurofins MWG Operon)
rv_OVA-toP7.5	CCCCTGTACATTAAGGGGAACACATCTG (Eurofins MWG Operon)
N1_F	GCTTTATTATACGCATTC (Eurofins MWG Operon)
N1_R	GTGGAAACTAAGTATTTTC (Eurofins MWG Operon)
FP_P4b	F: GATACAAGACCTTATTCGCG (Eurofins MWG Operon) R: GGTAATCATTTTTGAAGGGC (Eurofins MWG Operon)
mCherry	F: CCCCCTAATGCAGAAGAAGA (Eurofins MWG Operon) R: GGCCCTGTAGGTGGTCTTGA (Eurofins MWG Operon)
18S rRNA	F: AAACGGCTACCACATCCAAG (Eurofins MWG Operon) R: CCTCCAATGGATCCTCGTTA (Eurofins MWG Operon)
B8R	F: ATCCGCATTTCCAAAGAATG (Eurofins MWG Operon) R: ACATGTCACCGCGTTTGTA (Eurofins MWG Operon)
G8R	F: ATCGATAAACTGCGCCAAAT (Eurofins MWG Operon) R: CTCCGCGGTAGAACACTGAT (Eurofins MWG Operon)
H3L	F: GTCTTGAAGGCAATGCATGA (Eurofins MWG Operon) R: TCCCGATGATAGACCTCCAG (Eurofins MWG Operon)
MVA-N1LCin_fw	TCTATAAAAACGAGAATGACATAACTAGTTATCAAAGTGTTTATTTTACCATATAGATCAATC ATTAGATCATCAAATATGTTTCAATCATCTAAAGAGCCAGTGTTACAACCAATTAACC (Biomers)
MVA-N1LCin_rv	AAAGTGGCTAGAGACATTGGTGAACGTTTCAGAAATTAGATGGGAAGAGTCATTCACCATACTC TTTAGGATGATTGAAACATATTTTGATGATCTAATGATTTAGGGATAACAGGGTAATCGATTT (Biomers)
MVA-N1Lrev_fw	ACACTCTATAAAAACGAGAATGACATAACTAGTTATCAAAGTGCTAGGACGCGTAATTTTCAT ATGGTATAGATCCTGTAAGCATTGTCTGTATTCTGGAGCCAGTGTTACAACCAATTAACC (IDT)

MVA-N1Lrev_rv	TGCCAAAGTGGCTAGAGACATTGGTGAACGTTTCAGAAAATTAGATATAGAGAAAATAGCTCCAG AATACAGACAATGCTTACAGGATCTATACCATATGAAAATAGGGATAACAGGGTAATCGATTT (IDT)
P1_N1L	GCTTTATTATACGCATTC (Eurofins MWG Operon)
P2_N1L	GTGGAAACTAAGTATTTTC (Eurofins MWG Operon)

2.8. Plasmids

NAME	SOURCE
delVI P11 plasmid	Obtained from I. Drexler
delVI P11 plasmid-PmeI	Generated in this work
i-pIIIDHR-K1L	Obtained from I. Drexler
i-pIIIDHR-PmH5	Obtained from I. Drexler
i-pIIIDHR-P7.5	Obtained from I. Drexler
pIIIDHR-P11-OVA	Obtained from I. Drexler
pEPKan-S	Gift from K.Tischer
pEP-MVA-dVI-PmH5	Generated in this work
pEP-MVA-dVI-PmH5-mCherry	Generated in this work
pEP-MVA-dVI-P11	Generated in this work
pEP-MVA-dVI-P11-mCherry	Generated in this work
pEP-MVA-dVI-P11nsOVA	Generated in this work
pEP-MVA-dVI-P11nsOVA-LC3	Generated in this work
pEP-MVA-dVI-P7.5	Generated in this work
pEP-MVA-dVI-P7.5-mCherry	Generated in this work
pEP-MVA-dVI-P7.5OVA	Generated in this work
pEP-MVA-dVI-PG8R	Generated in this work
pEP-MVA-dVI-PG8R-mCherry	Generated in this work
pEP-MVA-dVI-PK1L	Generated in this work
pEP-MVA-dVI-PK1L-mCherry	Generated in this work
pMVA dVI-P11	Generated in this work

2.9. Synthetic Peptides

Antigen	Sequence	Origin	MHC	Type
B5R (46-60)	FTCDQGYHSSDPNAV	VACV / MVA	I-A ^b	Class II
L4R (176-190)	ISKYAGINI(V)LNVYSP	VACV / MVA	I-A ^b	
E9L (117-131)	PSVFINPISHTSYCY	VACV / MVA	I-A ^b	
OVA (265-280)	TEWTSSNVMEERKIKV	Chicken Ovalbumin	I-A ^b	
HBV-core(129-140)	PPAYRPPNAPIL	HBV	I-A ^b	
B8R (20-27)	TSYKFESV	VACV / MVA	H2-K ^b	
A8R (189-196)	ITYRFYLI	VACV / MVA	H2-K ^b	

K3L (6-15)	YSLPNAGDVI	VACV / MVA	H2-K ^b	Class I
OVA(257-264)	SIINFEKL	Chicken Ovalbumin	H2-K ^b	
β-Gal (96-103)	DAPIYTNV	β-Galactosidase	H2-K ^b	

2.10. Antibodies

NAME	SPECIES/ISOTYP E (Clone)	CONJUGATE	MANUFACTURER
anti-H3	Rabbit/Polyclonal	-	Gift from Bernard Moss (NIH)
anti-β-actin	Mouse/Monoclonal	-	
anti-Ovalbumin	Rabbit/Polyclonal	-	abcam
anti-N1	Rabbit/Polyclonal (serum)	-	Gift from Micheal Way (UK)
anti-N1	Mouse/Monoclonal (7E5)	-	Gift from Micheal Way (UK)
anti-mouse CD3ε	Hamster (500A2)	-	eBioscience
Goat-anti-mouse IgG	Polyclone IgG	horseradish peroxidase	Jackson ImmunoResearch Inc
Goat-anti-rabbit IgG	Polyclone IgG	horseradish peroxidase	Sigma
anti-mouse CD4α	Rat IgG2a, kappa (GK1.5)	eFluor450 (PB)	eBioscience
anti-mouse CD8α	Rat IgG2a, kappa (53-6.7)	eFluor450 (PB)	eBioscience
anti-mouse IFNγ	Rat IgG1, kappa (XMG1.2)	APC	eBioscience
anti-mouse IL-2	Rat IgG2b (JES6-5H4)	PE	eBioscience

2.11. Fluorescent Dyes

NAME	MANUFACTURER
EMA (Ethidium Monazide Bromide)	Sigma
7-AAD	BD-Pharmingen
APC Annexin V	BD-Pharmingen

2.12. Bacteria

NAME	DESCRIPTION	SOURCE
<i>E.coli</i> DHB10	Electro-competent	Gibco BRL
<i>E.coli</i> X-blue1	Chemical-competent	Stratagene
<i>E.coli</i> GS1783 #17	BAC clone: pMVAF No BAC self-excising	Gift from Matthew G.Cottingham
<i>E.coli</i> GS1783 #22	BAC clone: pMVAF-DX BAC self-excising	Gift from Matthew G.Cottingham

2.13. Cell lines

NAME	DESCRIPTION	SOURCE
BHK-21	Adhesive cell line, hamster fibroblast	ATCC CCL-10
Hela	Adhesive cell line, Human epithelioid carcinoma	ATCC CCL-2
BMDC	semi-adhesive primary cells, Murine Dendritic cells	Generated from OTI(Tg) mice
BM-MΦ	semi-adhesive primary cells, Murine macrophages	Generated from OTI(Tg) mice
CEFs	adhesive primary cells, chicken fibroblast	Generated from SPF eggs (VALO BioMedia)
CD4 _{OVA}	non adhesive lymph cell line, Murine CD4+ T cells	Generated by F.Thiele
CD4 _{B5R}	non adhesive lymph cell line, Murine CD4+ T cells	Generated by F.Thiele

2.14. Mice

All mice were derived from in-house breeding under specific pathogen-free conditions at the animal facility at the University Hospital Düsseldorf following institutional guidelines.

STRAIN	MHC RESTRICTION	SOURCE
C57BL/6	Class I : H2-K ^b and H2-D ^d Class II: I-A ^b	http://jaxmice.jax.org/strain/000664.html
IFNAR ^{-/-}	Class I : H2-K ^b and H2-D ^d Class II: I-A ^b	(Hwang <i>et al.</i> , 1995)
OT I (Tg)	Class I : H2-K ^b Class II: I-A ^b	(Hogquist <i>et al.</i> , 1994)

2.15. Viruses

NAME	SOURCE
MVA-P7.5 mCherry (SE)	Generated in this work
MVA-PH5 mCherry (SE)	Generated in this work
MVA-PK1L mCherry (SE)	Generated in this work
MVA-PG8 mCherry (SE)	Generated in this work
MVA-P11 mCherry (SE)	Generated in this work
MVA-PK1L mCherry (NSE)	Generated in this work
MVA-P11 mCherry (NSE)	Generated in this work
MVA-PH5 mCherry (NSE)	Generated in this work
MVA-N1L (SE)	Generated in this work

MVA-P7.5OVA	Obtain from I.Drexler
MVA-N1L-P7.5OVA (SE)	Generated in this work
MVA-N1L-P7.5OVA (SE)	Generated in this work
MVA-revΔN1L-P7.5OVA	Generated in this work
VV	Obtained from I.Drexler
VV-ΔN1L	Gift from Micheal Way (UK)
Rabbit Fibroma Virus (RFV)	Gift from K.Tischer (Berlin)
Fowlpox virus (FP-tyr)	Obtained from I.Drexler

2.16. Consumables

NAME	MANUFACTURER
Cell culture flasks (T25, T75, T185, T225)	Nunc Corning Greiner
Cell culture plates 6-, 12-, 24-, 96-well	Corning Nunc
Cell scraper	Nunc
Cell strainer 100µm	BD Pharmingen
FACS tubes	BD Falcon
Falcon tubes (15 ml, 50 ml)	BD Pharmingen
Gene Pulser cuvettes	Bio-Rad
Hyperfilm™ ECL	Amersham
Nitrocellulose membrane 0,45µM	Whatman
PCR reaction tubes	Eppendorf
Petri dishes	Nunc
Polyallomer Centrifuge Tubes (14×89mm, 25×28mm)	Beckman Coulter
Reaction tubes (0,5 ml, 1,5 ml, 2 ml)	Eppendorf
Sterile filters (Minisart 0,2-0,45 µm)	Sartorius AG
Syringes (5, 10, 20 ml)	BD Pharmingen
Whatman paper	Whatman

2.17. Laboratory Instrument

NAME	TYPE	MANUFACTURER
Centrifuge	Allegar X-152 L-70K	Beckman
CO ₂ Incubator	BBD6220	Thermo Heraeus
Cup sonicator	Sonopuls HD 200	Bandelin
DNA/RNA Calculator	Nanadrop	Thermo
Electrotransformator	E. coli Pulser	Bio-Rad

Film processor	Cawomat 2000IR	CAWO
Flow cytometer	FACS Canto	Becton Dickinson
Freezer (-20 °C)	-	Bosch
Freezer (-80 °C)	Hera freeze Ult 2090	Heraeus
Fridge (4 °C)	UT6-K	Bauknecht
Horizontal Electrophoresis System	A1 Gator A2 Gator	Owl Scientific
Ice machine	AF 200	Scotsman
Incubation shaker	Innova 4430	New Brunswick Scientific
Laminar flow	HERAsafe HS 12	Heraeus
Magnetic stirrer	Ikamag Reo	IKA Werke
Microscope	IX83	Olympus
Microwave	900W	Siemens
Nitrogen container	Cryo 200	Forma Scientific
PCR Cycler	GeneAmpR PCR	Applied Biosystems
pH-Meter	InoLab pH Level 1	WTW GmbH
Thermomixer	Thermomixer 5436	Eppendorf
Ultracentrifuge	ArantiJ-E	Beckman
Vortexer	L-46	Labinco
Waterbath	IV-205/5	Welabo
qPCR system	StepOne plus	Applied Biosystems
WB comb	TV400-NG	Bio-Rad

2.18. Software

NAME	MANUFACTURER
FlowJo 8.6	Treestar
GraphPadPrism 5	Graph Pad Software
Cytomics FC 500	Beckman Coulter
Clone manager	Scientific & Educational Software
Clustal X	EMBL-EBI
ESPrpt	Created by Patrice Gouet and Frédéric Metoz
MS Office	Microsoft
FacsDIVA	Becton Dickinson

3. Methods

3.1. Molecular biology

3.1.1. Generation of electrocompetent bacteria

Every step was performed under the sterile conditions. Bacteria from a suitable *E.coli* strain were streaked (Here DH10B) onto an LB agar plate (without antibiotic) and single colonies were picked and incubated at 37°C. The next day, the bacteria were inoculated in 50 ml of fresh LB medium and cultured overnight at 37°C under vigorous shaking (here 220 rpm, so as in following). 50 ml of the overnight *E.coli* culture were added to 500 ml of fresh LB medium and incubated at 37°C under vigorous shaking until the OD_{600nm} was approx. 0.4-0.6 indicating exponential growth. Cells were pelleted by centrifugation at 5000 rpm for 15 min at 4°C (Centrifuge Avanti J-25, rotor JA-10). The following steps were carried out on ice to achieve high transformation efficiency. The cells were resuspended in 500 ml of ice-cold sterile distilled water. The washing steps were repeated for 3 times. The cells were resuspended in a final volume of 2 ml ice-cold sterile 10% glycerol (~ (2-5)×10¹⁰ cells/ml). For storage electrocompetent cells were aliquoted to 50 µl per tube and immediately snap-frozen in a dry-ice ethanol bath and stored at -80°C.

3.1.2. Generation of competent *E.coli* bacteria

E.coli bacteria (XL1-blue) were cultured in LB-medium and streaked onto LB agar plates (without antibiotic) to obtain single colonies of freshly grown *E.coli* and incubated overnight at 37°C. Two ml of fresh *E.coli* culture was added to 200 ml LB-medium and cultivated at 37°C until density of OD_{600nm} 0.4-0.6 was reached. The culture was centrifuged at 5000 rpm for 15 min at 4°C. The pellet was resuspended in 25% culture volume ice-cold 0.1 M MgCl₂ and incubated for 10 min. Later on, the bacteria were pelleted, and resuspended in 25% culture volume ice-cold 0.1M CaCl₂ and incubated for 10 min. The bacteria were again centrifuged and resuspended in 5% culture volume 0.1M CaCl₂ with 15% glycerol. Finally, 100 µl aliquoted *E.coli* competent bacteria were snap-frozen in liquid N₂ and stored at -80°C.

3.1.3. Generation of electrocompetent GS1783 *E.coli*

GS1783 (2.5 µl) cells were incubated with 100 ml pre-warmed LB-medium with 30 µg/ml chloramphenicol and cultivated with 160rpm at 30-32°C until OD_{562nm} was

approx.0.5-0.7. The culture was transferred immediately into a water bath shaker at 42°C with 220rpm for 15 min. Bacteria culture was chilled on ice-water mix for 20 min with shaking. Later on, bacteria were pelleted at 6300 rpm (Beckman Coulter JA10) for 5 min at 4°C. The Pellet was further resuspended in 5 ml 10% ice-cold glycerol, and pelleted at 9800 rpm centrifugation for 1 min. The supernatant was then discarded. The washing steps were repeated 3 times with 5 ml 10% glycerol. The bacteria were resuspended with 900 µl 10% ice-cold glycerol. 50 µl aliquoted electrocompetent bacteria were snap-frozen using a dry-ice ethanol bath and stored at -80°C.

3.1.4. Transformation

To generate the *E.coli* that uptakes the desired plasmid or transfer vector DNA, electrocompetent *E.coli* were transformed by electroporation. 50 µl aliquots of electrocompetent *E.coli* were thawed on ice for 5 min. An appropriate amount of DNA was mixed into the bacteria. The mixture was then dropped into the pre-cooled cuvette (0.1 cm gene pulser, Bio-Rad) and then pulsed at 1.8 kV, 200Ω, 25µF (For GS1783 *E.coli*, setting was modified to 1.5 kV, 200Ω, 25µF). Then, new 900 µl LB medium without antibiotics was added to the pulsed cell sample immediately. Then bacteria were cultivated at 37°C (30°C-32°C for GS1783) to express the resistance gene product for antibiotics. After 1h incubation, 10% of bacteria were distributed directly to the LB agar plate containing the selecting antibiotics. The other 90% of bacteria were pelleted at 1000 rpm for 10 min, and resuspended with small amounts of (e.g 100 µl) new LB medium and distributed to another LB agar plate containing selecting antibiotics. The agar plates were incubated at 37°C for overnight or a desired period of time (30-32°C for GS1783 *E.coli*).

3.1.5. DNA isolation from bacteria

3.1.5.1. Isolation of plasmids for analysis (Mini-Prep)

The candidate single colonies were tip-picked and transferred to 4 ml antibiotic-containing LB medium and incubated at 37°C overnight. When bacteria grew faintly cloudy 1.2 ml of culture were taken, pelleted at 9000 rpm for 3 min at 4°C. Supernatant was discarded and the pellet was resuspended with 300 µl P1 solution (RNase added) (Qiagene). No cell clumps should be visible in the suspension. The EDTA containing P1 buffer would resolubilize the pellet. Then 300 µl P2 was added to lyse

the bacteria with Alkaline NaOH and SDS and kept at room temperature for 2-3 min. 300 µl P3 solution was added (Low PH acetic acid) on-ice and the mixture was carefully moved for several times. A milky pellet was observed (precipitated cell debris and proteins with bacterial chromosomes). The plasmid resolved in the supernatant and was centrifuged twice at 13000 rpm for 20 min at 4°C. The supernatant was transferred into a new reaction tube to improve purity (separation from the precipitate). After the second centrifugation step, the supernatant was again transferred to a fresh reaction tube. DNA was precipitated by adding 500-600 µl of isopropanol. After 5 min incubation at room temperature, the DNA was precipitated and pelleted by centrifugation at 13000 rpm for 20 min at 15°C. The supernatant was discarded and the pellet was slowly resolved with 500 µl 75% ethanol to wash away the remaining salt and then centrifuged with 13000 rpm for 10 min at 4°C. The fluids were carefully removed, and the pellet was air-dried for 20 min. The plasmid pellet was resolved with 45 µl water. Two to four µl of DNA could be used for digestion test.

3.1.5.2. Isolation of plasmid DNA for experimental use and storage (Maxi-Prep)

The correct clones as identified by restriction digest were chosen for plasmid maxi-preparation. Here, 600 µl bacteria culture was added to 250 ml LB culture with antibiotics, and then incubated at 37°C at 110 rpm overnight. On the next day, 600 µl bacteria culture was stored as a backup with LB medium containing 25% (V/V) glycerol in -80°C. The rest of bacterial cells was harvested by centrifugation at 5000 rpm for 15 min at 4°C. Qiaquick Maxi Kit was used for plasmid isolation following the manufacturer's instructions. Then, 500 µl TE was used to resolve the plasmid pellet. The DNA concentration was measured by a Nanodrop device. The plasmid DNA samples were then sent for commercial sequencing. (GATC Biotech, Eurofins MWG Operon and BMFZ).

3.1.6. Polymerase chain reaction (PCR)

3.1.6.1. Standard PCR

Target genes or gene fragments were amplified from plasmids by PCR reaction. Roche PCR master kit was used for the standard PCR. The commonly used master mix was carried out as follows:

PCR master 1	50 µl (25µl)
PCR master 2	46.5 µl (22.5 µl)

10 pmol/μl Primer F	1.25 μl
10 pmol/μl Primer R	1.25 μl
DNA template	1 μl (~ 1 μg)
Total	100 μl (50 μl)

Thermocycler program for each PCR reaction was usually determined according to primers, templates and product length. The standard cycle condition was used as follows:

Step	Temp.	Time	Cycle No.
Denaturation initial	95°C	5 min	× 1
Denaturation	95°C	30 s	× 30
Annealing	50°C-58°C	30-60 s	
Elongation	72°C	1-5 min (30-70 bp / sec)	
Final elongation	72°C	7 min	× 1
Cooling	4°C	Pause	

3.1.6.2. PCR method to introduce a long DNA fragment

For introducing long sequences to the 5' or 3' ends of target genes or gene fragments by long primer pairs, a two-step PCR cycle protocol was used:

Step	Temp.	Time	Cycle No.
Pre-denaturation	95°C	2 min	× 1
Denaturation	95°C	10 s	× 10
Annealing	50°C	10 s	
Elongation	68°C	1-5 min (30-70 bp / sec)	
Denaturation	95°C	30 s	× 25
Annealing	60°C	30-60 s	
Elongation	68°C	1-5 min (30-70 bp / sec)	
Final elongation	72°C	7 min	× 1
Cooling	4°C	Pause	

3.1.6.3. Small double strand DNA synthesis by stepwise annealing

To generate small double stranded DNA for cloning (< 100 bp) that is not convenient to be generated by PCR, a stepwise annealing method was used. The full complementary primer pairs (1000 pmol amount for each) were mixed at 1:1 ratio in a total volume of 100 μ l per reaction. The mixture was heated at 95°C for 5 min in the thermocycler, and then cooled down gradually to 37°C at a speed of 1°C per min. This was the so-call stepwise annealing process. Then the mixture was further incubated at 37°C for 2 h or overnight before electrophoresis.

3.1.6.4. Direct Colony PCR

The target gene specific primers were used for screening of positive clones by PCR. The aim of the screening was to verify the DNA insertion to the target region. Direct colony PCR circumvents the need to culture bacteria overnight in order to obtain sufficient DNA for further analysis. We used the colony PCR to screen the positive clones after the Red Recombination in MVA_BAC genome. DreamTaq Green PCR Master Mix (2X) kit was used for this PCR reaction. Twenty μ l reaction mix was prepared for each sample. A part of a colony was transferred to a fresh LB plate containing desired antibiotics and marked with a number. Then, the rest of the colony was transferred to a PCR tube containing reaction mixture by using pipet tips. Small amounts of bacteria are usually sufficient. The PCR reactions were performed in a thermocycler. The PCR products were examined by electrophoresis on an agarose gel. The colonies with correct fragment size were chosen for further usage and processed according to the number on new agar plate. (Figure 3.1)

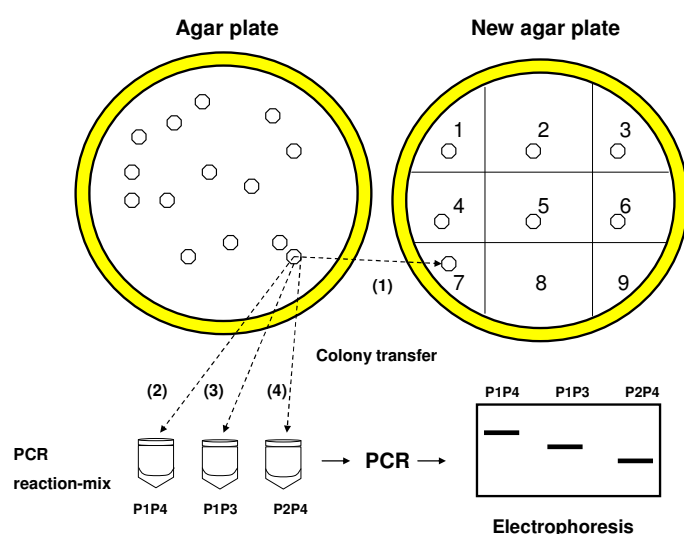


Figure 3.1. Schematic illustration of the direct colony PCR protocol.

3.1.7. Dephosphorylation and Ligation

A 5'-phosphate group presented in the digested DNA vector was required for ligation. To prevent self-re-ligation of the vector, dephosphorylation was performed. The 80 μ l of reaction mix contained 40 μ l digested vector, 6 μ l AP (Phosphatase alkaline), 8 μ l (10 \times) dephos. buffer, and 26 μ l H₂O. The reaction was incubated for 1 h at 37°C. Finally, 4 μ l EDTA (0.5M PH9.3) was added to bind Ca²⁺ and to avoid resistance of AP during heat inactivation.

Then the dephosphorylated DNA product was heated for 10 min at 70°C to inactivate the enzyme. PCR purification of the vector was performed by using the QIAquick PCR purification kit (50) following the manufacturer's instructions.

100 ng vector was used for ligation. Vector and PCR product (or DNA fragment) were measured at OD_{260nm} to determine the DNA concentration. The molar ratio was counted for the ligation according to the formula:

$$n = \frac{[\text{insert}]}{[\text{vector}]} = \frac{\frac{m_{\text{insert}}}{\text{bp}_{\text{insert}}}}{\frac{m_{\text{vector}}}{\text{bp}_{\text{vector}}}}$$

n : the ratio of insert : vector of molar amount
m : the amount of insert or vector
bp : the base-pairs length of vector or insert

For sticky end ligations, the molar ratio could be 3:1, while for the blunt end ligations the ratio is suggested to be 5:1. Ligation reactions were preferably carried out in ice water overnight. An additional 1 h incubation at 20 °C was performed to increase the blunt end ligation efficiency.

3.1.8. Generation of recombinant MVA_BAC genomes in GS1783 *E.coli*

3.1.8.1. Deletion of the *K1L* gene from the pVI-P11 plasmid

pVI-P11 plasmid (Fig.4.1.) was digested by *Pme*I. After electrophoresis, a 4552 bp fragment was extracted using the QIAquick gel extraction kit according to the manufacturer instruction and used for re-ligation. The re-ligated product was verified by *Acc*I digestion (mini-prep). The resulting plasmid was termed pVI-P11-*Pme*I (Fig.4.1.).

3.1.8.2. Introducing an additional *PacI* site at the *HindIII* site of pVI-P11-PmeI

Primer pairs, Hind Pac PL fw and Hind Pac PL rv, were taken for the stepwise annealing procedure. The plasmid pVI-P11-PmeI and the annealed primer DNA fragment were digested by *HindIII* cutting enzyme and then ligated at a molar ratio of 3:1. Mini-preps of clones were further tested by *PacI* digestion. The fragments pattern for positive colonies was expected to be 2737 bp plus 1830 bp in electrophoresis. Further sequencing guaranteed that correct clones contained a single *PacI* site inserted in the desired locus. The resulting construct was named pMVA-dVI-P11(Fig.4.1.) .

3.1.8.3. Construction of transfer plasmid pEP MVAAdVI-P11

For construction of the MVA deletion VI targeted transfer plasmids, an 1059 bp aphAI-I-SceI cassette was amplified from plasmid pEPKan-S (A generous gift from Karsten Tischer, Institute of Virology, Freie Universität Berlin, Germany) using primers MVAExpEPfw and MVAExpEPrv. The cassette contained a kanamycin resistance gene, an *I*-SceI homing endonuclease site and a 50 bp viral sequence duplication. The plasmid pMVA-dVI-P11 was digested with *Bam*HI and *Pme*I. The resulting 4551 bp fragment was ligated to the *Bam*HI and *Eco*RV cut aphAI-I-SceI cassette to generate the plasmid pEPMVAAdVI-P11. The sequence was verified by commercial sequencing.

3.1.8.4. Construction of transfer plasmids containing different VV promoters

To create the transfer plasmids with different VV promoters, a PK1L promoter containing fragment was amplified from i-plIIDHR-K1L with PK1L primer fw and PK1L primer rv; a PG8R promoter containing fragment was generated by stepwise annealing with PG8 primer fw and PG8 primer rv; a PmH5 promoter containing fragment was amplified from i-plIIDHR-PmH5 with PH5 primer fw and PH5 primer rv; a P7.5 promoter containing fragment was generated from digestion of i-plIIDHR-P7.5 with *Sna*BI and *Bam*HI; finally plasmid pEPMVAAdVI-P11 was digested with *Sac*I and *Pme*I, and ligated with *Sac*I and *Pme*I cut PK1L, PG8 and PmH5 promoter containing fragments respectively resulting in vectors pEPMVAAdVI-PK1L, pEPMVAAdVI-PG8 and pEPMVAAdVI-mH5 in which the P11 promoter had been substituted by the respective promoters. Plasmid pEPMVAAdVI-P7.5 was generated using a similar strategy. Briefly, previously generated plasmid pEPMVAAdVI-longP7.5 was digested with *Pme*I and

*Bam*HI to get rid of an inactive sequence in the 7.5 promoter region. The resulting 5489 bp fragment was ligated to a 156 bp fragment derived from plasmid ipIIIDHR-P7.5 digested with *Sna*BI and *Bam*HI, which contained the P7.5 promoter sequence.

3.1.8.5. Construction of VV transfer plasmids expressing mCherry

To generate the transfer vectors in which mCherry was inserted as a reporter gene, pEPMVAdVI- (PK1L, PG8, P11, P7.5, PmH5) plasmids were digested by *Sac*I. T4 DNA Polymerase was used for 5' overhang fill-in to obtain blunt ends. They were ligated with mCherry fragments obtained from pmCherry-N1 digested with *Afe*I and *Hpa*I resulting in pEPMVAdVI-PK1L-mCherry, pEPMVAdVI-PG8R-mCherry, pEPMVAdVI-P11-mCherry, pEPMVAdVI-P7.5-mCherry and pEPMVAdVI-PmH5-mCherry, respectively. Unwanted ATG sequences between promoter regions and mCherry were deleted from each vector.

3.1.8.6. Red Recombination

GS1783 *E.coli* harbouring the bacmid MVA_BAC pMVA-F-DX (a generous gift from Matthew G.Cottingham, Oxford,UK) were grown in the presence of 30 µg/ml chloramphenicol (CAM). To introduce the VV promoter-mCherry expression cassettes into the MVA_BAC deletion VI region, linearized 3.7 Kb VV promoter-mCherry DNA fragments flanked by left and right homologous sequences to the MVA natural deletionVI site were extracted from *Pac*I cut pEPMVAdVI-VV promoter-mCherry (in the following, pEPMVAdVI-P11-mCherry will be used as an example for the further steps of recMVA generation), and introduced into GS1783 by electroporation (refer to 3.1.4). The bacteria were shaken for 1-2 h, and grown on LB agar plates containing 30 µg/ml CAM and 30 µg/ml kanamycin (Kana) for 24h. The correct colonies were identified by direct colony PCR (refer to 3.1.6.4). For the 2nd Red Recombination in order to remove the aphAI-I-SceI cassette, the bacteria having the correct co-integrates were inoculated into 1 ml of LB broth with 30 µl/ml CAM. After 2 h of incubation at 32°C at 220 rpm the solution became faintly cloudy. One ml of pre-warmed LB broth with 30 µl CAM plus 2% L-arabinose (g/100ml) was added including sterile 10 µl tips to enhance oxygen transduction. The bacteria were shaken for 1 h at 220 rpm at 32°C. Then the bacteria were further incubated at 42°C (water bath shaker) for another 30 min at 220 rpm and at 32°C for further 2-3 h at 220 rpm. The bacterial growth density was measured at OD_{600nm}. Five to 10 µl of the bacterial

suspension at 1:100 ($OD_{600nm} < 0.5$) or 1:1000 ($OD_{600nm} > 0.5$) dilution were streaked to LB agar plates containing 30 μ l/ml CAM and 1% L-arabinose. The plates were incubated at 30-32 °C for 1-2 days until bacterial colonies with desired size were formed. The correct integration of the cassettes was verified by direct colony PCR and sequencing.

3.1.8.7. *E.coli* MVA_BAC genome extraction for recMVA rescue

For this protocol, pipet tips here must be cut at the end. Five ml LB medium containing 30 μ l CAM was used to grow recMVA_BAC GS1783 *E.coli* at 30-32°C at 250 rpm. The bacteria were centrifuged at 11000 rpm for 5 min. The rest of the procedure was done on ice. The pellet was resuspended with 100 μ l P1 solution (Qiagen) by pipeting up and down, then 200 μ l P2 lysis solution were added. Tubes were inverted for 5 times and 150 μ l P3 solution were added. After 5 min incubation on ice, the suspension was subsequently centrifuged at 11000 rpm for 15 min. The supernatant was transferred into a new tube and 320 μ l cold isopropanol added. The mixture was carefully shaken for 5 times and the DNA was precipitated at 11000 rpm for 15 min. Two hundred μ l 70% ethanol were used to wash the pellet. The remaining ethanol was removed and the DNA was air-dried for 10-15 min. The pellet was resolved in 30 μ l TE/RNase (40 μ g RNase/ml). After 30 min incubation at 37 °C to allow for or the RNase reaction, the DNA was stored at 4°C before usage for the BAC rescue.

3.1.8.8. Viral DNA extraction from infected cells

The cell monolayer of one well in a 6-well plate was infected with virus at a MOI of 10, and was incubated for 1 day in the 5% CO₂ incubator. The cells were then harvested in 400 μ l sterile Mili-Q water and subsequently transferred into a 1.5 ml EP tube. 50 μ l 10X TEN (pH 7.4) were added. After 3 times of freeze/thawing and sonification, cellular debris was removed by centrifugation at 450g for 5 min at RT and the supernatant was transferred into a new EP tube. Fifty μ l proteinase K and 23 μ l SDS were added and mixed by pipetting. The suspension was then incubated for 1 to 4 hours at 56 °C. Suspension was extracted twice with phenol-chloroform (P-I): equal volume of P-I was added and then the mixture was centrifuged at top speed for 5 min at RT. The supernatant was then transferred into the new EP tube. Then 1/10 volume of 3M NaAc and 2 volumes of pure ethanol were added and mixed gently. Subsequently, the solution was cooled for 30 min at -80 °C and centrifuged at top

speed for 10 min at 4 °C. The supernatant was washed twice with 70% ethanol and air dried for 10 min. Finally, the pellet was resuspended in 1X TE buffer.

3.1.8.9. Construction of MVA-N1L, MVA-OVA-N1L, MVA-OVA-revΔN1L

Generation of the MVA-N1L_BAC genome (pMVAF-DX-N1L) was performed by the two-step red-mediated recombination as described. Briefly, for reconstitution of the truncated C terminal 71 nucleotides of N1L in MVA ortholog with C terminal 83 nucleotides of wild type N1L, plasmid pEP-MVA-dVI-P11 was used as template for a PCR using primer pair MVA-N1LCin_fw and MVA-N1LCin_rv. The PCR product contained the following parts: homologous sequences for the first Red Recombination, 83 nucleotides of wild type *N1L*, a duplication of a *N1L* sequence that was necessary for the second step of the Red Recombination and the selection cassette I-SceI-aphAI. The PCR product was electroporated into the recombination-competent GS1783 *E.coli* strain harbouring the pMVAF-DX. The following steps for generating the MVA-N1L_BAC were carried out as the two-step Red Recombination (Section 3.1.8.6 and Fig. 4.10 A).

To generate the MVA-OVA-N1L_BAC genome (pMVAF-DX-(OVA)-N1L), we first constructed transfer plasmid pEP-MVA-dVI-P7.5OVA. Briefly, the OVA ORF was PCR-amplified from template plasmid pIIIDHR P11-OVA using primers fwd_OVA_toP7.5 and rv_OVA-toP7.5. The resulting 1181 bp PCR product and plasmid pEPMVAdVIP7.5 were cut with *Bam*HI and *Bsr*GI. The cut 1167 bp PCR product and the 5632 bp plasmid were ligated, yielding the transfer plasmid pEP-MVA-dVI-P7.5OVA. To generate the MVA-OVA-N1L_BAC genome, pEP-MVA-dVI-P7.5 OVA was digested with *Pac*I and the resulting linearized insertion cassette was used for a two-step Red-mediated recombination in MVA-N1L_BAC (GS1783 *E.coli* containing pMVAF-DX-N1L; Strategy in Appendix Fig.8.2).

The MVA-OVA-revΔN1L_BAC genome (pMVAF-DX-(OVA)-revΔN1L) was created using a similar strategy as for MVA-N1L_BAC generation. Briefly, plasmid pEP-MVA-dVI-P11 was used as a template for a PCR using primers MVA-N1Lrev_fw and MVA-N1Lrev_rv. The resulting 1191 bp PCR product was taken for the two-step red-mediated recombination into the MVA-OVA-N1L_BAC genome (GS1783 *E.coli* containing pMVAF-DX-(OVA)-N1L; Strategy in Appendix Fig.8.3).

3.2. Cell biology

All the cell lines were handled under the sterile conditions. The cell culture was always fostered at 37°C with 5% CO₂ and 95% humidity.

3.2.1. Adherent eukaryotic cell culture

CV₁, HeLa and BHK-21 cells are adherent cell lines. HeLa and BHK-21 cells were cultured with RPMI medium (DMEM medium for CV₁ cells) supplemented with 10% fetal bovine serum (FBS) and 1% penicillin-streptomycin (Pen/Strep). Cell lines were grown as monolayers in cell culture flasks. When cell confluency reached around 90% of the flask, cells were split for passaging at the ratio of 1:2 to 1:10 depending on intended usage. For passaging, cells were washed once by PBS. Then 3 ml 0.25% trypsin were added and incubated at 37°C for a few minutes until cells were detached. Seven ml 10% FBS RPMI medium were added to stop the trypsin reaction. The trypsin containing medium was removed from the cells by centrifugation at 1500 rpm at RT for 5 min. Cells were resuspended and singularized by pipetting with fresh medium. The required fractions were transferred into a new flask supplemented with fresh medium.

3.2.2. Cyro-preservation of cell lines

When in the exponential growth phase, the cells could be stored. Cells were harvested by trypsination from flasks and counted for the cell number. Subsequently, they were pelleted by centrifugation, resuspended and singularized with freezing medium (here using 90% FBS plus 10% DMSO) with the desired cell density. Cells were transferred into cryotubes at 1 ml per tube and placed to the Mr. Frosty freezing containers surrounded by isopropanol (abs.). After 1 day of cooling at -70°C at the speed of -1°C per min, the cryotubes were transferred to liquid nitrogen for long-term storage.

3.2.3. Recovery of cell culture

To re-culture the frozen cells, they were taken from the liquid nitrogen and thawed rapidly in a 37°C water bath. The thawed cells were diluted immediately into pre-warmed growth medium. Cells were centrifuged at 1200 rpm for 3 min and resuspended with new culture medium.

3.2.4. Primary chicken embryo fibroblast (CEF) culture

Embryos were bred in a breeder for 10 or 11 days of age at 37°C with optimal humidity. Air cell was faced up to breed. The eggs used for CEFs preparation were disinfected with Bioguard or 70% EtOH. A hole was punched in the shell at the top of the egg and the part covering the air cell was removed with a sterile scissor. Forceps were used to remove the chorioallantois membrane to open the allantoic cavity. The embryo was transferred to a petri dish containing PBS without calcium and magnesium. The eyes and splanchna were removed from the embryo. A cannula was attached to a 20 or 50 ml syringe. The plunger was removed. Subsequently, the tissue chunks were poured into the barrel and forced through the cannula with the plunger into a 30 ml beaker. The embryo was washed 3 times to remove the red blood cells. 100 ml pre-warmed trypsin solution (0.25 %) was added to the stirrer containing flask and set on a magnetic plate for 25 min. The supernatant was filtered through double-layer sterile gauzes into a 500 ml beaker. The remaining tissue was trypsinated again as described above and filtered into a new 500 ml beaker. After 3 times of tissue trypsination and filtering, the trypsinated cells were divided into 50 ml falcons and centrifuged at 1800 rpm for 6 min. The cells were resuspended and washed in 50 ml PBS per falcon by centrifugation at 1800 rpm for 6 min. After 3 times of washing, the cells were resuspended in CEFs medium at a volume of 60 ml per embryo, and filtered again through the gauze. The CEF cells were diluted in the desired volume of CEFs medium and cultivated in T225 or T185 flask in normal cell culture incubator (approx. 1 embryo for 2 × T225 flask).

3.2.5. Preparation of bone marrow-derived dendritic cells (BMDC) and bone marrow-derived macrophages (BMΦ)

Femurs and tibiae were removed from the mice and transferred to petri dishes containing 70% ethanol. Muscles were removed from the bones which were placed in a new petri dish containing M2 medium. Both ends (epiphyses) of each bone were cut off with scissors and transferred to a separate dish. The marrow was obtained by flushing out each of the shafts 2-4 times using a syringe with 1 ml M2 medium until the shaft became white. The epiphyses were minced and clumps were broken up with Pasteur pipets. The suspension was passed through 70 µm strainer into a 50 ml falcon to remove the particles. The red blood cells were lysed by adding 3 ml (for 2 bones) TAC lysis buffer at room temperature for 2 min. The cells were then diluted in

PBS up to 50 ml and centrifuged for 5 min at 1500 rpm at RT. The cells were resuspended with appropriate M2 medium to obtain a cell density of 5×10^6 per ml. One ml cell suspension was grown in 10 ml fresh 10% GM-CSF M2 medium (M-CSF used for BMΦ) in 150 mm petri dishes and cultured in 37°C incubator. On day 3, 10 ml 10% GM-CSF (M-CSF) containing M2 medium were added to the culture. On day 6, change of medium was carried out by aspirating 10 ml of supernatant and adding 10 ml fresh 10% GM-CSF (M-CSF) containing M2 medium. The BMDCs were used for experiments on day 7 to day 9.

3.2.6. Antigen specific CD4+ T cell re-stimulation and culture

Splenocytes from C57BL/6 background mice were used (OT I B6 or OT I × CD45.1 B6) for T cell re-stimulation. The spleen was transferred to 5 ml M2 medium containing falcon tubes, and then transferred on metal grids in petri dishes. A stamp was used to mince and homogenize the spleen. Homogenized materials were poured over 70 μm cells strainers into fresh falcon tubes. The cells were centrifuged at 1500 rpm for 4 min. Pellets were erythrocytolyzed by 3 ml TAC buffer (one spleen) for 2 min at room temperature. Then PBS was added to dilute the cells to 50 ml. Cells were centrifuged at 1500 rpm for 4 min and the pellet was resuspended with 10 ml M2 medium. 10 kGy γ irradiation was applied on cells. The cell number was counted and cells split equally to 3 falcon tubes containing 5 ml RPMI medium (without FBS). The FBS was washed away from the cells using RPMI medium and resuspended with 1 ml fresh M2 medium. 2 μg of peptide (OVA₍₂₆₅₋₂₈₀₎, B5R₍₄₆₋₆₀₎, L4R₍₁₇₆₋₁₉₀₎) were used to load splenocytes for 30 min in a 37°C incubator. Then the peptides were washed away with 10 ml fresh M2 medium. Fresh medium was used to resuspend the cell pellet (final cell density of 1.2×10^7 cells / ml.) The splenocytes were transferred into 24- well plates (6×10^6 cells per well). A 0.5 ml TCGF was added to the splenocytes at a final concentration of 5%. CD4+ T cells (CD4^{OVA}, CD4^{B5R}, CD4^{L4R}) were harvested and pelleted. Fresh M2 medium was used to resuspend the cells. T cells were split at a ratio of 1:2 and cultured with the peptide stimulated splenocytes. The total volume of the new culture was 2 ml per well.

3.2.7. CD4+ T cell re-activation assay

1×10^5 APCs (BMDCs or macrophages) were infected with MVA or VV at the desired MOI (0.1-20) in 500 μl M2 medium for 90 min. During incubation, the falcon tube was slightly shaken every 20 – 30 min. Next, 1×10^5 APCs were plated out to 96-well

plates in 100 µl M2 medium per well. Peptides were added at a final concentration of 2 µg/ml per well as positive controls. MHC-mismatched peptides or DMSO were added as negative controls. Six hours later, 3×10^5 Ag-specific CD4⁺ T cells (CD4^{OVA} and CD4^{B5R}) were prepared in 100 µl M2 medium together with BFA at a final concentration of 1 µg/ml. CD4⁺ T cells were then co-cultivated with the APCs for 12-15 hours at 37°C in a CO₂ incubator. T cell activation was further determined by intracellular cytokine staining for IFN γ and IL-2 secretion (see section 3.5.3).

3.2.8. Annexin staining

STS treated- or MVA-infected cells were washed twice with cold PBS and then resuspended in 1X binding buffer at a concentration of 1×10^6 cells/ml. 1×10^5 cells in suspension (100 µl) were transferred to 96-well plates. Five µl of APC-conjugated Annexin V and 5 µl of 7-AAD were added to the cells. After gently vortexing, the cells were incubated for 15 min at room temperature in the dark. After incubation, 400 µl binding buffer was added to each well. The subsequent analysis was carried out by flow cytometry within 1 hour.

3.3. Virology methods

3.3.1. MVA_BAC rescue

There exist two distinct established protocols to be used for our MVA_BAC rescue depending on the helper virus used for MVA_BAC reconstitution in eukaryotic BHK-21 cell lines.

- 1) **Fowlpox virus (FPV) as helper virus.** FPV (MOI of 1) was diluted in 1000 µl OptiMEM medium. The culture medium of BHK-21 cells was replaced with the OptiMEM/FPV mixture, and then incubated for 1-2 h at 37°C CO₂ incubator. During the incubation period, 3-5 µg MVA-BAC DNA were mixed with 300 µl OptiMEM. Meanwhile, 10 µl of Lipofectamin 2000 was mixed with 300 µl OptiMEM medium in a separate transfection tube. Five min later, BAC DNA and transfection reagent were mixed and incubated at room temperature for 20 min. The helper virus was removed from the cell monolayer, and washed once with OptiMEM. Then the transfection mixture was dropped on the cell monolayer for incubating with additional 200 µl serum-free medium. Eight h later, the cell culture medium was exchanged with 2 ml

fresh pre-warmed 10% FBS RPMI medium and incubated for another 24 h until fluorescence monitoring started.

2) **Rabbit fibroma virus (RFV) as helper virus.** 10 μ l of MVA-BAC DNA (~50 μ g) was mixed with 4 μ l X-tremHP transfection reagent in 68 μ l OptiMEM serum-free medium. After 20 min incubation, the mixture was dropped evenly on the BHK-21 cell layer (60-70% confluency). The plate was softly whipped every 15 min to avoid drying of the cells and incubated for 1 h at 37°C in an CO₂ incubator. RFV virus (MOI 1) was added to the cell monolayer in 1 ml 2% FCS RPMI medium. Forty-eight h later, GFP expression was monitored under the fluorescent microscope.

All recMVA expressing mCherry in this dissertation were generated by FPV helped rescue, while the recMVA used for N1 function analysis were produced by RFV assisted rescue.

3.3.2. Subcloning of BAC-excised recMVA

After 3 passages in permissive cells, recMVA_BAC self-excising constructs were monitored under the microscopy for fluorescence of infected cells. GFP negative cells with CPE (or mCherry expression for certain vectors) were picked using 10 μ l tips and transferred to EP-tubes containing new virus growth medium. After 3 times of freeze/thawing and homogenizing, the suspension was cultured in 6-well plates with monolayers of permissive cells. The GFP negative cells with CPE were chosen for further virus amplification. A second round of plaque picking was needed when GFP expressing cell remained.

An alternative way to subclone the BAC-excised recMVA is the limiting dilution method. RecMVA_BAC at serial 10-fold dilutions were grown in 96-well plates. After 3 days of virus growth, GFP expression and CPE were checked under the microscope. GFP negative cells with CPE were chosen for further virus amplification.

3.3.3. Virus amplification and crude stock preparation

To produce a larger scale of virus, 10-40 T185 (T225) flasks were seeded with CEFs. Flasks with 80-90% confluency were infected with virus at an MOI of 0.3. Two days later or when CPE was recognized, cells were harvested and centrifuged for 10 min at 1800g at 4°C. Pellets were resuspended in appropriate volumes of 10 mM Tris PH9 (1 ml per T225 flask) and stored as crude stock in -80°C or used for further purification.

3.3.4. RecMVA purification

The crude stock virus material was freeze/thawed 3 times and then sonicated. It was further transferred to a dounce homogenizer and dounced for 5 sets on ice (5 times each sets). After centrifugation, the supernatant was transferred to a new falcon tube. The virion-containing fluids were then slowly dropped on sterile 36% sucrose cushions in SW28 centrifuge tubes. The pellets were resuspended with 1 mM Tris after 60 min centrifugation at 13500 rpm at 4°C, and then dropped on 36% sucrose cushions in SW41 centrifuge tubes. After 1 h of centrifugation at 13500 rpm at 4°C, the pellets were resuspended in 1mM Tris buffer (PH of 9) for long-term storage at -80°C. This virus preparation was considered as purified stock.

3.3.5. Virus titration and growth kinetic analysis by TCID₅₀

CEFs (or BHK-21) were seeded into 96-well plates. The virus material was serially diluted (ranging from 10⁻¹ to 10⁻¹⁰), plated and grown in 96-well plates for 1 week. During day 4 to day 7, CPE containing wells were marked under the microscope. TCID₅₀ was counted by the fomula:

$\log_{10} 50\% \text{ endpoint dilution} = x - d/2 + (d\sum r/n)$
x = highest dilution in which all eight wells (8/8) are counted positive
d = the log10 of the dilution factor (d = 1 when serial 10-fold dilutions are used)
r = number of positive wells per dilution
n = total number of wells per dilution (n = 8 when dilutions are plated out in replicates of eight)

To test the growth kinetics of recombinant MVA, CEFs were infected at MOI 0.01 and harvested at indicated time points (0 h is the harvest from a sample infected for 45 min at 4°C, which was used as the control for virus attachment). The samples harvested at each time point were titrated by TCID₅₀.

3.4. Biochemistry methods

3.4.1. Quantitative real time PCR assay

Hela cells were seeded at approximately 5×10⁵/well in 12-well plate 18h prior to virus infection. Each well was infected with desired virus at MOI 10, and synchronized for virus attachment at 4°C for 45 min. Unattached virus was washed away by cold PBS and the cells were cultivated at 37°C in a CO₂ incubator with fresh 2% FBS containing RPMI medium for the desired time period. The cells of each time point

were lysed and total mRNA extracted with RNeasy[®] Mini Kit (Qiagen). Genomic DNA was eliminated from mRNA before RNA reverse transcription to cDNA using the QuantiTect[®] Reverse Transcription kit (Qiagen). For quantitative real time PCR, each cDNA was mixed into the FastStart SYBR Green Master (Roche) following the manufacturer's instructions. Corresponding primer pairs were added into the mastermix as shown in section 2.7. The qPCR reaction and quantification analysis was carried out on the thermocycler system Step One Plus (Applied Biosystems). The ΔCt between the target gene and the reference gene (18S rRNA) was calculated for each sample ($\Delta Ct = Ct_{\text{target}} - Ct_{18S}$). The difference between the ΔCt of the unknown and the ΔCt of the calibrator (here $t = 0$ sample) is calculated, giving the $\Delta\Delta Ct$ value: $\Delta\Delta Ct = (Ct_{\text{target}} - Ct_{\text{reference}})_{\text{calibrator}} - (Ct_{\text{target}} - Ct_{\text{reference}})_{\text{sample}}$. Finally, the $2^{-\Delta\Delta Ct}$ value was used to denote the expression levels in the samples.

3.4.2. Fluorescent protein quantification by FACS

Hela cells were seeded at approximately 5×10^5 /well in 12-well plates 18h prior to virus infection. The virus infection and synchronization at desired time points was carried out as described in section 3.4.1. At each time point, the supernatant was collected. The cells were washed once by PBS, and detached with 0.25% trypsin before FBS containing medium was added for neutralization. PBS and trypsin/FBS medium cell suspensions were pooled to the supernatant which was collected before. Cells were centrifuged and the cell pellet was resuspended in ice-cold FACS blocking buffer (PBS with 5% BSA). Relative mCherry expression of 20,000 cells per sample was quantified on a Cytomics FC 500 (Beckman Coulter). Data were analyzed using FlowJo v9.4.10 (Tree Star, Inc.USA).

3.4.3. Western blot

Western blot is an antibody-based method to detect and quantify the target protein synthesis after proteins have been separated by sodium dodecyl sulphate polyacrylamide gel electrophoresis (SDS-PAGE) according to their molecular weight.

1) **Sample preparation.** Cells were infected at a MOI of 10-20 TCID₅₀ recMVA or pfu VV (e.g. MOI 10 = 1×10^7 cells with 1×10^8 TCID₅₀ of virus). Infected cells were incubated at on ice for 45 min, and were shaken every 10 min during the incubation. Then cells were washed twice to remove the free virus particles. Fresh medium was added and cells incubated for additional hours at 37 °C in 5% CO₂-atmosphere

depending on the experimental conditions. Cells were then harvested (0 h is the harvest from samples incubated for 45 min at 4°C, which used as the control for virus attachment as described in section 3.4.1.). Subsequently, the cells were transferred into 1.5 ml Eppendorf tubes, and centrifuged at 4000 rpm for 3 min at 4 °C. The pellet was resolved by desired RIPA buffer and stored immediately at -80°C.

2) **SDS-PAGE.** Cell lysates were thawed on ice for 20-30 min, and then centrifuged for 30 min at top speed. Supernatant was transferred into a new EP tube on ice. When required, protein concentration was measured using a Bradford assay kit. The protein sample was then mixed with loading buffer. Subsequently, the samples were incubated at 95 °C for 5 min to denature the proteins and break the disulfide bonds. Samples were then loaded into the pockets of stacking gel for electrophoresis. The proteins were separated according to their molecular weight.

3) **Blotting.** The separation gel was used for blotting to transfer the proteins from the gel onto the nitrocellulose membrane (0.45 µl pore size). A semi-dry blotting method was used here. The gel/membrane was sandwiched by whatman papers and then blotted (<15 V, <1000mA, <8 W). Seventy min later, the membrane was stained with Ponceau S to check the presence of the transferred proteins. Ponceau S was washed away with TBS-T.

3) **Antibody incubation.** After 1 h of blocking with 5% w/v nonfat dry milk, the membrane was incubated with 1st Ab (e.g. mouse-anti-N1) (1:1000) in blocking buffer overnight. Unbound Ab was washed away with TBS-T. The secondary Ab (e.g. anti-mouse IgG) was incubated with the membrane for 45 min in blocking buffer. Unbound 2nd Ab was also washed away with TBS-T. Two to 3 ml substrate solution (a 1:1mix of Lumi-Light solution A and B) were added to the membrane for 2-3 min which was later used for exposure. The protein specific signal was detected on a photographic film.

3.5. Immunologic methods

3.5.1. Immunizations

Male and female mice between 6-10 weeks of age were used for immunization. Mice were injected i.p. with 10^7 - 10^8 TCID₅₀ MVA in 500 µl PBS. BD Micro-Fine needles were used for injection.

3.5.2. Preparation of splenocytes

Spleens were extracted and homogenized with a syringe plunger over a metal grid in petri-dishes. Homogenized spleen materials were given over 70 micron cell strainers and centrifuged (5min, 15000 rpm). Splenocyte pellets were lysed with 3 ml TAC-buffer for erythrocytolysis (2 min, 37°C) and washed with 40 ml RPMI 1%. The cells were again filtered over a cells strainer.

3.5.3. Intracellular Cytokine Staining (ICS)

1) **Peptide stimulation of lymphocytes.** 4×10^6 splenocytes were transferred to flat-bottomed 96-well plates in 200 μ l RPMI 10% FCS. A master-mix for 10 peptides for stimulation were used as: 600 μ l RPMI 10% FCS + 3 μ l peptide + 0.6 μ l BFA. 50 μ l of this mastermix were dropped on the splenocytes. α -CD3 was added at 3 μ l per master-mix. Cells were incubated with peptides for 5 hours for CD8⁺ T cell stimulation and for 12-15 hours for CD4⁺ T cell stimulation, respectively at 37°C in a CO₂ incubator.

2) **EMA-Staining.** Cells were transferred to a V-bottom 96-well plate, and then washed once. Cell pellets were incubated with 100 μ l EMA (1:1000) for 20 min under light to stain the dead cells. Cells were washed twice with FACS buffer in a total volume of 200 μ l for 2 min at 1400 rpm. EMA staining was used for live/dead discrimination by the entry of photo-activated molecules into the dead or damaged cells which lost intact membranes. EMA may form stable links to nucleic acids within the cell. EMA stained cells can be specifically detected by excitation with a laser at 488 nm.

3) **Surface marker and intracellular cytokine staining.** After EMA staining, washed cells were stained with 50 μ l of the surface markers CD4 or CD8 α for 30 min in the dark on ice with desired antibody dilutions (1:400). Subsequently, the cells were washed 3 times with FACS-buffer and then treated with 100 μ l Cytotfix/Cytoperm to permeabilize cell membranes for 15 min in the dark on ice. Cells were washed with PermWash buffer 3 times before they were stained with 50 μ l intracellular antibodies. Here we used diluted anti-IFN γ /APC-conjugated (1:250), anti-IL-2/PE-conjugated antibodies (1:250) in 50 μ l Perm-Wash buffer for 30 min in the dark on ice. Finally, cells were washed again for three times, and fixed with 0.4% PFA (final concentration) and stored until usage for FACS analysis.

3.5.4. Statistics

Student's two-tailed t-test was used for each pairwise comparison. The p values deemed significant are indicated in the figures as follows: ns, no significance; *, $p < 0.05$; **, $p < 0.01$; ***, $p < 0.001$.

4. Results

4.1. Construction of VV-specific promoter transfer plasmids targeting MVA deletion VI

In order to generate the transfer plasmids, we employed the plasmid pVI-P11 as an initial construct, which contained MVA DNA homologous flanking sequences FlankVI₁ and FlankVI₂ adjacent to the MVA deletion VI region. The vaccinia virus natural promoter P11 is positioned between these two flanking sequences. There was a multiple cloning site (MCS) in conjunctions of both upstream and downstream of the P11 sequence to facilitate the exogenous DNA insertion. First, the unwanted VV gene *K1L* cassette with its promoter PK1L was removed by *PmeI* cleavage (Fig.4.1A). After re-ligation, a *PacI* recognition sequence was inserted into the plasmid *HindIII* site of plasmid pVI-P11-*PmeI*. The resulting plasmid pMVA-dVI-P11 contained two *PacI* sites flanking the deletion VI flanking sequences (Fig.4.1B). Second, an *aphAI*-I-*Scel* cassette was amplified from plasmid pEPKan-S and inserted upstream of the MCS for promoter P11 in pMVA-dVI-P11. This cassette consisted of: i) a kanamycin resistant gene for antibiotic selection, ii) an *I-Scel* homing endonuclease for cleavage at the flank of *aphAI*, and iii) a sequence homologous to the vector sequence for Red Recombination. As a result, we had generated the vector transfer plasmid pEPMVAdVI-P11. In order to control the transgene expression with different strength and kinetics, the promoter P11 was replaced by other VV specific promoter elements using standard PCR for generating respective DNA sequences and restriction digest and ligation for integration. Consequently, we obtained a series of transfer plasmids with VV-specific promoters for transgene expression which targeted MVA deletion VI (Fig.4.2A). The properties of these promoters have been listed in Table 4.1. To monitor and evaluate the transgene expression under control of these promoters, we used fluorophore mCherry as a reporter. Here, the mCherry ORF was inserted into each transfer vector downstream of the respective promoters (Fig.4.2B). Subsequently, a transient mCherry expression experiment (transfection + infection) was carried out which confirmed that all of the transfer plasmids (except pEPMVAdVI-PK1L) allowed for successful transgene expression (Data not shown). Transient expression of mCherry driven by promoter PK1L was not detectable due to the different localization of the

early transcription machinery in the infectious viral particles and the transfer plasmid in the cell.

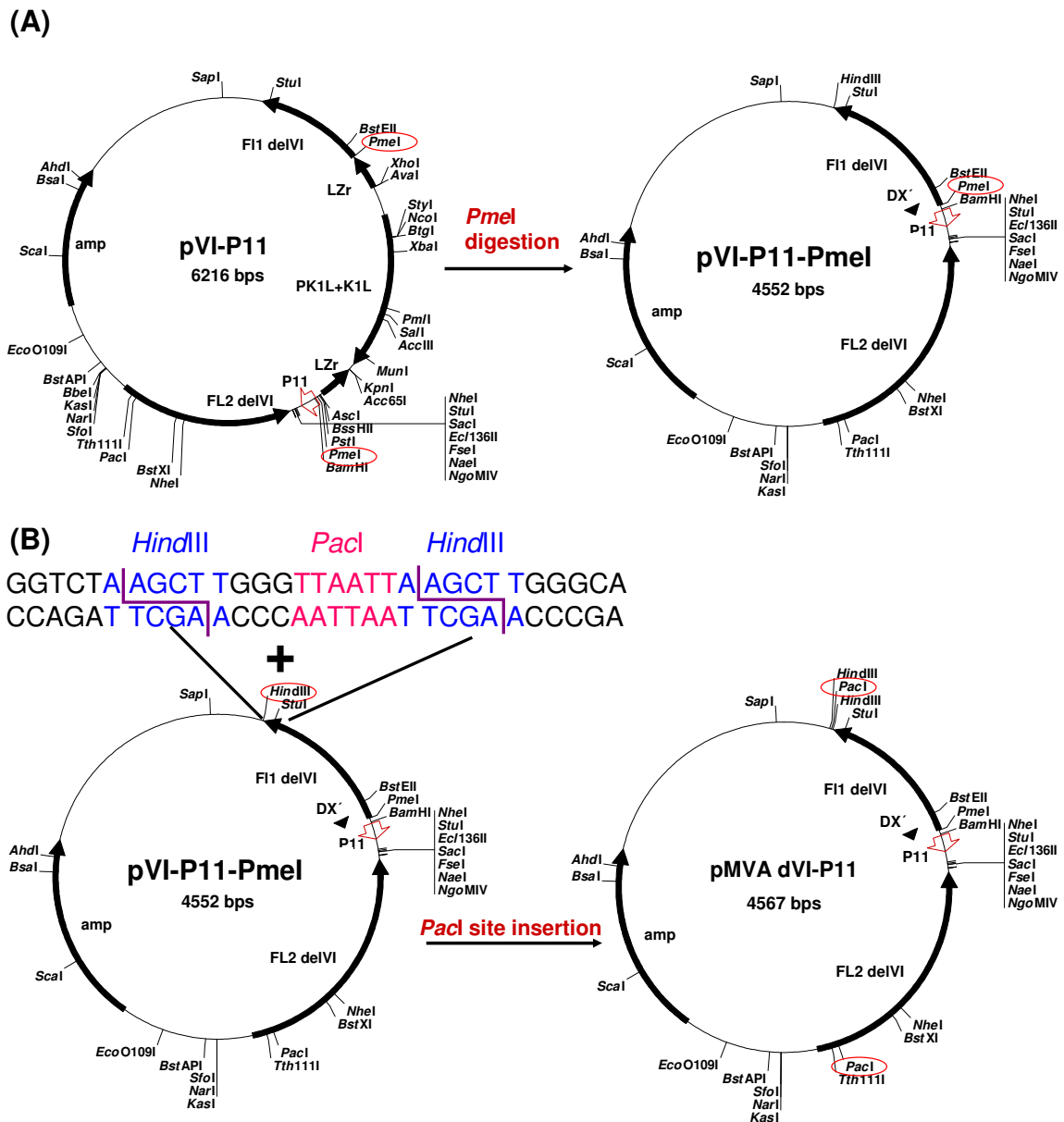


Figure 4.1. Schematic cloning strategy for the plasmid pMVA dVI-P11. A VV *K1L* gene with its promoter cassette was deleted by *PmeI* endonuclease cleavage from pVI-P11 plasmid, resulting in plasmid pVI-P11-PmeI (A). A *HindIII*-*PacI*-*HindIII* restriction sites containing DNA fragment was synthesized by PCR and digested by *HindIII*. The cut fragment was inserted into the *HindIII* cut plasmid pVI-P11-PmeI, resulting in plasmid pMVA-dVI-P11 which contained two *PacI* sites flanking the expression cassette close to or at the delVI flanks(B).

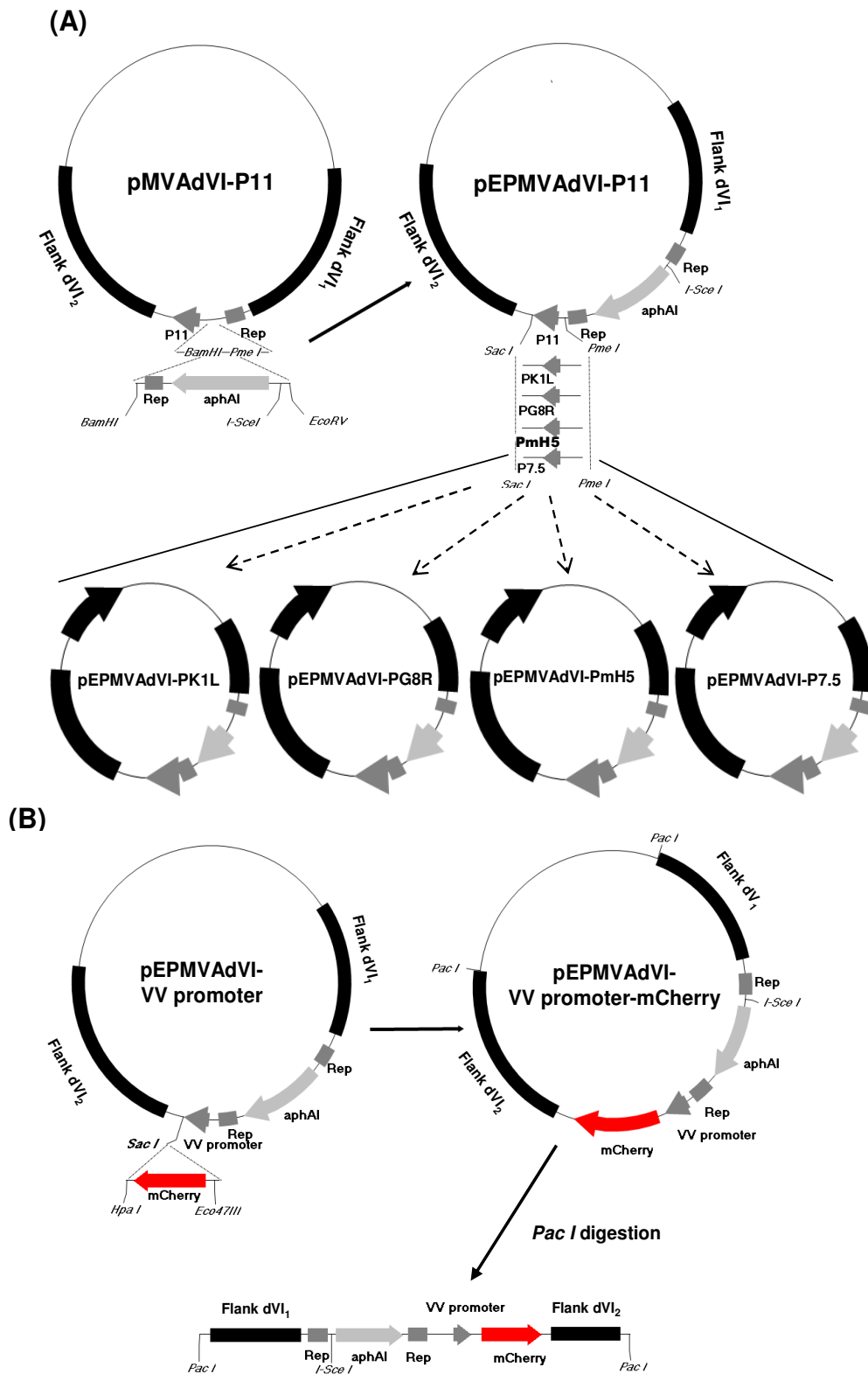


Figure.4.2. Schematic maps of vector transfer plasmids and cloning strategy. (A) To construct vector pEPMVAdVI-P11, an *aphAI-I-SceI* cassette was amplified from plasmid pEPKan-S and inserted into vector pMVAdVI-P11 after cleavage with *BamHI* and *PmeI*. Two identical 50 bp DNA sequences were flanking the *aphAI* gene. By exchanging the P11 promoter sequence with those from the other VV promoters

(Table 4.1) in vector pEPMVAdVI-P11 after cleavage with *SacI* and *PmeI*, transfer plasmid pEPMVAdVI-PK1L, pEPMVAdVI-PG8R, pEPMVAdVI-PmH5 and pEPMVAdVI-P7.5 were generated. (B) To generate the respective recombinant mCherry expressing transfer vectors, the mCherry ORF fragment was PCR amplified from pmCherry-N1, enzymatically cut and inserted into the *SacI* digested transfer vectors to bring mCherry expression under the control of each VV promoter respectively. *PacI* digestion of pEPMVAdVI-VVpromoter (pVV)-mCherry vectors was finally applied to generate the linearized insertion cassette for Red Recombination in *E.coli*.

Table 4.1. Promoter sequences and properties

Promoter	Activity ^a	Strength	Sequence ^{b,c,d}
PK1L	E	Weak	ccatgattaagattggctcttcggtggctgggtaccccctcccgatccgcatagccatgtatctactaatcagatctattagagatattattaattctgggcaaatgacaaaattataa AAAATGAAAAAATATA cactaattaGcgctcgtttcagacggatccattgctagatct – MCS
PG8R	IM	Moderate	t TAACTTTAAATAA ttacaaaaatt TAAA ggatccattgctagatct - MCS
P11	L	Strong	caatcaccactttcataittagaatatatgtatgtaaaaaatagggagaattcatgggggg TTTTT Tcctgcta TAAATTA gctagcaggcctggctaccggactc – MCS
P7.5	E/L (Constitutive)	Moderate	atcactaattccaaccaccgcttttatagtaag TTTTTcaccataaataaTAAATA caataattaattctcgt AAAAGTAGAAAAATATA ttctaatttattGcA cggt aaggaagtagaatcataaagaacagtgc – MCS
PmH5	E/L (Constitutive)	Very strong	gcaggtcagctt AAAAATTGAAAAATAAATA caaaaggttctt GA gggttggt TAAATTG aaagcgagaaataatcataaataagggtgactctagaggatcgatccattgctagatct – MCS

^a E - early, IM - intermediate, L - late.

^b Putative core elements are shown in bold capitals. Initiators are shown in boldface underlined.

^c In P7.5 and PmH5 promoters sequences, the initiators are corresponding to their nearest upstream early or late core elements.

^d Dashes indicate appendage of multiple clone sites (MCS)

4.2. Insertion of the transgene cassette in MVA deletion VI by Red Recombination

To create recombinant MVA_BAC, transfer vectors were cleaved at the *PacI* sites flanking FlankVI₁ and FlankVI₂. The linearized transfer cassette was subsequently transfected into GS1783 *E.coli* containing the MVA_BAC for Red Recombination (Fig. 4.3A). GS1783 is an artificially engineered *E.coli* strain. In its bacteria genomic DNA, the λ -red recombinase genes are under the control of a heat inducible promoter, while an *I-SceI* homing endonuclease gene is under the control of an L-(+)-arabinose inducible promoter. Besides, in the bacterial cytoplasm, a copy of MVA_BAC genome is harboured, containing a BAC-GFP cassette in the MVA deletion III region. This cassette consists of a mini-F sequence and a poxviral promoter controlled *gfp* gene (driven by the late *FP4B* gene promoter) and a

chloramphenicol acetyltransferase gene. After the 1st Red Recombination, the transfer cassette was recombined into MVA deletion VI. The correct integration was rapidly verified by a colony PCR covering the insertion cassette in MVA deletion VI (Fig. 4.3A). For the convenience of further MVA_BAC manipulations, we deleted the selective marker gene *aphAI*. Here, the BACs were treated with 1% L-arabinose to induce the *I-SceI* endonuclease gene expression which led to the formation of a genomic double-strand break adjacent to *aphAI*. Raising the temperature up to 42°C triggered the 2nd Red Recombination, which hereby excised the *aphAI* gene from the viral genome. This is the so-called *en passant* mutagenesis. The correct sequences were again confirmed by colony PCR, and the expected fragment size reduction was observed for both fragments spanning the whole dVI region and the regional *aphAI* gene (Fig. 4.3B). Both 1st and 2nd Red Recombination were highly efficient in that more than 90% of the colonies tested were correct. Moreover, the accuracy of the insertion region including promoter and mCherry ORF was further confirmed by DNA sequencing.

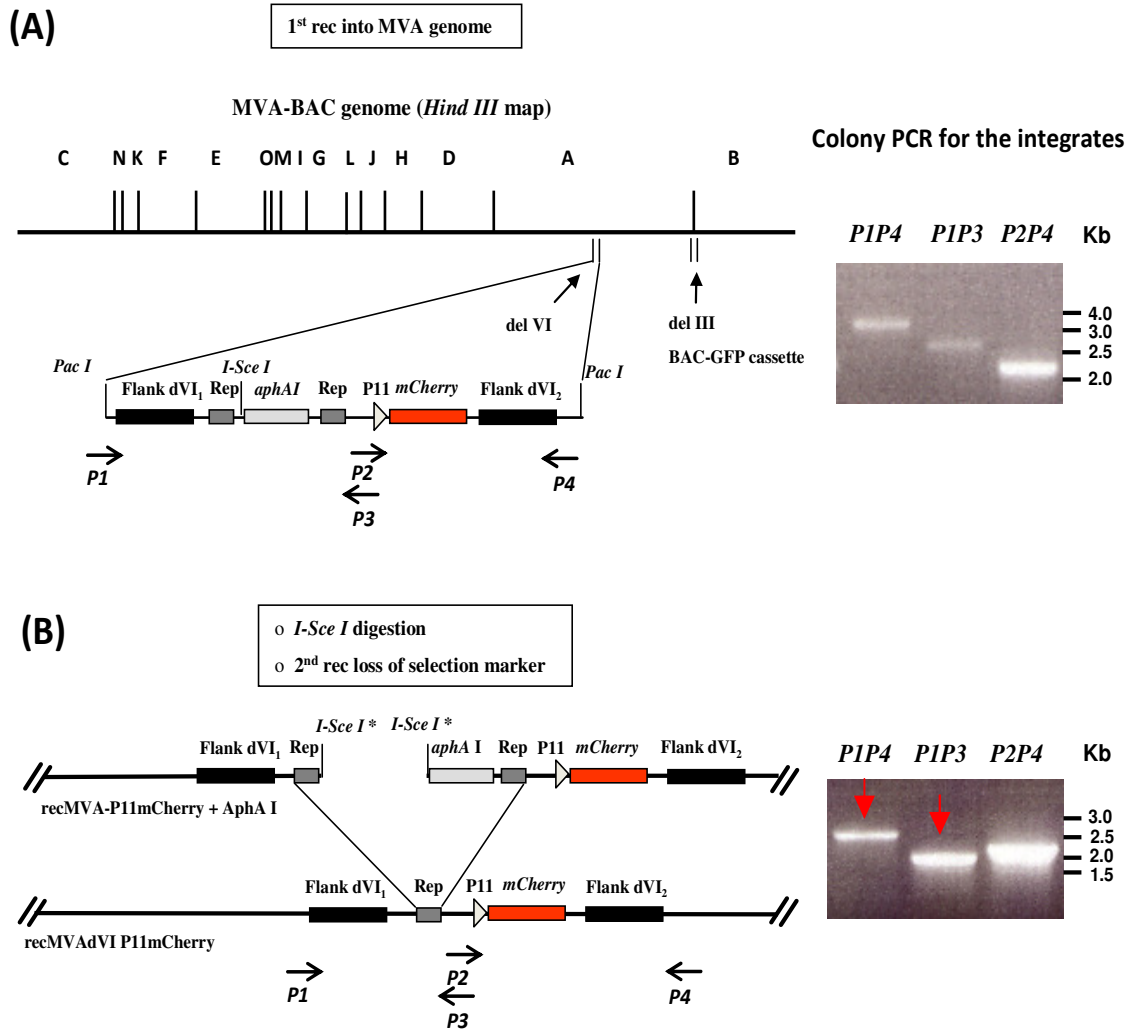


Figure 4.3. Targeting expression cassette into MVA deletion VI. P11 promoter is shown as a representative for other VV promoters. (A) Schematic map of the linearized P11-mCherry containing expression cassette which was transfected into GS1783 *E.coli*. The 1st Red Recombination inserted the cassette into the MVA deletion VI. Colony PCR for the correct integration denoted 3.8 kb, 2.9 kb and 2.2 kb fragments, which correspond to PCR products obtained by the primer combinations: P1+P4, P1+P3 and P2+P4. (B) Schematic map of 2nd Red Recombination showing *I-Sce I* cleavage and selective marker *aphAI* deletion. Colony PCR denoted 2.7 kb, 1.8 kb and 2.2 kb fragments, which correspond to PCR products obtained by the primer combinations: P1+P4, P1+P3 and P2+P4.

4.3. Generation of recombinant viruses by MVA_BAC recombineering

The recombinant MVA_BAC genomes were extracted from GS1783 *E.coli*. They were transfected to BHK-21 cells. Fowlpox virus (FPV) was used as helper virus for infection of non-permissive BHK-21 cells as previously described (Cottingham *et al.*, 2008). It provides the recMVA-BAC genome with the poxviral initial transcriptional

machinery to trigger the initiation of the replication cycle of the recMVA. There are two reported MVA_BAC strains used in our system: 1) One in which the BAC cassette containing GFP and the mini-F is always kept as a scar in the recombinant viral genome. 2) Another in which the BAC cassette can be efficiently eliminated from the genome due to an inverse-oriented sequence duplication between the selection marker and the bacterial replicon (so-called self-excising BAC) (Fig.4.3B) (Cottingham and Gilbert, 2010; Tischer *et al.*, 2007). We amplified the BAC containing recMVA in the BHK-21 cells which can be easily identified due to dual-fluorescence of both GFP and mCherry (Fig. 4.4A). Nevertheless, when growing the BAC self-excising recMVA, a sizable amount of recombinant viruses lost their BAC cassette from the deletion III locus after 3 rounds of amplification. This was indicated by a dramatical switch of dual-fluorescent populations to mCherry-only expressing populations (Fig. 4.4B). In order to obtain pure BAC-excised recMVA stocks, we subcloned mCherry-only expressing cells by plaque picking (Fig. 4.4B). Usually, 2 rounds were sufficient to get 100% BAC-excised recMVA. An alternative method for subcloning based on limiting dilution to obtain single clones was also performed for this purpose, preferably for constructs that do not contain reporter genes in the expression cassette. Since MVA has a higher virus yield when propagated in CEFs, we switched the amplification of recMVA from BHK-21 to CEFs. Given that the helper virus FPV could replicate in CEFs, it was necessary to measure whether FPV had been cleared from recMVA preparations before crude stocks were generated. Viral DNA was extracted for PCR analysis with specific primers for the fowlpox viral *P4b* gene (Table.2). We found that after more than 5 rounds of recMVA passaging in BHK-21 cells, FPV helper virus became undetectable (Fig. 4.6). The resulting recMVAs were further amplified, crude stocks produced and titrated by the TCID₅₀ method in CEFs. To confirm functionality, mCherry expression by different recMVA was detected in infected Hela cells by using fluorescent microscopy (Fig.4.5). A graphic overview for the MVA-BAC *en passant* workflow is presented in Appendix Fig.8.1.

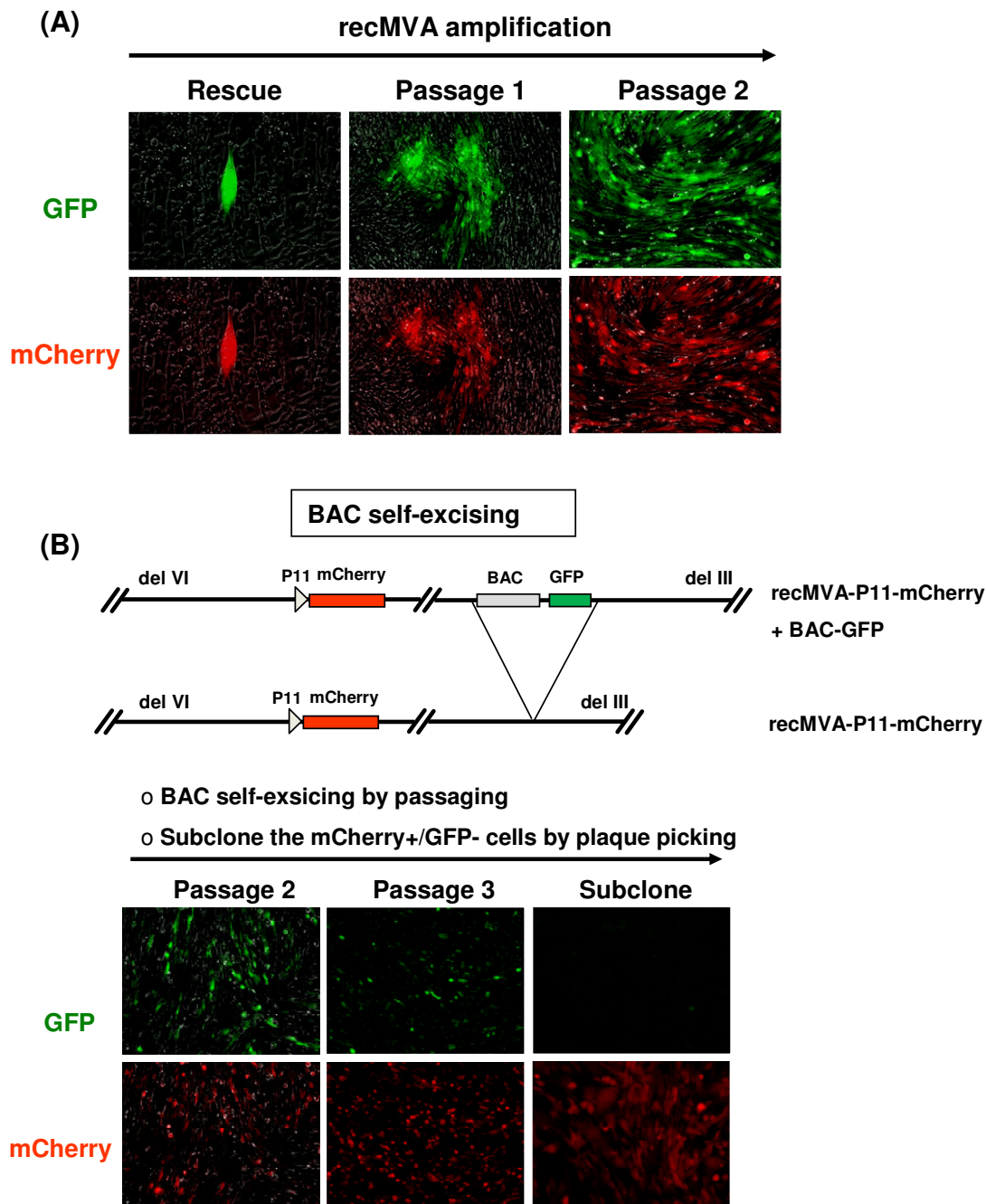


Figure 4.4. BAC rescue and amplification of the recombinant MVA. (A) The MVA-P11mCherry_BAC rescue was done as described in Materials and Methods. RecMVA were rescued in BHK-21 cells. After the 1st passage only some discrete cells were colored both, green and red. After re-plating, successfully rescued recMVA grew as plaques with dual-fluorescence of green and red and was amplified. (B) Schematic map of self-excising BAC. The BAC mini-F-GFP cassette was spontaneously lost from the viral genome when recMVA were passaged in CEFs. After more than 3 passages after the rescue, BAC-excised recMVA were obtained by 2 rounds of plaque picking of GFP-/mCherry+ cells. MVA-P11-mCherry_BAC strain was used as an example.

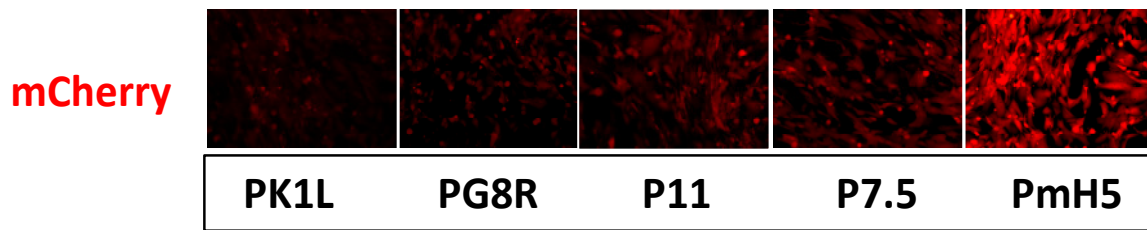


Figure 4.5. Representative pictures of mCherry expression in recMVA infected HeLa cells. HeLa cells were 2 days post infection with MVA-PK1LmCherry, MVA-PG8R-mCherry, MVA-P11-mCherry, MVA-P7.5-mCherry or MVA-PmH5-mCherry. mCherry was detected by fluorescent microscopy.

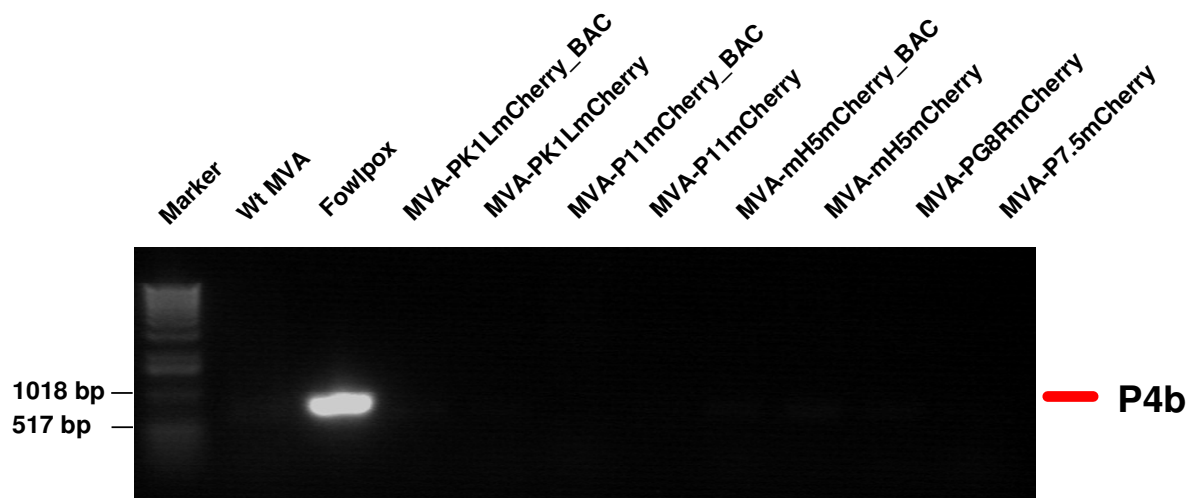


Figure 4.6. Elimination of helper virus in recMVA preparations. Detection by P4b gene-specific PCR analysis. BHK-21 cells were infected with indicated viruses for 72 hours at low MOI. Total viral DNA was extracted using the phenol-chloroform method. Fowlpox virus gene *P4b*-specific primers were used for PCR analysis of the indicated viral DNA (expected size of 811 bp). Resulting DNA fragments were analyzed in a 1% agarose gel.

4.4. Growth kinetics of BAC-derived recMVAs

It had been reported that in some cases mutant recMVA occur due to genomic instability which lost the ability to express foreign genes and may overgrow the original recMVA during the passages (Wyatt *et al.*, 2008; Wyatt *et al.*, 2009). Besides, it also needs to be investigated whether the stability of recMVA is influenced by the BAC cassette, since the BAC region may cause the virus attenuation *in vivo* (Wagner *et al.*, 1999). To address these concerns, we infected permissive CEFs with all of the BAC-derived recMVA to compare their replication ability with wild-type MVA. Multi-

step growth kinetics experiments were performed and the amount of viral progeny was determined at 0, 24, 48, 72 hours post infection (hpi). The titres of all recMVA were measured by counting mCherry positive cells, while the titre of wt MVA was determined by counting CPE (see section 3.3.5). The growth curves for all of the 7 recMVA expressing mCherry indicated comparable growth properties as wt MVA (Fig.4.7). Besides, also presence or absence of the BAC cassette in the recMVA showed the similar replication kinetics.

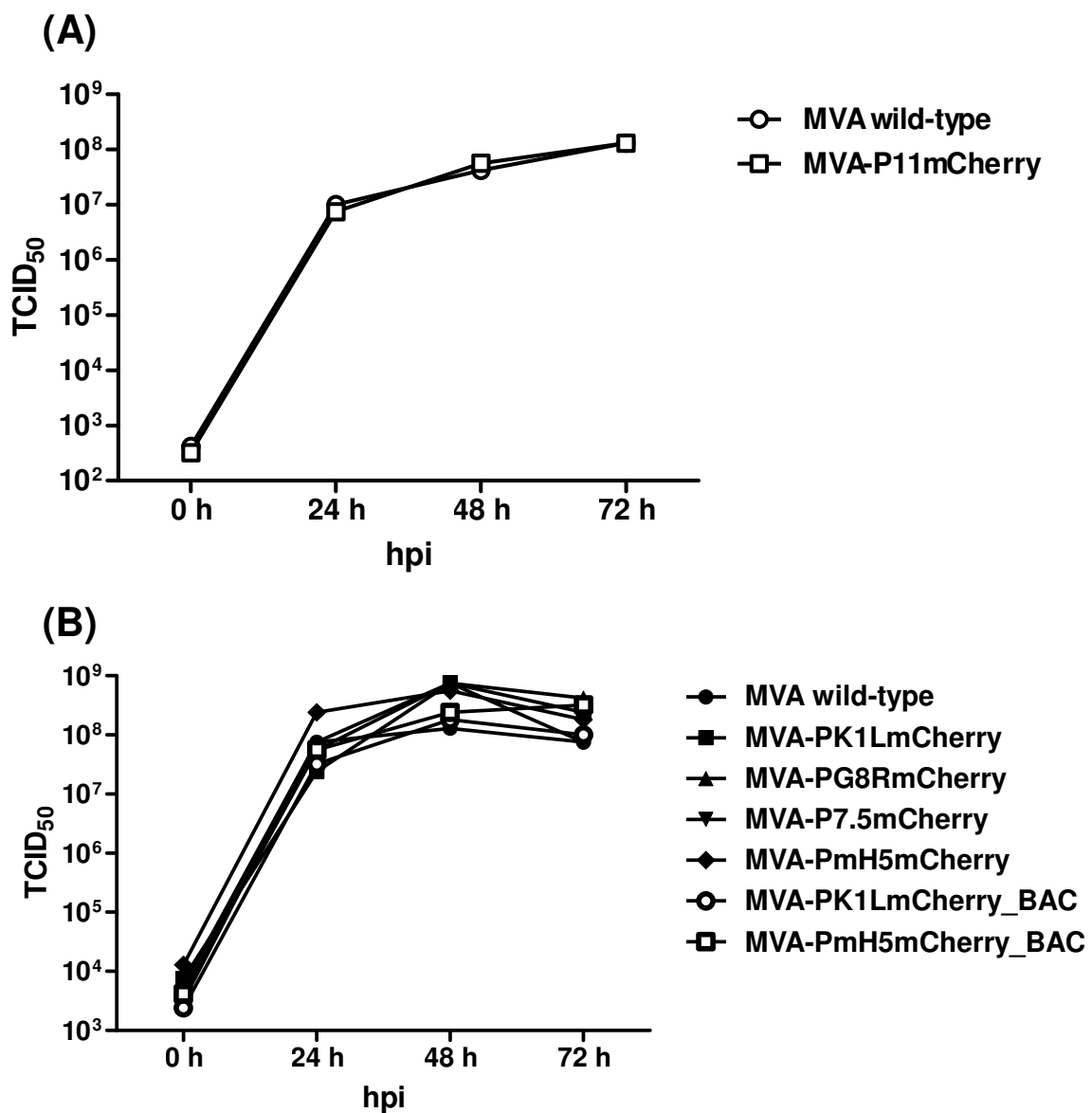


Figure 4.7. RecMVA showed normal viral growth kinetics. Permissive CEF cells were infected with various recMVA and harvested at the indicated time points. Multiple step growth curves were determined after titration of the respective TCID₅₀.

4.5. VV promoter-specific gene transcription kinetics

We generated recMVA expressing mCherry under the control of 4 different temporal classes of VV specific promoters (early, early/late, intermediate, late). In order to verify that the transgene had promoter-specific transcription kinetics, we gained total RNA from HeLa cells infected with these recMVA for 0 to 24 hpi and reversely transcribed them into cDNA for quantitative real-time PCR (qPCR). For a more precise control and discrimination of recombinant gene transcription, only BAC-excised recMVAs were used in this context. We employed the house keeping gene 18S ribosomal RNA (18S rRNA) as the reference gene for the qPCR because its transcription was unaffected in HeLa upon MVA infection (Frank Thiele/Korbinian Pröls personal communication). Besides, in order to precisely compare the transcription kinetics of the transgenes, we simultaneously used MVA endogenous genes representative for different temporal classes as control. Gene-specific primers were utilized for quantitative PCR (see Material section 2.7). Accordingly, *B8R* was used as early transcription control for mCherry expression in MVA-dVI-PK1L-mCherry infected cells. Subsequently, *G8R* and *H3L* were applied as intermediate and late transcription controls for mCherry expression in MVA-dVI-PG8R-mCherry- and MVA-dVI-P11-mCherry- infected cells, respectively. The transcription levels of these genes were evaluated by comparing with the transcription level of the corresponding 18S rRNA. Of note, we found that both, *B8R* gene driven by viral early promoter PB8R and mCherry driven by PK1L, initiated transcription consistently at 0.5 hpi and transcription levels were dramatically elevated within the first 4 hpi. The small spike of gene transcription seen at late time points (6 hpi) was likely due to some prolonged virus infection (Fig. 4.8A). Next, we tested the *G8R* intermediate gene promoter which was rarely investigated before. We observed that PG8R-driven mCherry transcription started at 1-2 hpi, and peaked at 5-6 hpi. This kinetics was almost identical to that of the endogenous *G8R* gene driven by the same promoter. Moreover, the strength of PG8R was similar with some biological variation which might be explained by the different genomic sites (authentic locus v.s recombinant deletion VI locus) (Fig. 4.8A). For the late promoter P11, the mCherry transcriptional

activity was first detectable at 2.5-3 hpi which was equivalent to that of the late gene H3L used as control. The maximum transcription levels for late genes mounted at 6-10 hpi (Fig. 4.8A). We then focused on the kinetics of the constitutive promoters P7.5 and PmH5. The PmH5 has been reported as a stronger VV promoter compared to P7.5. To evaluate their activity in our system, we checked the transcription properties of these two promoters. In agreement with early gene transcription of PB8R and PK1L, both promoters allowed for mRNA production as early as 0.5 hpi, but additionally had another elevated transcription period at later time at 6-10 hpi. Accordingly to the relative expression (compared to the corresponding 18S rRNA) PmH5 triggered a much more vigorous transcription of mCherry than P7.5 (Fig. 4.8B).

Taken together, 3 distinctly temporally active classes of mCherry transcription kinetics were observed for i) early and early/late promoters starting from 0-0.5 hpi (PK1L, P7.5 and PmH5); ii) intermediate promoter PG8R starting from 1-2 hpi; and later promoter P11 starting from 2.5-3 hpi. It has to be noted that PmH5 had the strongest early transcriptional efficacy (Fig. 4.8C).

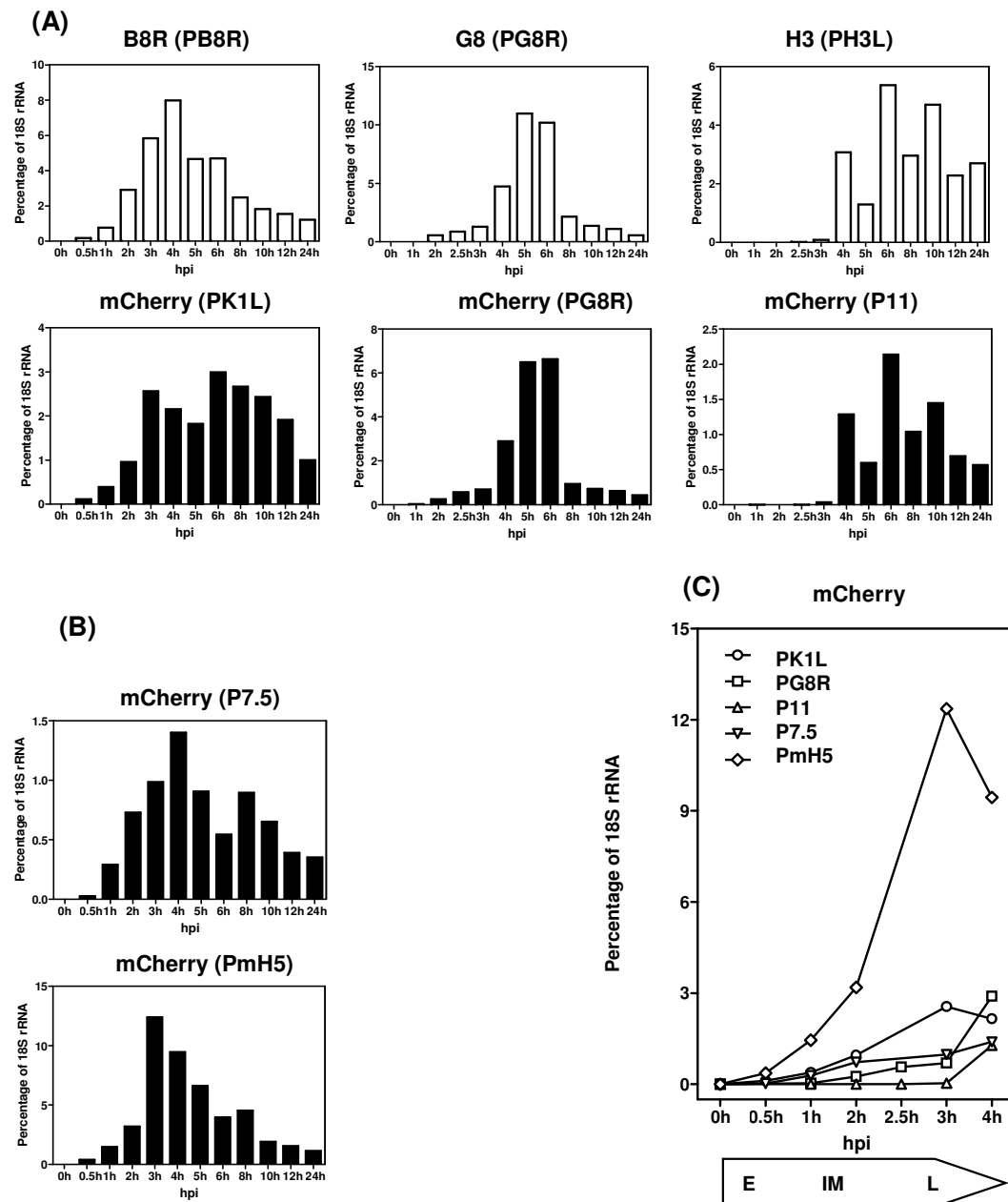


Figure 4.8. VV-promoter-specific transcription kinetics for recMVA expressing mCherry . Hela cells (5×10^5) were infected with respective recMVA at MOI 10 and harvested at indicated time points. Whole cell mRNA was extracted and reversely transcribed to cDNA with specific primer sets to detect mCherry or the internal viral gene control. Real-time PCR was carried out for each cDNA. Transcription kinetics is shown in (A) for MVA *B8R* - viral early gene control in MVA-PK1LmCherry infected samples; for MVA *G8R* - viral intermediate gene control in MVA-PG8RmCherry infected samples; and for MVA *H3L* - viral late gene control in MVA-P11mCherry infected samples. (B) Compares transcription kinetics for MVA-P7.5mCherry infected samples and MVA-PmH5mCherry infected samples. (C) Overlap of kinetics for the first 4 hpi for a detailed overview of the transcription of mCherry for all recMVA tested. Time course of promoter activity is shown. Each cDNA was triplicated for qPCR and the average value was counted for evaluation. Results for a representative experiment of three are shown. E = early, IM = intermediate, L = late.

4.6. VV promoter-specific kinetics of target protein synthesis

To extend our findings from mRNA level to protein level, we sought to evaluate the kinetics for target protein synthesis as determined for mCherry driven by various promoters in recMVA. The relative mean fluorescent intensity (MFI) of mCherry in infected Hela cells was counted during 0 to 20 hpi by flow cytometry. From the panoramic point of view, early/late promoter PmH5 had the most vigorous mCherry expression and double-peaked early (6 hpi) and late (12 hpi). Late promoter P11 was strong as well and peaked late at 16 hpi. Early/late promoter P7.5 showed moderate promoter strength in both, early and late phase, and mCherry expression peaked at early (5-6 hpi) and late (12 hpi) time points. In contrast, PK1L and PG8R showed relatively weak promoter strength. PK1L mounted mCherry expression at 4 hpi (Fig. 4.9). In addition, focusing on the expression initiation, early promoter PK1L as well as early/late promoters P7.5 and PmH5 allowed for mCherry expression detectable as early as 1 hpi. PG8R and P11 initiated mCherry expression at 2-3 hpi. Unlike gene transcription, it was hardly to dissect the temporal difference between PG8R and P11. A possible explanation is that PG8R has a relatively weak promoter strength, thus the fluorochrome needs to be accumulated for a period of time to meet the threshold of detection. Due to posttranscriptional translation and subsequent maturation of mCherry (Merzlyak *et al.*, 2007), we observed an overall delay for the kinetics of protein expression compared to mRNA transcription (Fig. 4.9).

Our experimental data showed 3 phases of mCherry expression: At 0-4 hpi phase I in which viral gene expression started according to the respective promoter activity and early promoter activity peaked; at 4-12 hpi phase II in which early/late, intermediate and late promoter activity continued to promote gene expression; at 12-20 hpi and later phase III in which mCherry expression plateaued and even ceased because of MVA-induced cell death (Fig. 4.9).

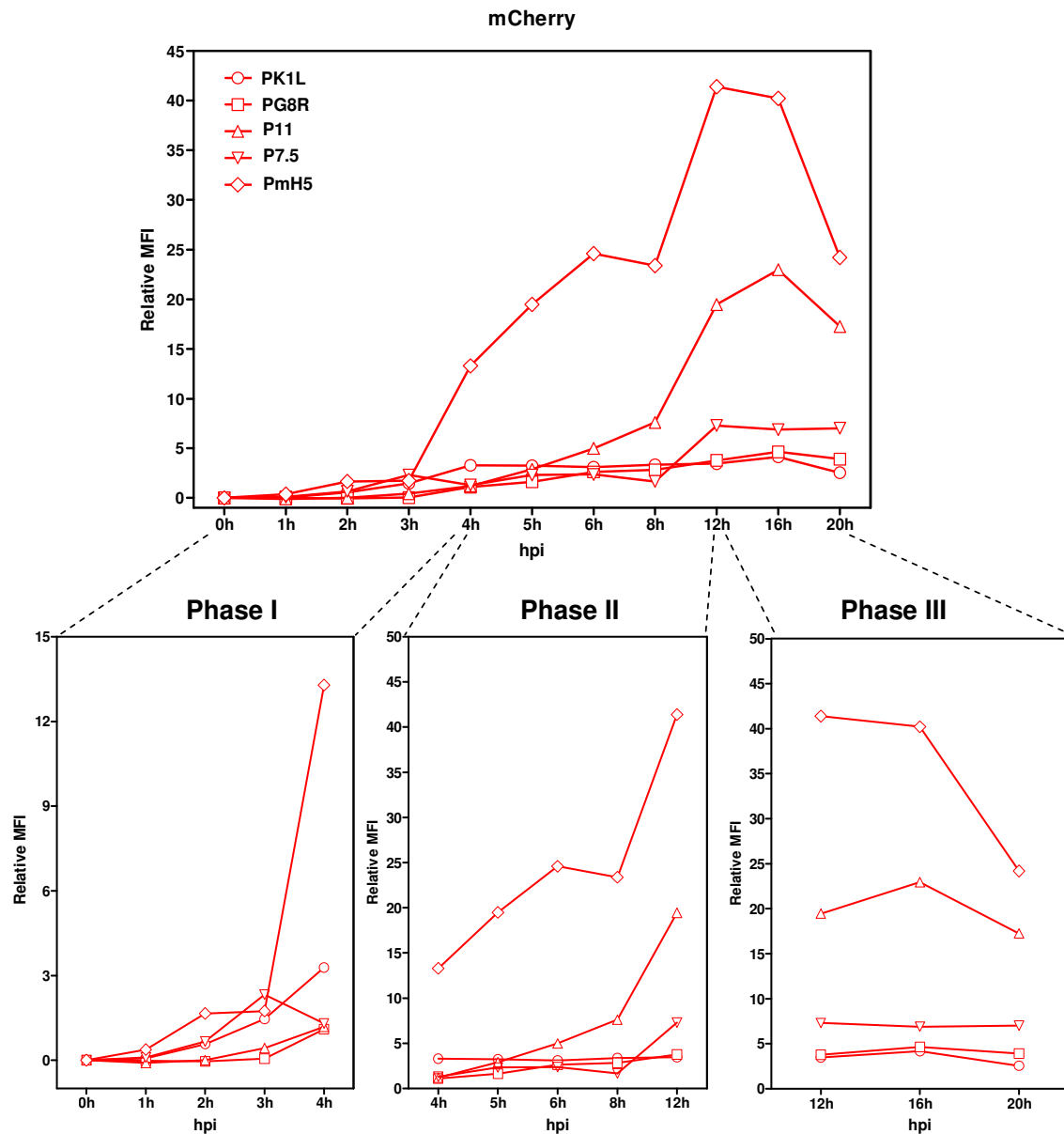


Figure 4.9. RecMVAs showed the VV-promoter specific protein expression. HeLa cells (5×10^5) were infected with recMVA at MOI 10 and harvested at indicated time points. mCherry expression was detected by FACS analysis (absorbance at 600 nm - 630 nm). MFI in infected cells was determined for mCherry expression by FlowJo v9.4.10. The MFI at each time point had been calibrated to the MFI in 0 hpi for each recMVA. Results for a representative experiment of two are shown.

4.7. Construction and generation of MVA-N1L and related recombinant or revertant viruses using the two-step red-mediated recombination system

Vaccinia virulence gene *N1L* is highly conserved among orthopoxviruses, and is able to impair the host innate immunity. The *N1L* gene in VV consists of 396 bp nucleotides. However, in the MVA genome *N1L* contains at the C-terminus a frame shift mutation at position nt 266, which results in a pre-mature stop codon leading to a 83-nucleotide truncated and potentially inactive protein (Fig. 1.3). To investigate the function of *N1L* gene product, we orthotopically replaced the C-terminally fragmented 71 nucleotides with 83 nucleotides of wt *N1L*. The resulting MVA-N1L contains a full length *N1L* ORF in its authentic locus in the MVA genome (Figure 4.10).

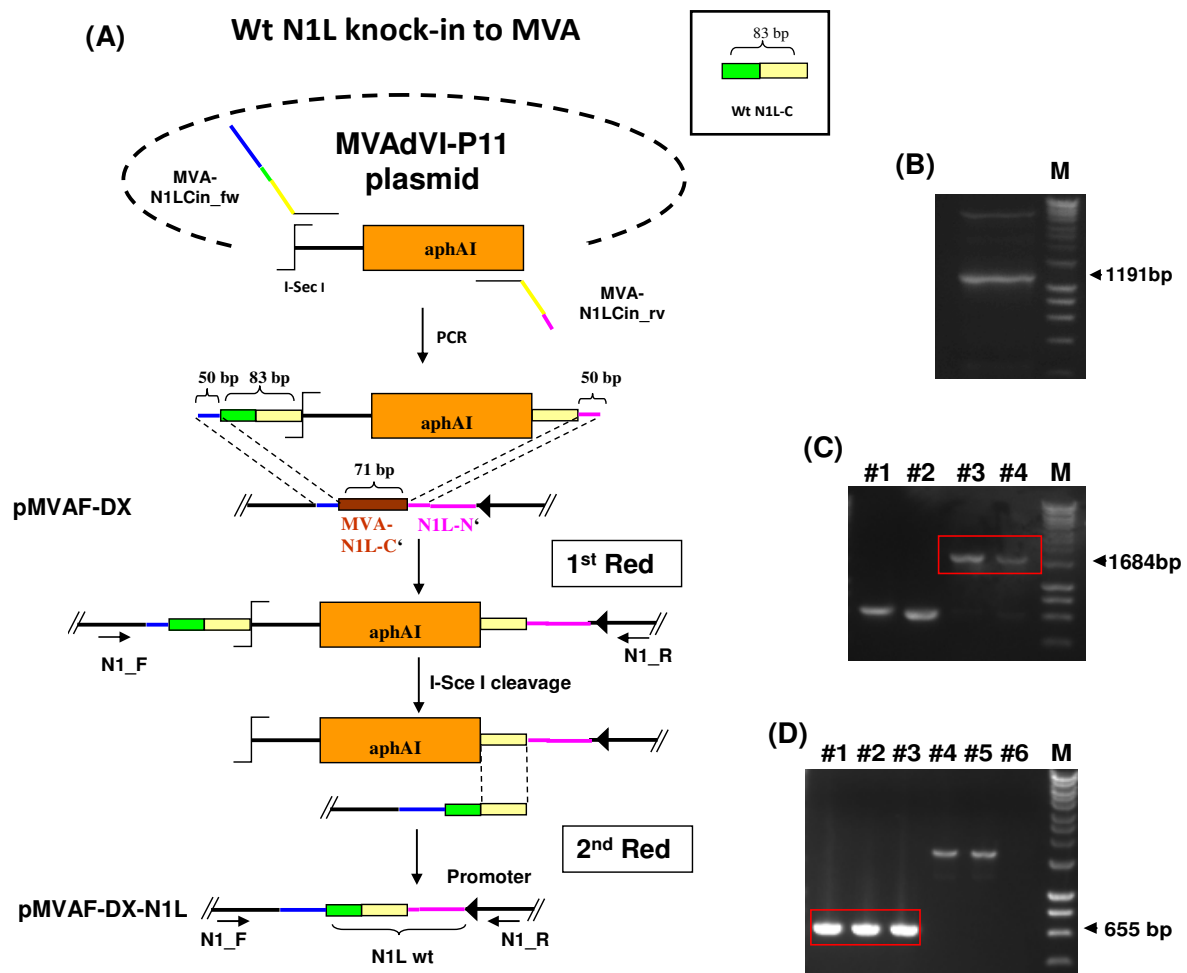


Figure 4.10. Construction of MVA-N1L by BAC *en passant*. Schematic map of the cloning strategy is depicted in (A). MVAdVI-P11 plasmid was used as PCR template and amplified by primers pair MVA-N1LCin_fw and MVA-N1LCin_rv. The expected PCR product (1191 bp) was used as linearized DNA for homologous recombination

in GS1783 *E.coli* harbouring the MVA_BAC genome (B). Primers N1_F and N1_R contained sequences of the C terminus and the putative *N1L* promoter adjacent region. Colony PCR was used to identify clones with correct integration. Clones #3 and #4 were correct 1st Red Recombinants (C). Clones #1, #2 and #3 were correct 2nd Red recombinants (D). Sequence colour blue indicates MVA backbone; Green indicates *N1L* C' terminal sequences; Yellow indicates *N1L* sequences identical for both primers; Pink indicates *N1L* N' terminal sequences.

Since MVA-N1L can be used for further manipulation, we subsequently used it to generate recMVA expressing OVA named MVA-OVA-N1L or a revertant from MVA-OVA-N1L in which the original *N1L* from MVA has been reconstituted (MVA-OVA-revΔ*N1L*) (Figure. 4.11). Briefly, the full-length of OVA ORF was amplified by PCR and inserted into the transfer plasmid pEPMVAdVI-P7.5 to be controlled by the P7.5 promoter as described before. Next, the P7.5-OVA cassette was recombined into MVA-N1L_BAC by the two-step BAC- *en passant* system as described before. Based on MVA-OVA-N1L_BAC, the MVA-OVA-revΔ*N1L* BAC-genome was subsequently created by reconstituting the C-terminal 83- nucleotides of functional *N1L* with the C-terminal 71-nucleotides of the MVA ortholog. As the result, we created OVA expressing recMVA which regained the truncated *N1L* gene under the transcriptional control of its authentic promoter. The recombinant viruses were then rescued with the help of RFV in BHK-21 cells and amplified in CEFs. The integrity of *N1L* and its ortholog including their putative promoters were further confirmed by sequencing the respective genomic regions in all of the recMVA.

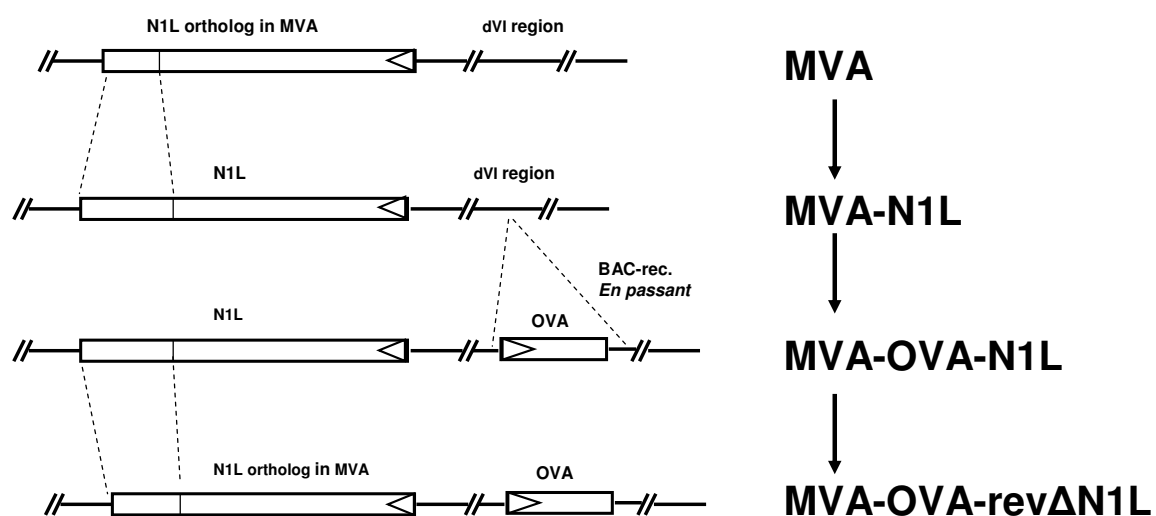


Figure 4.11. Construction of MVA-N1L recombinant and revertant viruses. The generation of MVA-N1L was described above. Based on the MVA-N1L-BAC genome, we inserted the OVA gene into deletion VI region of MVA (Under the control of P7.5 promoter) and generated the MVA-OVA-N1L. Based on MVA-OVA-N1L, we reversely deleted the 83 bp of the N1L C-terminus and replaced it with the C terminal 71 bp of N1L ortholog from MVA, resulting MVA-OVA-recΔN1L.

4.8. MVA-N1L and related recMVA show comparable growth kinetics

To determine whether the knock-in, recombinant or revertant viruses are affected in growth, multiple-step viral growth kinetics were performed. Permissive CEF cells were infected with MVA-N1L, MVA-OVA-N1L and MVA-OVA-recΔN1L and compared to wild-type MVA and MVA-OVA. As shown in Fig. 4.12, MVA-N1L, MVA-OVA-N1L and MVA-OVA-recΔN1L had comparable growth ability to control viruses, which indicates that genetic reconstitution and genome manipulation did not influence viral replication and growth.

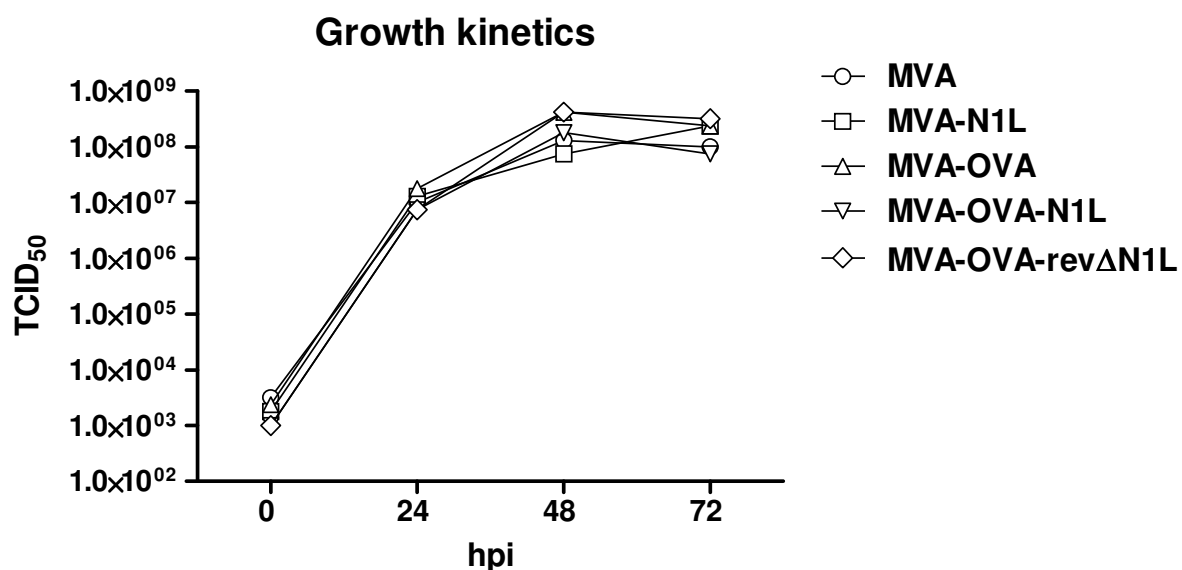
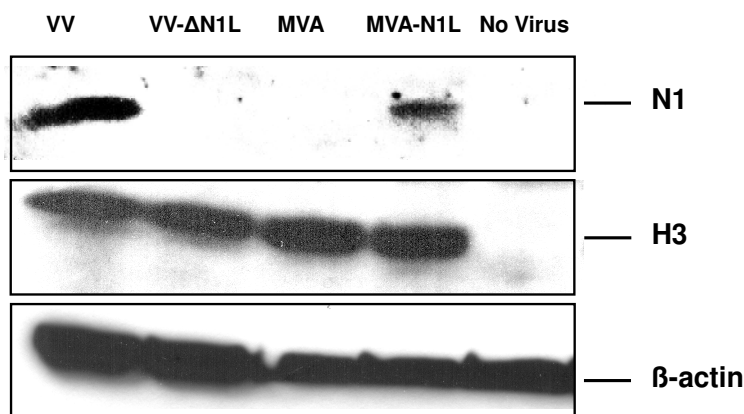


Figure.4.12. RecMVA showed normal viral growth kinetics. Permissive CEF cells were infected with the indicated viruses (MOI of 0.01) and harvested at indicated time points. Viral titres were determined by titration (TCID₅₀) and multiple step growth curves were established.

4.9. Western blot analysis of N1 and OVA synthesis upon recMVA infection

To confirm the presence and absence of *N1L* gene expression in MVA-N1L and VV- Δ N1L, we monitored the N1 protein synthesis in infected Hela cells. VV and MVA infections were used as positive and negative control, respectively. In agreement with our expectations, we observed that N1 was detectable in MVA-N1L- and VV- infected cell lysates using a polyclonal antibody that recognizes the C terminus of the protein, whereas it was not found in VV- Δ N1L and MVA-infected cell lysates (Fig. 4.13A). Compared to VV, N1 expression levels in MVA-N1L were weaker (Fig. 4.13).

(A)



(B)

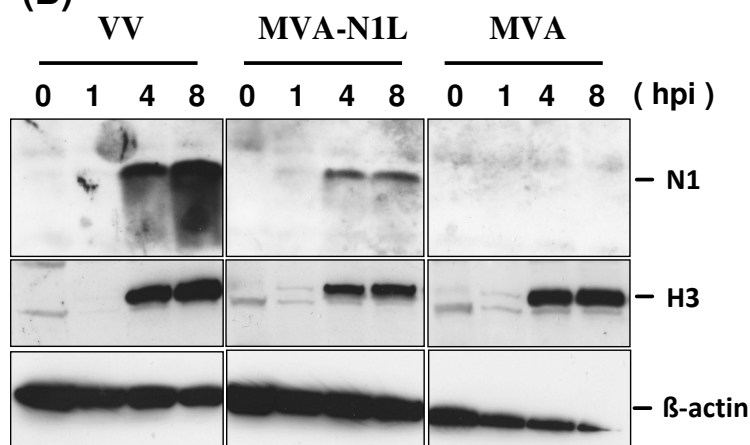


Figure.4.13. Expression of *N1L* in Hela and murine BMDCs infected by MVA-N1L. (A) Western blot analysis of Hela cells (2×10^6) infected with VV, VV- Δ N1L, MVA or MVA-N1L at MOI 5, or mock. (B) Western blot analysis of GM-CSF-BMDC (2×10^6) infected with indicated viruses at MOI 20 or mock. Whole cell lysates were prepared. Proteins were subjected to SDS-PAGE. Immunoblot was performed using mouse polyclonal anti-N1 antibody (A) or monoclonal anti-N1 (7E5) antibody (B). H3 and β -actin were used as loading control.

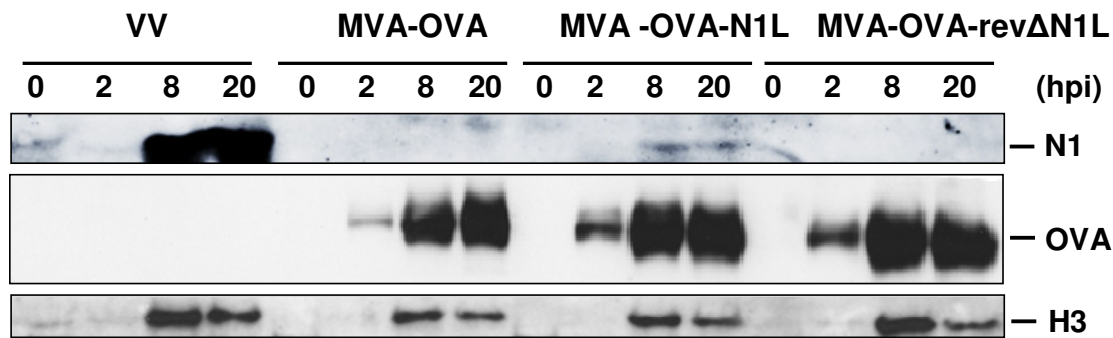


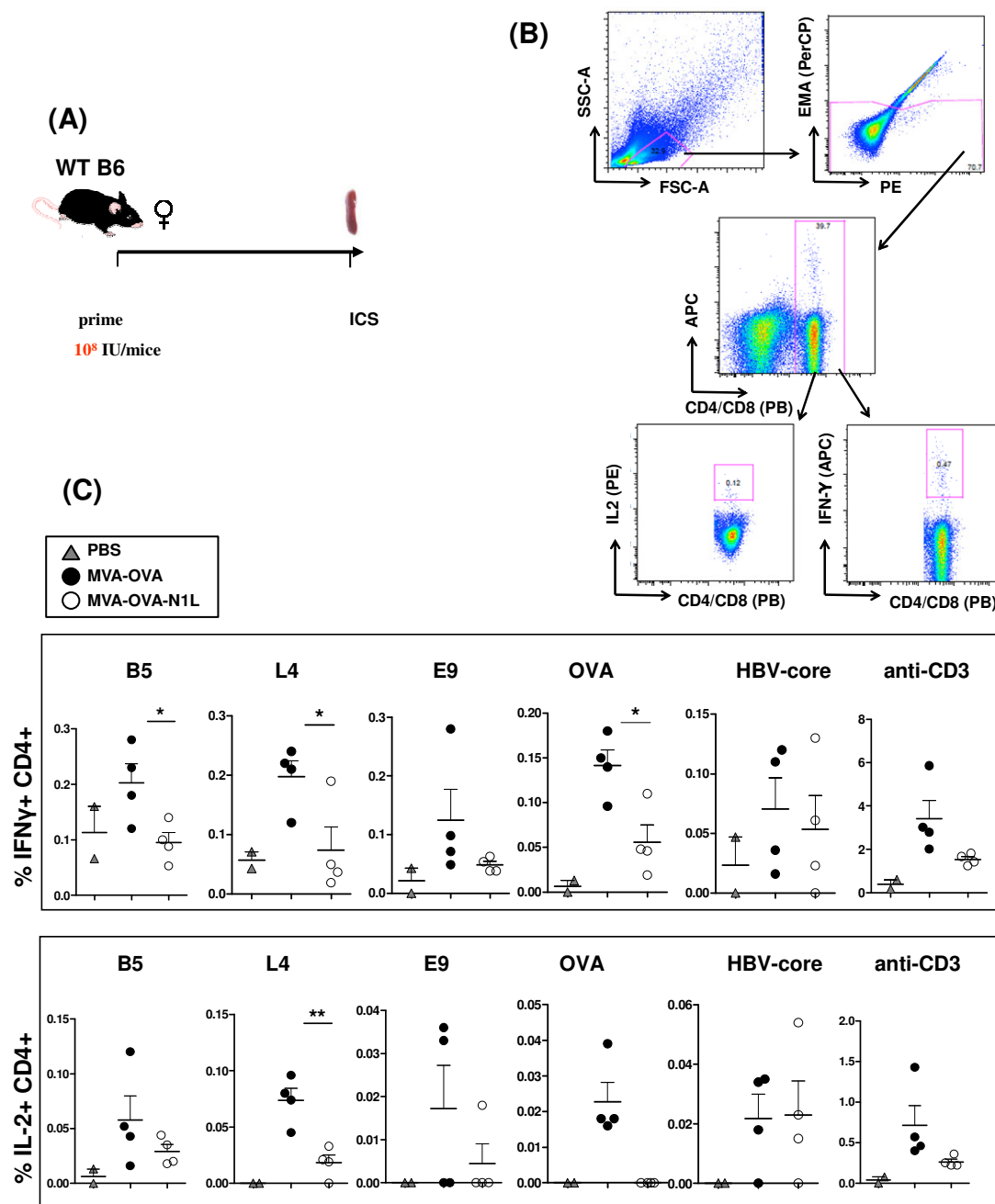
Figure.4.14. Expression of N1 and OVA in murine BMDC infected with MVA-OVA-N1L. Western blot analysis of GM-CSF-BMDC (2×10^6) infected with indicated viruses at MOI 20 or mock. WT VV was used as N1-positive and OVA-negative control. MVA-OVA was used as N1-negative and OVA-positive control. Whole cell lysates were prepared. Proteins were subjected to SDS-PAGE. Immunoblot using mouse monoclonal anti-N1 antibody (7E5) (N1), mouse polyclonal anti-OVA antibody (OVA) or anti-H3 polyclonal rabbit serum (H3).

In order to address the immune-relevant questions related to this gene, we were interested in expressing N1 in APCs. Conventional DC (cDC) represent one of the major antigen presenting cells (APCs). Cell lysates from MVA-N1L infected GM-CSF-derived murine BMDCs were analyzed by western blot. VV and MVA were used as positive and negative controls, respectively. In agreement with our expectation, we observed that N1 was detectable after 1 hpi in the lysates, and corresponded to a band seen in VV-infected BMDC lysates (Figure. 4.13B). Next, in order to verify that 1) both N1 and OVA proteins were expressed in MVA-OVA-N1L-infected BMDC and 2) N1 protein synthesis was abrogated in MVA-OVA-revΔN1L-infected BMDC, western blot analysis was carried out (results shown in Fig. 4.14). Consistently, we observed N1 expression in VV and MVA-N1L-OVA samples, whereas the protein was undetectable for MVA-OVA and MVA-OVA-revΔN1L. Moreover, the presence or absence of OVA in the corresponding viruses was confirmed as well. Taken together, we demonstrated that all of the viruses tested had the expected target protein expression profile, therefore were eligible for the following assays.

4.10. N1 impairs MVA-induced T cell priming

N1 has been reported as an innate immunomodulator of VV. However, little is described about its role in adaptive immunity. We asked whether N1 could impact MVA-elicited T cell responses. A proof of concept experiment was carried out in a murine infection model to compare T cell responses induced by the *N1L* knock-in

MVA and wild type MVA. Intracellular cytokine staining (ICS) and subsequent FACS analysis were used for this purpose. Since intracellular staining of cytokines was conducted with saturating concentrations of fluorochrome-conjugated antibodies, the specific increment of mean fluorescence intensity can be an indicator of relatively increased amounts of synthesized cytokines per cell. On day eight post vaccination, ICS analysis of splenic T cell activation was carried out after *ex vivo* stimulation with I-A^b- or H-2^b-restricted peptides (Fig.4.15A). Gating strategy is shown in Figure 4.15B for the measurement of IFN γ and IL-2 production of T cells. Interestingly, for CD4⁺ T cell priming, we observed that MVA-OVA-N1L induced lower frequencies of MVA vector- and OVA- specific cytokine producing Th1 cells as indicated by the



(D)

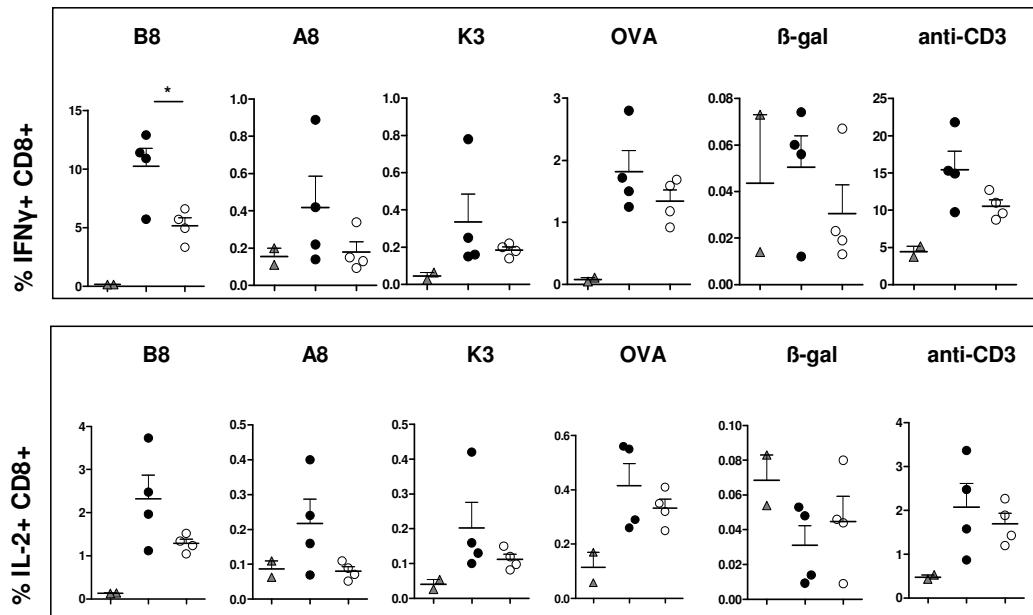


Fig.4.15. N1 impairs MVA-induced CD4+ and CD8+ T cell priming. Groups of C57BL/6 mice (n=2-4) were vaccinated i.p with 10^8 TCID₅₀ of MVA-OVA, MVA-N1L-OVA or PBS as control. MVA vector- and OVA- specific CD4+ and CD8+ T cell responses in the spleen were analyzed on day 8 post infection by intracellular cytokine staining (ICS) as schematically shown in (A). The gating strategy (B). Percentage of CD4+ T cells producing IFN γ (upper panel) or IL-2 (lower panel) (C). Percentage of CD8+ T cells producing IFN γ (upper panel) or IL-2 (lower panel) (D). Data are means \pm SE.. * P<0.05. Results for a representative experiment of two are shown.

diminished percentage of IFN γ and IL-2 producing populations (Fig.4.15C). For CD8+ T cell priming, a significant impairment of B8R-specific T cell responses (IFN γ and IL-2) was observed in MVA-OVA-N1L vaccinated mice, while only a marginal impact on other antigen-specific CD8+ T cells (A8R, K3L and OVA) could be observed (Fig.4.15D).

To preclude the possibility that the inhibitory effect of N1L knock-in MVA shown above was caused by other genetic mutations within MVA-OVA-N1L which may have occurred in the process of generating the recombinant virus, we included MVA-OVA-rev Δ N1L vaccinated mice as a control (Fig.4.16A). On day eight post vaccination, The ICS analysis for splenic T cell activation showed that, consistently, MVA-OVA-N1L elicited the lowest frequencies of MVA vector- and OVA- specific cytokine producing Th1 cells (IFN γ and IL-2). The marginal difference between the groups immunized

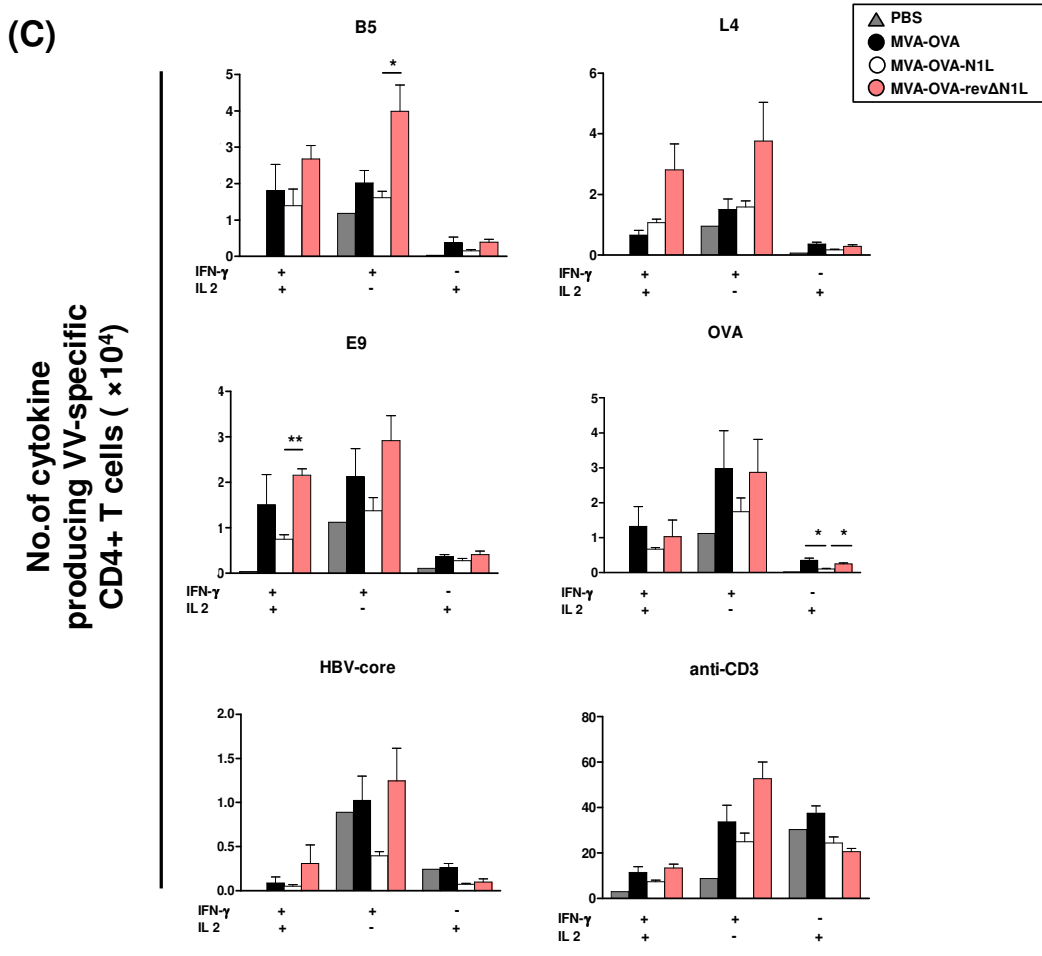
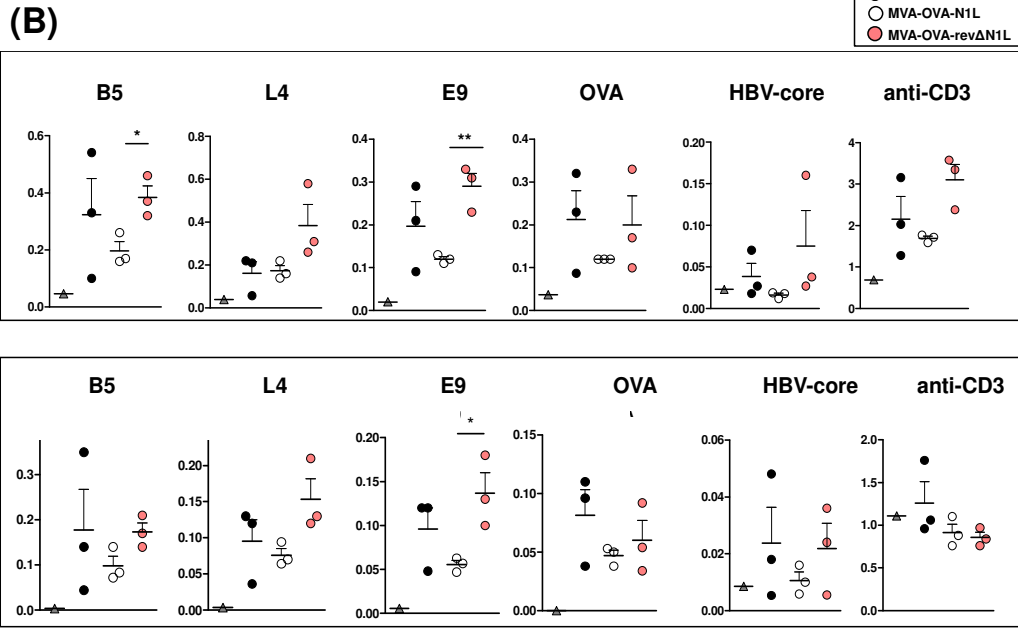


Fig. 4.16. N1 impairs MVA-induced CD4+ T cell priming. Groups of C57BL/6 mice (n=3, mock group n=1) were vaccinated i.p. with 10^7 TCID₅₀ of MVA-OVA, MVA-OVA-N1L, MVA-OVA-revΔN1L or PBS (as mock). MVA vector- and OVA- specific CD4+ T cell responses in the spleen were analyzed on day 8 post infection by intracellular cytokine staining (ICS) as schematically shown in (A). Percentage of CD4+ T cells producing IFN γ (upper panel) IL-2 (lower panel) (B). Number of MVA vector- and OVA-specific cytokine producing CD4+ T cells are indicated for each spleen for IFN γ +IL-2+, IFN γ +IL-2- or IFN γ -IL-2+ populations (C) Data are means \pm SEM. * P<0.05; ** P<0.01. Results for a representative experiment of one are shown.

with MVA-OVA and MVA-OVA-N1L was likely due to the weak immunogenicity in a single mouse shown in the MVA-OVA vaccinated group (Fig.4.16B). To determine whether N1 in MVA also impacts the amount of activated Th1 cells, we counted the absolute number of splenic CD4+ T cells in each group after short peptide restimulation. Consistent with what we found in frequency, diminished numbers of IFN γ +, IL-2+ and cytokine double-positive Th1 cells were observed in the group of MVA-OVA-N1L immunized mice (Fig. 4.16C). These results suggested that N1 protein may play an inhibitory role in the priming of IFN γ -secreting Th1 cells. To evaluate the impact on CD8+ T cell priming in mice vaccinated with the N1 knock-in MVA, a comparable ICS assay was performed for CD8+ T cell responses. Interestingly, in line with what has been shown in figure 4.15, we found that unlike its ubiquitous inhibitory effect on Ag-specific CD4+ T priming, N1 weakened mainly the immunodominant CD8+ T cell response against a peptide from MVA B8 protein (Fig 4.17B). There was evidence that both, frequency and number of B8R-specific CD8+ T cell were highest in MVA-OVA-revΔN1L vaccinated mice, which was shown by the upregulation of both IFN γ and IL-2. In contrast, MVA-OVA-N1L elicited a lower frequency and number. Nevertheless, other subdominant Ag-specific CD8+ T cells were hardly influenced by the presence of N1. A8R-, K3L-, OVA- specific CD8+ T cells showed no obvious difference in their activation level (Fig 4.17B,C). It has to be mentioned that for B8R-specific CD8+ T cell activation, MVA-OVA and MVA-OVA-N1L vaccinated mice exhibited only marginal differences (Fig 4.17B,C). This was possibly due to the lower dose (10^7 TCID₅₀), since other independent experiments had shown a significant difference when the virus inoculum was increased to 10^8 TCID₅₀ (Fig 4.15D).

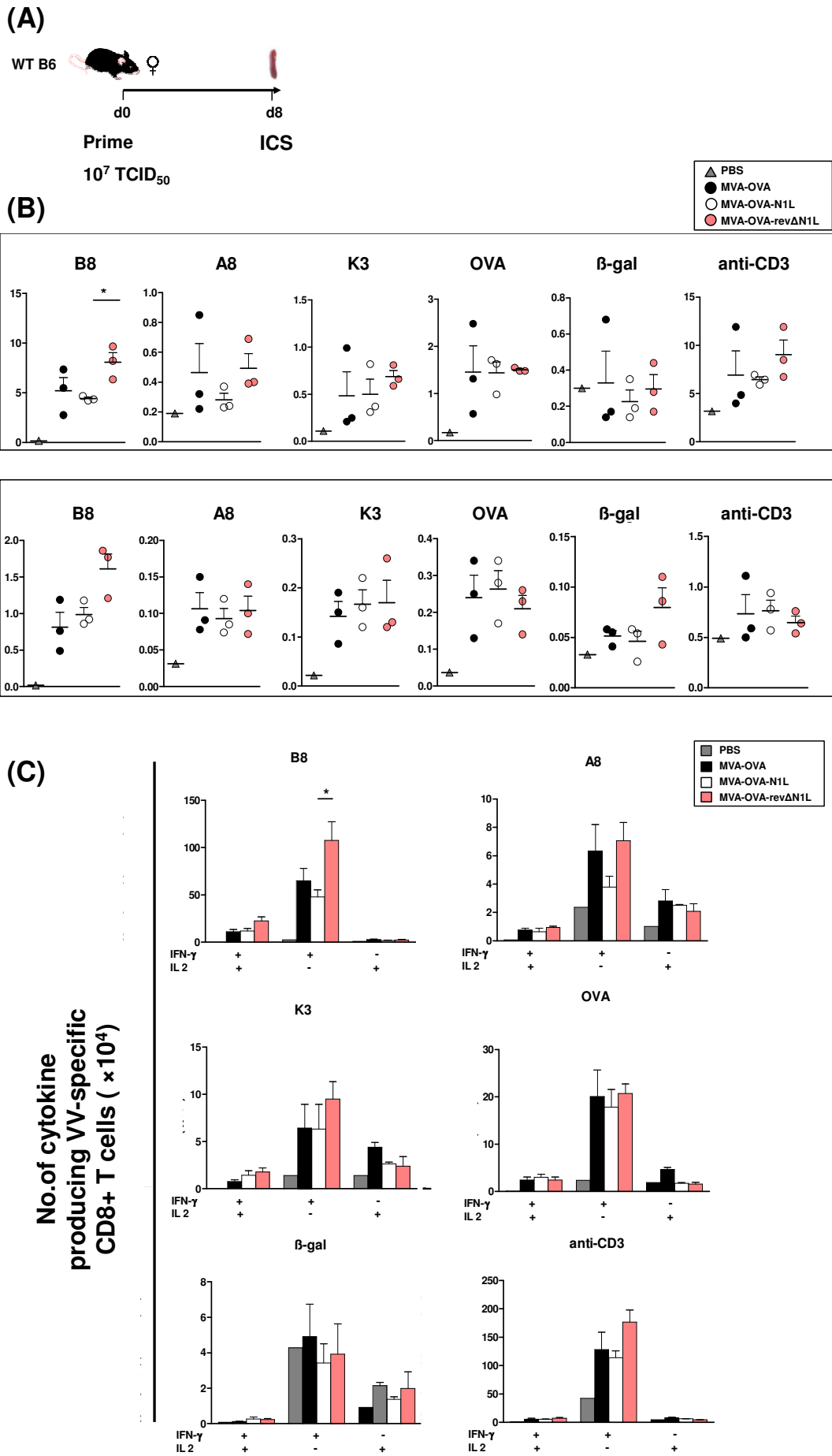


Fig.4.17. N1 impairs MVA-induced specific CD8+ T cell priming against the immunodominant B8R epitope. Groups of C57BL/6 mice (n=3, mock group n=1) were vaccinated i.p. with 10^7 TCID₅₀ of MVA-OVA, MVA-OVA-N1L, MVA-OVA-revΔN1L or PBS (as mock). MVA vector- and OVA- specific CD8+ T cell responses in the spleen were analyzed on day 8 post infection by intracellular cytokine staining (ICS) as schematically shown in (A). ICS assay and FACS analysis. Percentage of antigen-specific cytokine producing CD8+ T cells. The upper and lower panels indicate IFN γ and IL-2 producing cells, respectively (B). Number of MVA vector- and OVA- specific cytokine producing splenic CD8+ T cells (C). Data are means \pm SEM, * P<0.05. Results for a representative experiment of one are shown.

Since the *B8R* gene product accounts for up to the half of the total VV-specific CD8+ T cells, it clearly dominates the immune response against VV in C57BL/6 mice (Tschärke *et al.*, 2005). According to this hypothesis, our finding suggests that MVA-OVA-N1L suppresses the CD8+ T cell priming by mainly impairing the immunodominant B8R-specific T cell priming rather than one against subdominant epitopes.

4.11. Interference with IFN-I signalling inhibits T cell priming after MVA-OVA-N1L vaccination

N1 has been proven to be able to suppress the type I interferon induction by interfering with IRF3 activation (Dai. *et al.*, 2014; DiPerna *et al.*, 2004) . Given that IFN-I can promote naive CD4+ T cell differentiation towards IFN γ -secreting Th1 cells, and increase the IFN γ production by CD8+ T cells (Brinkmann *et al.*, 1993; Nguyen *et al.*, 2002), we asked whether the impaired T cell priming by MVA-OVA-N1L was dependent on inhibitory effects of N1 on IFN-I production. To answer this question, we vaccinated interferon alpha receptor deficient mice (*IFNAR*^{-/-}) or C57BL/6 mice with 10^8 TCID₅₀ of MVA-OVA-N1L or MVA-OVA. Eight days post vaccination, ICS and FACS analysis of IFN γ and IL-2 producing antigen-specific T cell primary responses was carried out as shown in Fig. 4.18A. For CD4+ T cell priming, in line with previous findings in C57BL/6 mice immunized with MVA-OVA-N1L, we observed dramatically reduced frequencies and numbers of specific Th1 cells against all determinants derived from both, MVA vector and OVA antigen (Fig. 4.18B,C). The decline ranged from 50% to 75% (P<0.05 for B5, P<0.01 for L4 and OVA, P<0.001 for E9), while polyfunctional CD4+ T cells (IFN γ + IL-2+) were reduced up to 50-80% (P<0.001 for B5, P<0.01 for L4, E9 and OVA).

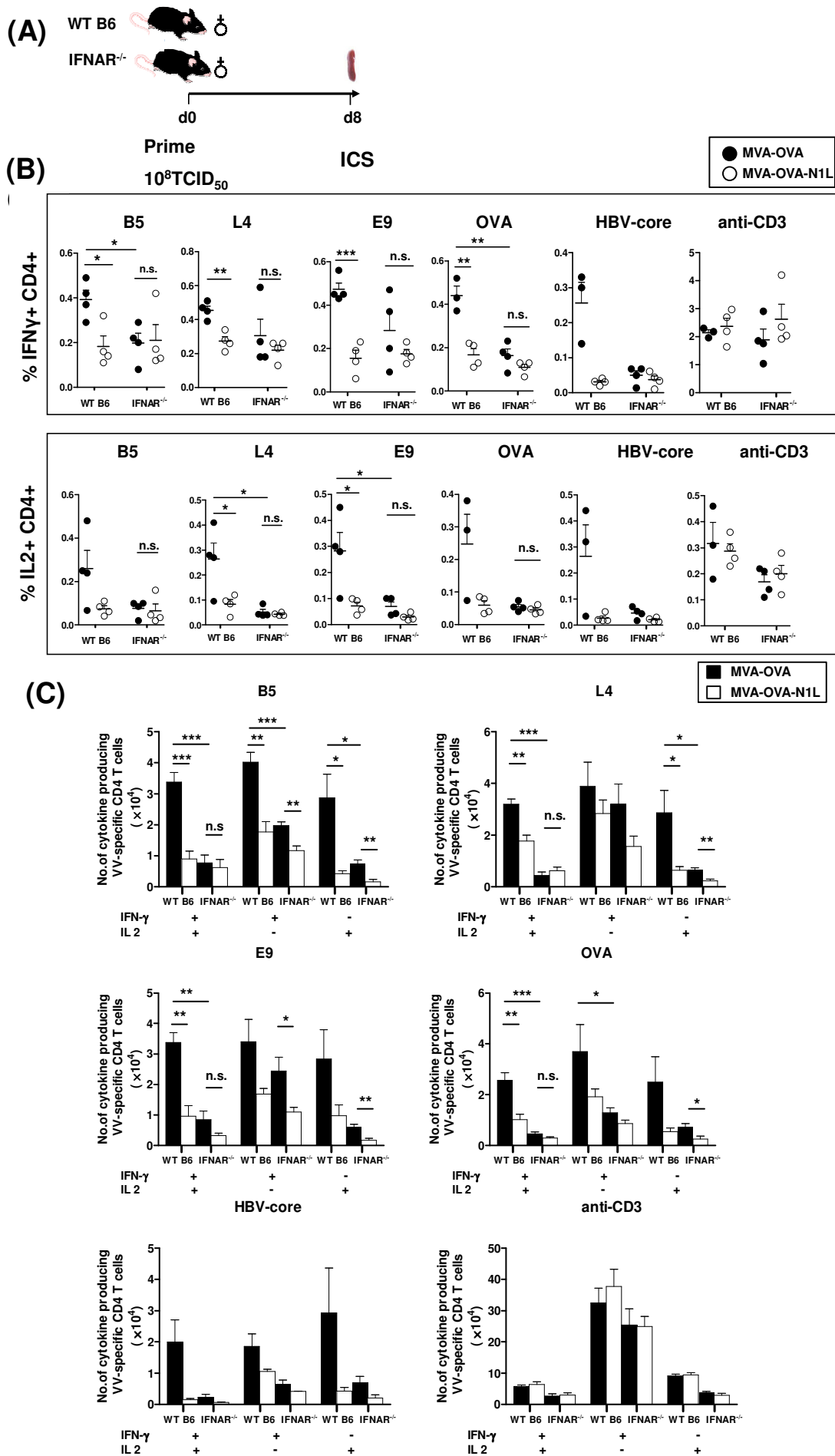


Fig.4.18. Interference with IFN-I signaling is responsible for suppression of CD4+ T cell priming after MVA-OVA-N1L vaccination. Groups of C57BL/6 and *IFNAR*^{-/-} mice (n=3 or 4) were vaccinated i.p with 10⁸ TCID₅₀ of MVA-OVA or MVA-OVA-N1L. MVA vector- and OVA- specific CD4+ T cell responses in the spleen were analyzed on day 8 post infection by intracellular cytokine staining (ICS) as schematically shown in (A). Percentage of CD4+ T cells producing IFN-γ (upper panel) or IL-2 (lower panel) (B). Numbers of MVA vector- and OVA- specific cytokine producing CD4+ T cell in each spleen (C). Data are means ±SEM. n.s. P>0.05, * P<0.05, ** P<0.01, *** P<0.001. Results for a representative experiment of one are shown.

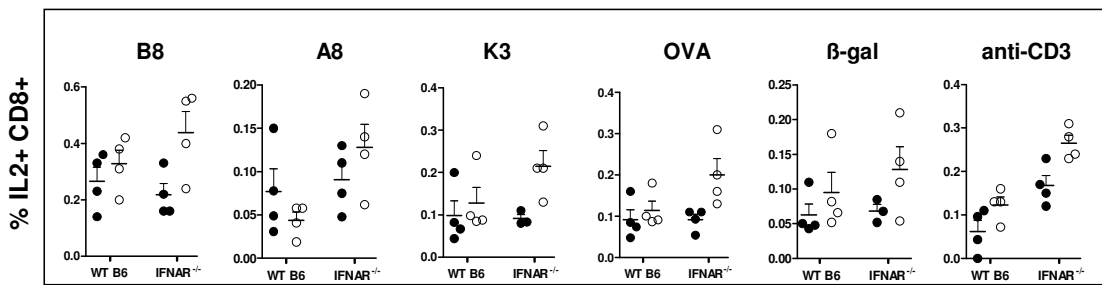
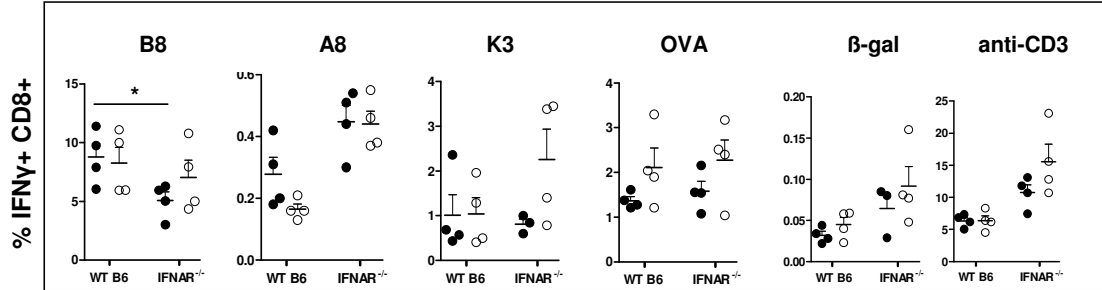
Accordingly, the number of Ag-specific CD4+ cells which only secreted IFNγ or IL-2 were also diminished showing the same tendency as found for polyfunctional CD4+ T cells. Interestingly, in MVA-OVA vaccinated *IFNAR*^{-/-} mice, the frequency and number of cytokine producing CD4+ T cells for all antigen specificities were significantly decreased compared with that from wt mice. Nevertheless, *IFNAR*^{-/-} mice showed comparable weak CD4+ T cell responses and statistically equivalent numbers of polyfunctional Th1 cells for MVA-OVA or MVA-OVA-N1L, in spite of smaller populations of single cytokine positive CD4+ T cells found in the MVA-OVA-N1L vaccinated group (Fig.4.18B,C). Taken together, in the context of MVA-OVA-N1L vaccination, N1 is responsible for the impaired CD4+ T cell priming in this murine model. This impairment is dependent on interference with type I interferon signalling.

Given that IFN-I receptor-triggering is required to promote optimal MVA-induced B8R-specific CD8+ T cell expansion (Frenz *et al.*, 2010), we therefore asked whether the inhibition of CD8+ T cell priming caused by N1 is also dependent on type I IFN receptor signalling. Consistent with what has been reported, MVA-OVA vaccinated *IFNAR*^{-/-} mice showed a massive reduction in frequency and number of IFNγ+ secreting B8R-specific CD8+ T cells as compared to WT C57BL/6 mice (nearly 50% less). However, we observed only a marginally decline in frequency and number of IFNγ+ secreting B8R-specific CD8+ T cells for MVA-OVA-N1L in C57BL/6 mice compared to MVA-OVA, This effect was not as significant as in the previous finding shown in figure 4.15D (Fig. 4.19B,C). In contrast, MVA-OVA-N1L did not result in reduced frequency and number of B8R-specific CD8+ T cells when immunizing *IFNAR*^{-/-} mice. On the contrary, IFNγ+ and IL-2+ T cell frequency seemed slightly increased after MVA-OVA-N1L vaccination of *IFNAR*^{-/-} mice, despite reduced



(B) Prime 10^8 TCID₅₀ ICS

● MVA-OVA
○ MVA-OVA-N1L



(C) ■ MVA-OVA □ MVA-OVA-N1L

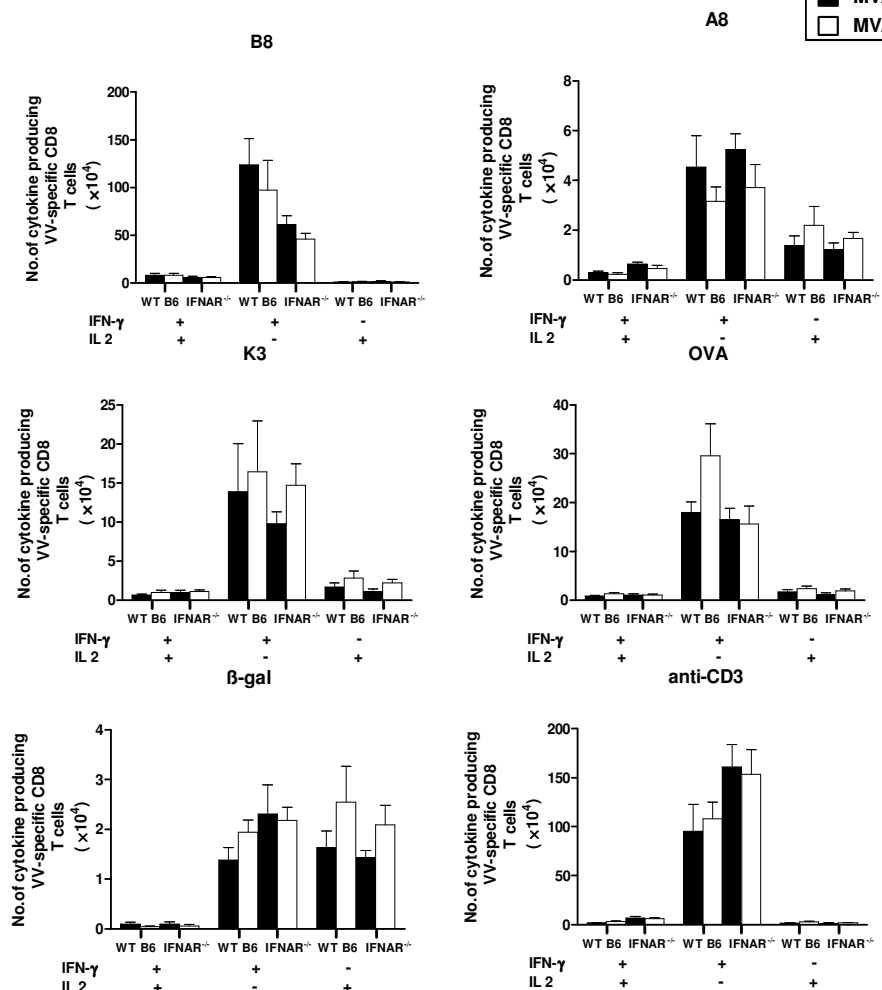


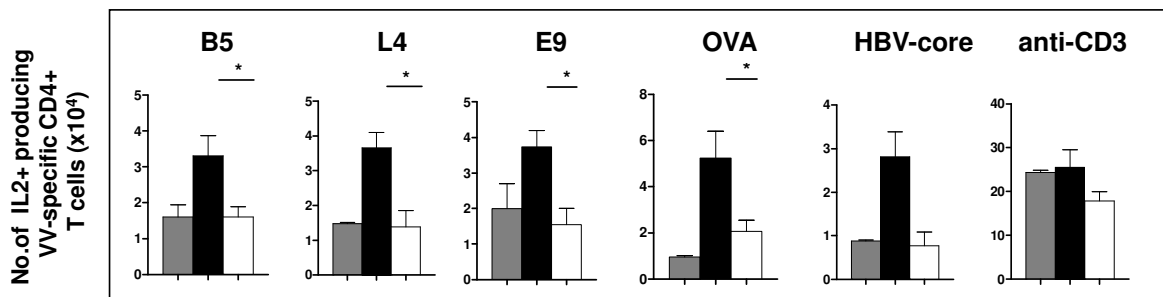
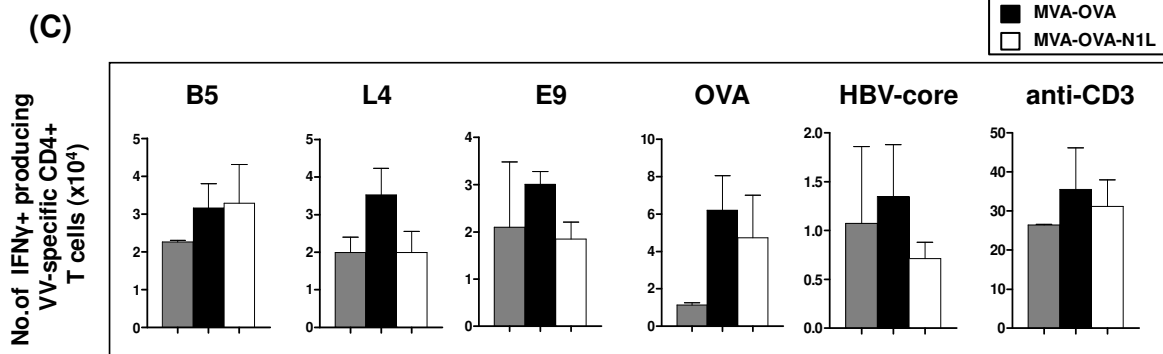
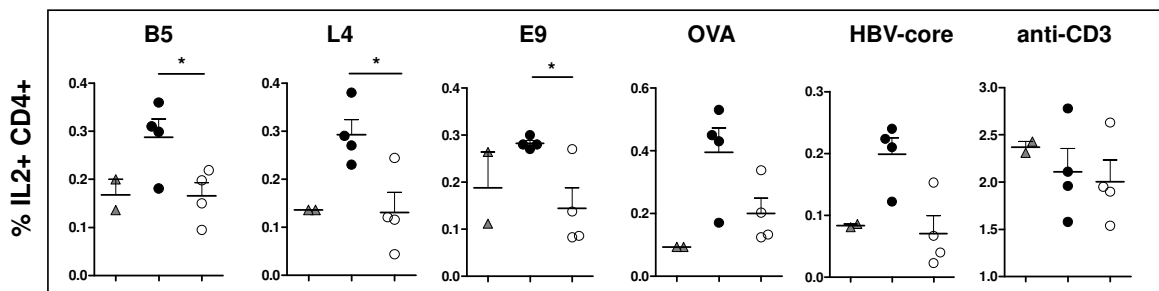
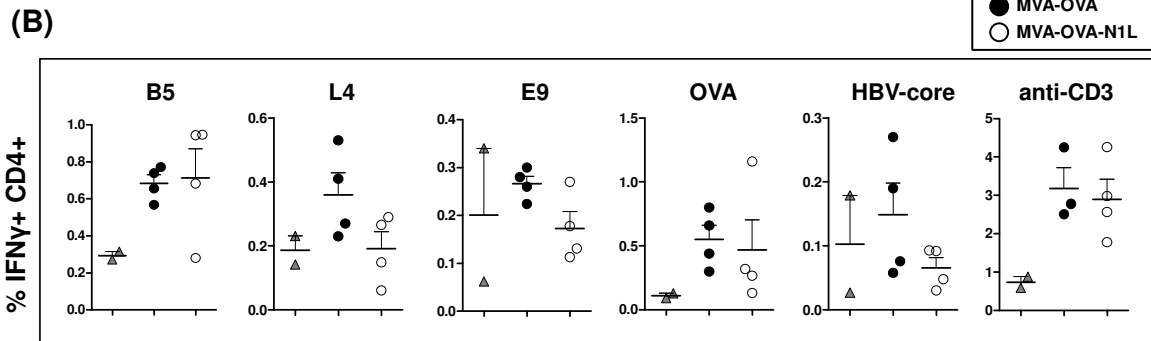
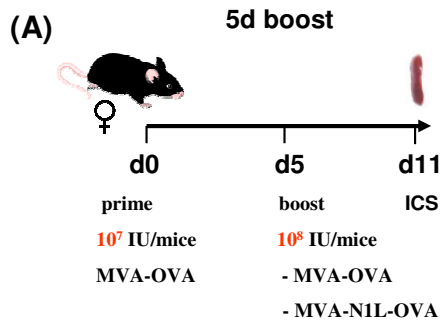
Fig.4.19. Immunodominant B8R-specific CD8+ T cell priming is suppressed due to interference with IFN-I signaling but independent of N1. Groups of C57BL/6 and *IFNAR*^{-/-} mice (n=3 or 4) were vaccinated i.p with 10⁸ TCID₅₀ of MVA-OVA or MVA-OVA-N1L. MVA vector- and OVA- specific CD8+ T cell responses in the spleen were analyzed on day 8 post infection by intracellular cytokine staining (ICS) as schematically shown in (A). FACS analysis after ICS for the percentage (B) and number (C) of antigen-specific CD8+ T cells expressing cytokines. Data are means ±SEM. * P<0.05. Results for a representative experiment of one are shown.

number. We also could not observe the decrease of other antigen-specific CD8+ T cells in frequency and number in *IFNAR*^{-/-} mice. Paradoxically, the frequency of A8R-specific CD8+ T cell even showed an obviously upregulated in MVA-OVA-N1L vaccinated mice.

4.12. MVA-OVA-N1L inhibits IL-2 secretion in secondary T cell responses

Recombinant MVA is most efficient as vaccine when used as a boosting agent in heterologous prime/boost vaccination protocols (Cottingham and Carroll, 2013). How vaccinia virus immunomodulators influence the boosting of antigen-specific memory T cell responses is an important issue. To dissect the role of N1 in secondary immune responses, we performed so-called short-interval prime/boost immunizations (Kastenmuller *et al.*, 2007). C57BL/6 mice were vaccinated with 10⁷ TCID₅₀ of MVA-OVA for comparable T cell priming. Five days later, vaccinated mice were split into 3 groups which were then boosted with 10⁸ TCID₅₀ of MVA-OVA or MVA-OVA-N1L or PBS, respectively. Six days later, splenocytes were prepared for ICS and FACS analysis. We found that after boosting, CD4+ B5R- and OVA- specific Th1 cells secreting IFN γ or IL-2 expanded stronger than that for L4R and E9L. This indicates that B5R- and OVA-specific CD4+ T cells had the higher immunodominance hierarchy. Surprisingly, for these two CD4+ T cell populations, there was no difference in IFN γ -secreting frequencies and numbers between MVA-OVA- and MVA-OVA-N1L- boosted mice. (Fig.4.20B,C, upper panels) Only a slight decline was observed in L4R- and E9L-specific IFN γ -secreting Th1 cell populations when mice were vaccinated with MVA-OVA-N1L. Therefore, MVA-OVA-N1L did not influence the recall CD4+ T cell response concerning IFN γ -secretion. Unexpectedly, when we

analysed the IL-2 secretion of CD4⁺ T cells, a significant reduction was detected in MVA-OVA-N1L vaccinated mice for all antigen-specific Th1 cells. Frequency and number decreased more than half compared to the MVA-OVA vaccinated group, demonstrating a serious impairment for IL-2 production (Fig.4.20B,C, lower panels). Subsequently, we tested the secondary CD8⁺ T cell response. As demonstrated in previous sections, N1 impaired the naïve CD8⁺ T cell priming if at all for the immunodominant B8R-specific epitope. In line with that, after boosting, MVA-OVA-N1L did not exert any suppressive action on IFN γ secreting B8R-specific CD8⁺ T cells (percentage and number) (Fig.4.20D,E). Nevertheless, MVA-OVA-N1L dramatically decreased both, relative and absolute numbers of IL-2 secreting CD8⁺ T cell populations (frequency, $P < 0.05$; number, $P < 0.01$) specific for the immunodominant epitope derived from B8R. Consistently, there were no obvious differences for all other antigen-specific CD8⁺ T cells tested for IFN γ or IL-2 production between MVA-OVA and MVA-OVA-N1L vaccinated mice (Fig.4.20D,E)



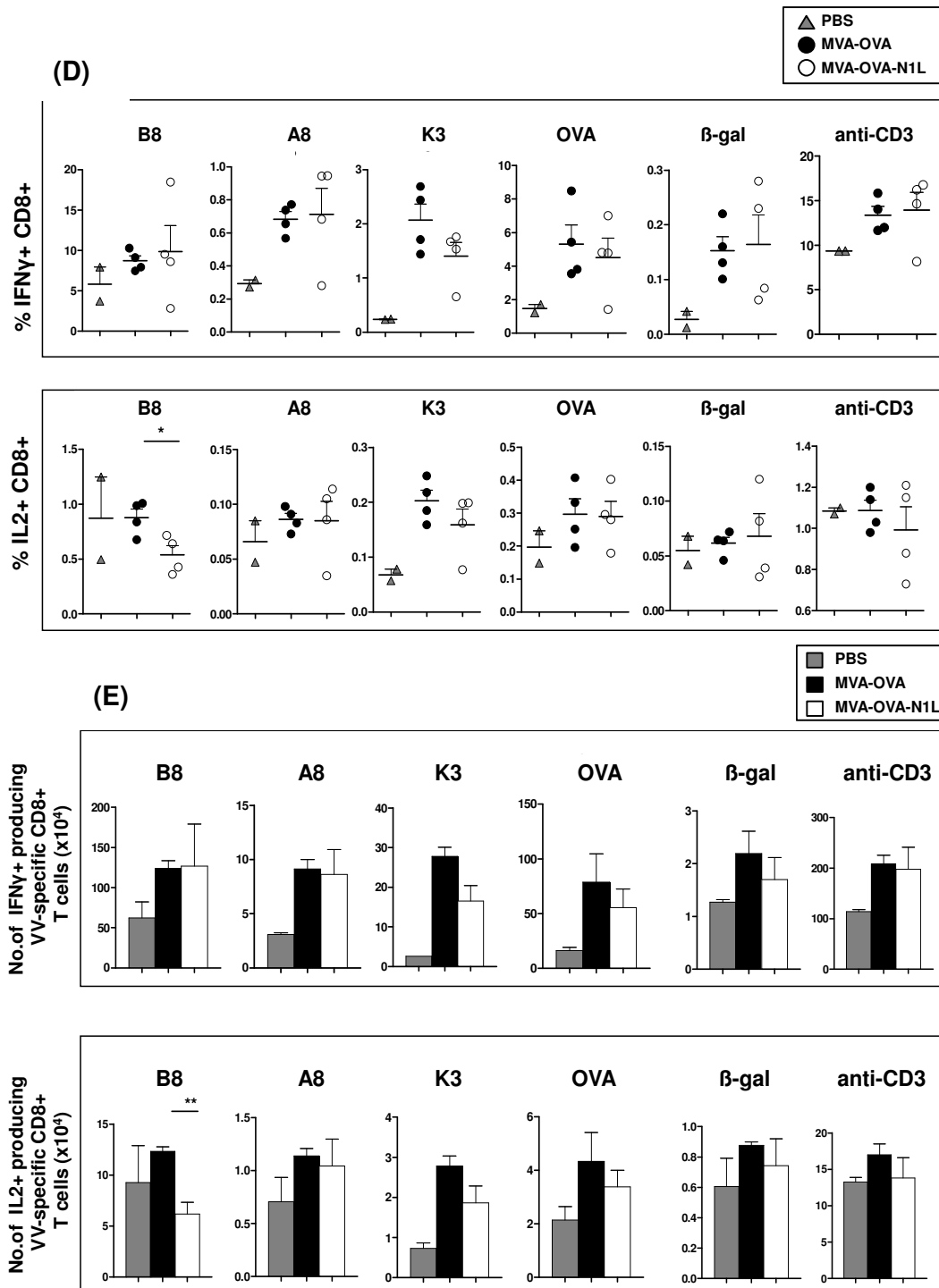
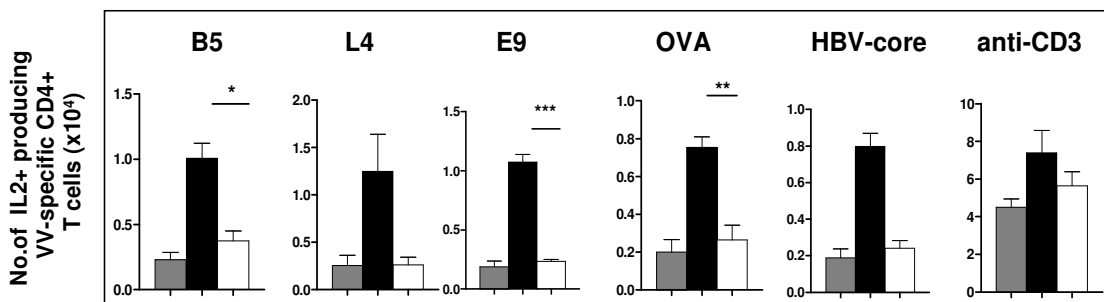
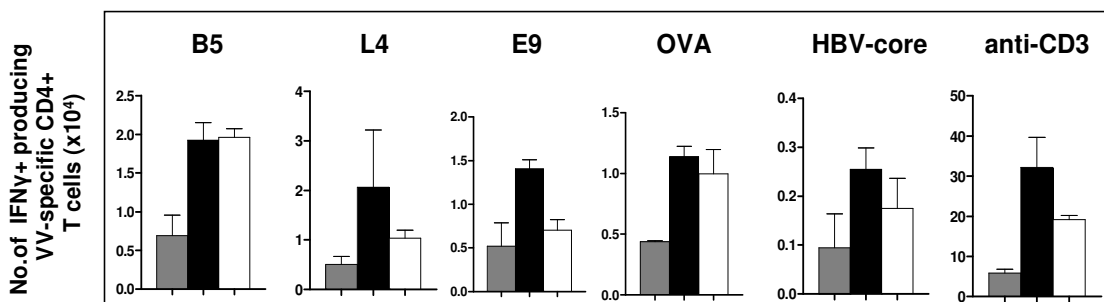
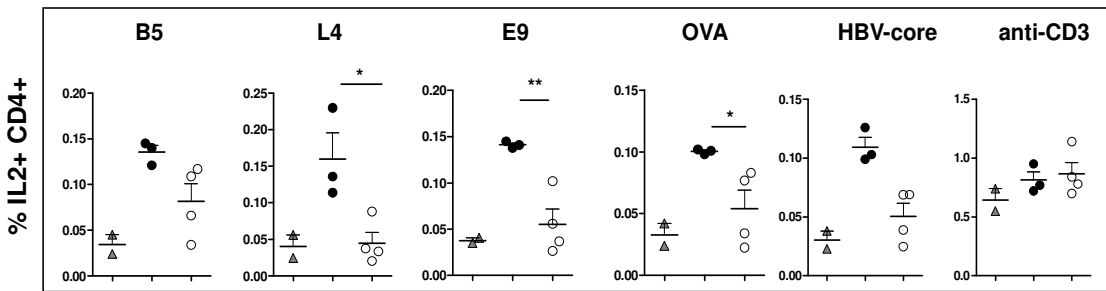
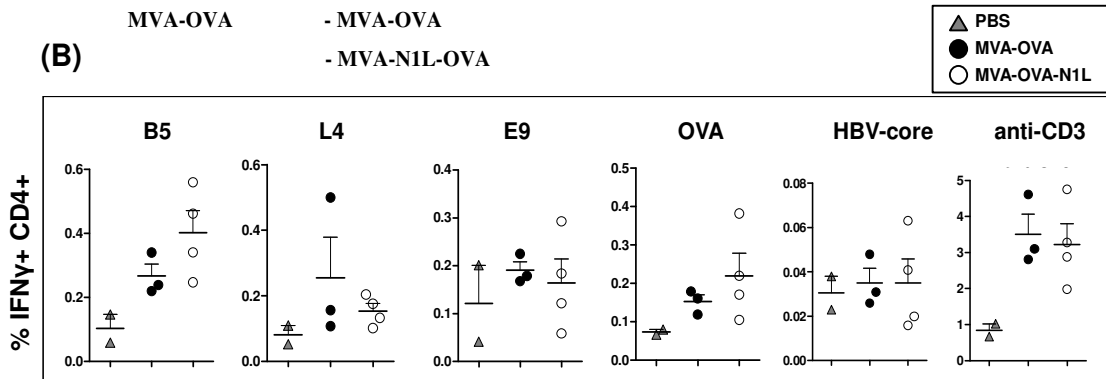
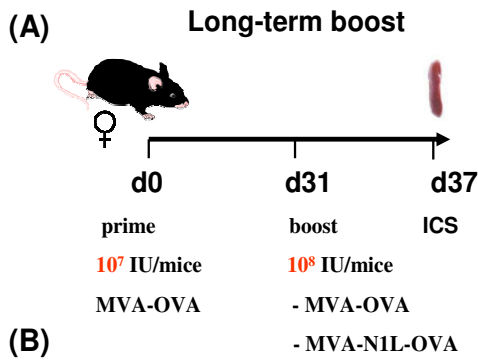


Fig.4.20. MVA-OVA-N1L selectively impairs IL-2 secretion after short-interval boost. C57BL/6 mice were vaccinated i.p with 10^7 TCID $_{50}$ of MVA-OVA. Five d post infection, groups of mice (n=3 or 4, mock PBS =2) were boosted with 10^8 TCID $_{50}$ MVA-OVA, MVA-OVA-N1L or PBS. Six days later, MVA vector- and OVA- specific CD4+ and CD8+ T cell responses in the spleen were analyzed by ICS as depicted in (A). Percentage of antigen-specific IFN γ + (upper panel) and IL-2+ (lower panel) CD4+ and CD8+ T cells (B,D) and absolute numbers of antigen-specific IFN γ + and IL-2+ CD4+ and CD8+ T cells (C,E) are shown for ICS after FACS. Data are means \pm SEM. * P<0.05, ** P<0.01. Results for a representative experiment of one are shown.

In order to preclude unwanted interference by the T cell primary response after short-interval prime/boost immunizations, we performed long-term prime/boost immunization experiments to investigate the recall response (memory T cells). The vaccination strategy was designed similar to the short-interval immunization, but the boosting was carried out on day 31 after priming. Impressively, in line with what we had found in short-interval prime/boost immunizations, MVA-OVA-N1L did not suppress the recall CD4⁺ T cell response for IFN γ (only slightly diminished numbers were observed for L4R- and E9L- specific CD4⁺ T cells). On the contrary, even substantially elevated levels of B5R- and OVA- specific IFN γ producing CD4⁺ T cells were observed in MVA-OVA-N1L vaccinated mice (Fig.4.21B). Interestingly, however, we found again a remarkable decline of secondary responses for IL-2 production in all antigen-specific CD4⁺ T cells from MVA-OVA-N1L vaccinated mice. The frequencies were reduced approx. 40-60% (L4R, P<0.05; E9R, P<0.01; OVA, P<0.05), whereas absolute numbers were reduced up to approx. 60-80% (B5R, P<0.05; E9R, P<0.001; OVA, P<0.01). This result is consistent with what had been revealed in short-interval prime/boost immunizations. Subsequently, we also tested the CD8⁺ T cell recall immune response. In line with the results from short-term boosting, we could not find any suppressive effect on all antigen-specific CD8⁺ T cells for IFN γ production in MVA-OVA-N1L vaccinated mice. On the contrary, moderately higher frequencies of IFN γ ⁺ antigen-specific CD8⁺ T cells were observed in all peptide cohorts. Nevertheless, a decreased frequency and number of IL-2 producing cells were shown for B8R in MVA-OVA-N1L immunized mice.

Taken together, we conclude that the knock-in of functional N1L into MVA did not inhibit secondary immune responses (reactivated memory T cells) to produce IFN γ , however, it reduced the amount of IL-2-secreting T cells. Interestingly populations with higher immunodominance were more sensitive to this inhibitory effect.



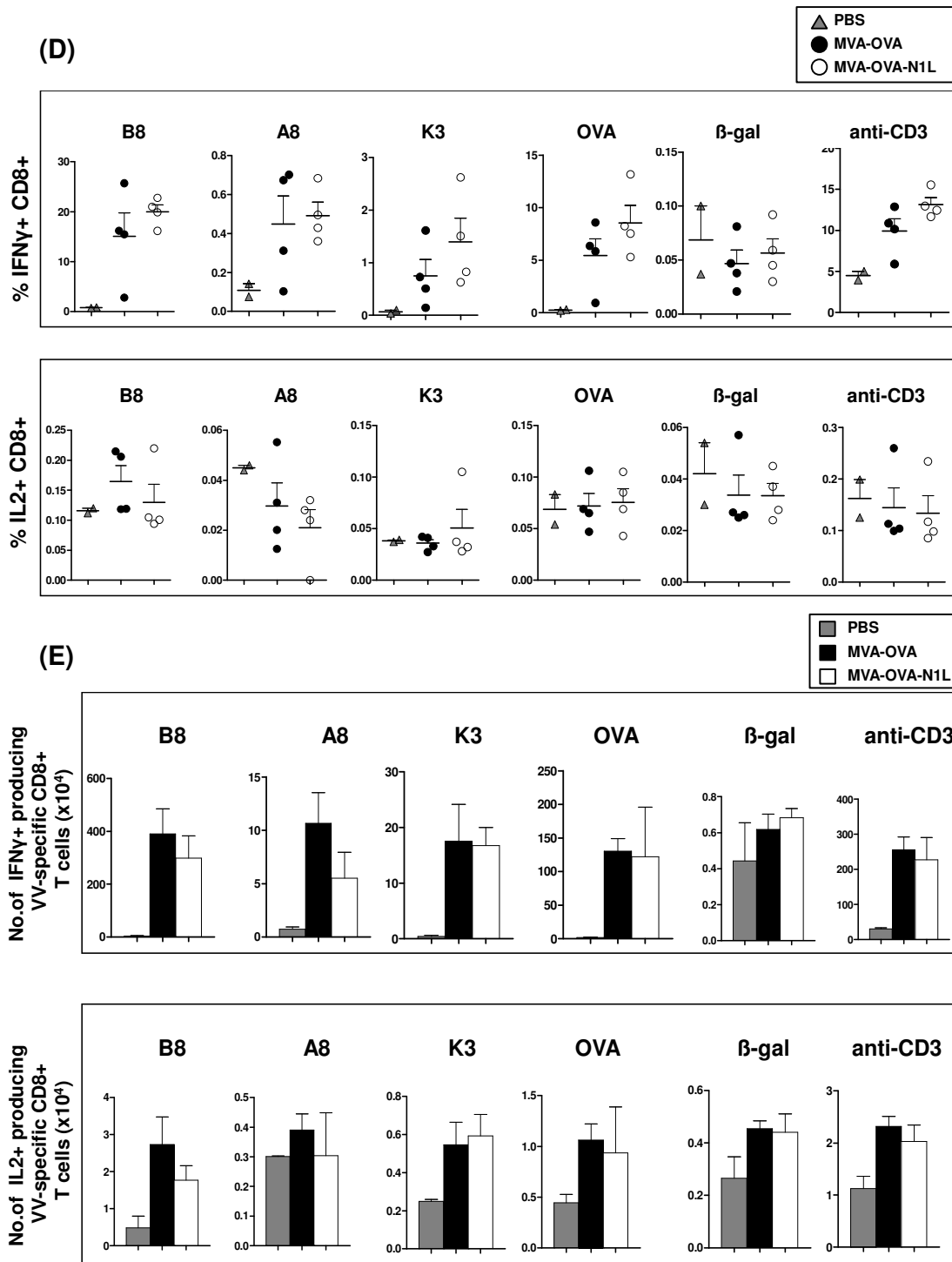


Fig.4.21. MVA-OVA-N1L selectively impairs IL-2 secretion in longterm-interval recall T cell responses. C57BL/6 mice were vaccinated i.p with 10^7 TCID $_{50}$ of MVA-OVA. At 31 d post infection, groups of mice (n=3 or 4, mock PBS =2) were boosted with 10^8 TCID $_{50}$ of MVA -OVA, MVA-OVA-N1L or PBS. Six d later, MVA vector- and OVA- specific CD4+ and CD8+ T cell responses in the spleen were analyzed by FACS (ICS) as depicted in (A). Percentage of antigen-specific IFN γ + (upper panel) and IL-2+ (lower panel) CD4+ and CD8+ T cells (B,D) and number of antigen-specific IFN γ + (upper panel) and IL-2+ (lower panel) CD4+ and CD8+ T cells (C,E) are shown. Data are means \pm SEM.* P<0.05, ** P<0.01, *** P<0.001. Results for a representative experiment of one are shown.

4.13. Vaccinia N1 has a marginal effect on antigen-specific CD4+ T cell reactivation *in vitro*

To investigate whether N1-mediated inhibitory effects on T cell priming and secondary immune responses observed *in vivo* were due to impaired antigen presentation, we utilized antigen-specific T-cell lines as read out tools *in vitro*. Given that *N1L* knock-in MVA was able to suppress priming of CD4+ T cells for all tested antigen-specificities, we subsequently focused on its role in CD4+ T cell responses. Two well-established antigen-specific CD4+ T cell lines were used, termed CD4^{OVA} and CD4^{B5R}. The amount of cytokine producing CD4+ T cells (IFN γ +, IL-2+) was determined to evaluate the quantity and quality of the T cell response. T cells were weekly restimulated using murine splenocytes (MHC class II I-A^b) pulsed with the corresponding peptides. As expected, they exerted a specific response against the cognate peptide (OVA₂₆₅ or B5R₄₆) which were loaded on BMDCs. The background activity was very low as determined by using both, negative control peptides and DMSO (Fig.4.22). BMDC is one of the major professional antigen presenting cells and plays a critical role in activating T cell responses against VV or MVA. To assess the function of N1, we infected BMDCs with 1) MVA versus MVA-N1L, 2) VV versus VV Δ N1L or 3) MVA-OVA versus MVA-OVA-N1L. Antigen-specific CD4+ T cells were co-cultivated with infected BMDCs, and were analyzed for their specific response.

As expected, MVA, MVA-N1L, VV and VV Δ N1L could not activate CD4^{OVA} T cells (no IFN γ or IL-2) expression. They elicited background levels of response similar to negative control peptides. MVA-OVA and MVA-OVA-N1L could induce potent responses in CD4^{OVA}, but no difference in magnitude was found (Fig.4.23A,C). For CD4^{B5R} activation, we found that all of these viruses were able to trigger a robust T cell response in an infectious dose-dependent manner before a saturation was reached (from MOI=1 to 20). Likewise, all viruses tested showed maximal activation level of the T cell response. Of note, VV showed a stronger inhibitory effect on CD4^{B5R} activation, compared with VV Δ N1L, when BMDCs were infected with high MOI (10 or 20). There were approx. 20% less IFN γ + and 0.8% less IL-2+ CD4+ T cells elicited by VV. (Fig.4.23B,D). This indicated a marginal impact of N1 on antigen presentation of B5R₄₆. Consequently, our data suggest that N1 did not obviously impair antigen presentation and T cell

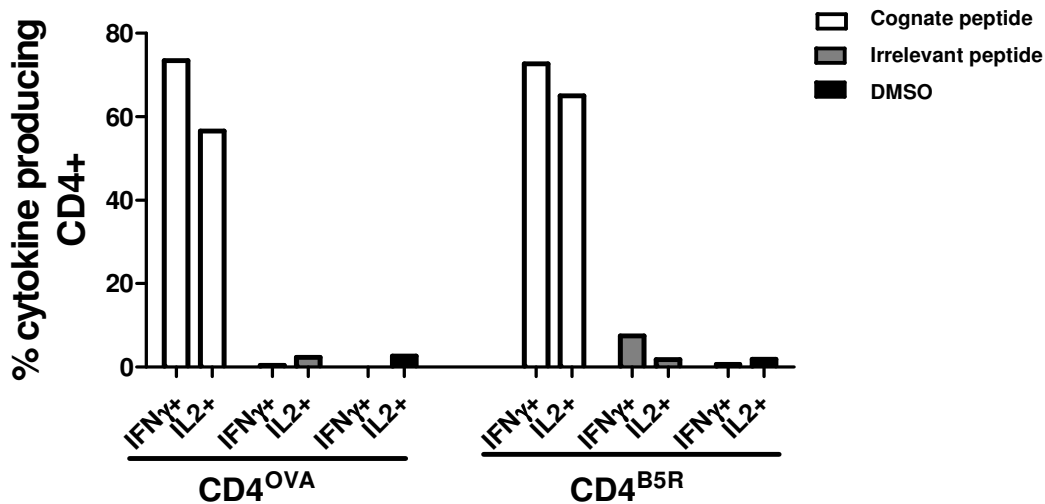


Figure.4.22. Stimulation of CD4⁺ T cell lines with peptides pulsed BMDCs. BMDCs were pulsed with the respective cognate peptide (OVA₂₆₅ or B5R₄₆), irrelevant peptide (E9L₁₇₉), or DMSO and co-cultivated with CD4^{B5R} and CD4^{OVA}. The percentage of IFNγ and IL-2 expressing CD4⁺ T-cells was determined by ICS and quantified by FACS analysis.

reactivation by MVA infected BMDCs but slightly impede CD4^{B5R} activation in context of VV infection.

Since MVA-OVA-N1L showed an IFN-I signaling dependent inhibition of CD4⁺ T cell priming *in vivo*, therefore we wanted subsequently to check whether antigen-specific CD4⁺ T cell responses would be influenced when this signaling pathway is missing *in vitro*. GM-CSF-derived BMDCs from *IFNAR*^{-/-} mice were infected with MVA-OVA or MVA-OVA-N1L, and used to stimulate antigen-specific CD4⁺ cell lines. Of note, cognate peptide-pulsed *IFNAR*^{-/-} BMDCs could induce similar magnitude of CD4⁺ T cell responses for both CD4^{OVA} and CD4^{B5R} compared to that induced by pulsed BMDCs from C57BL/6 mice (Fig.4.23 and Fig.4.24). Furthermore, MVA-OVA induced similar CD4^{OVA} and CD4^{B5R} responses via BMDCs from *IFNAR*^{-/-} or C57BL/6 mice. This tendency was also found for MVA-OVA-N1L (Fig.4.23 and Fig.4.24). In addition, when *IFNAR*^{-/-} BMDCs were used as targets, MVA-OVA and MVA-OVA-N1L showed comparable activation competence for IL-2 production of CD4^{OVA} and IFNγ production of CD4^{B5R} (Fig.4.24B,C). Nevertheless, *IFNAR*^{-/-} BMDCs targeted for T cell activation were more sensitive to MVA-OVA-N1L for which in high dose virus infections IFNγ⁺ CD4^{OVA} and IL2⁺ CD4^{B5R} were diminished (Fig.4.24A,D). Our results

indicate that antigen-specific CD4⁺ T cell activation was highly effective for epitopes presented by MHCII on the surface of infected APCs, but was insensitive to the IFN-I receptor signaling feedback loop in BMDC. The inhibitory role of N1 in antigen presentation of BMDC was marginal.

Given that macrophages (MΦ) represent another group of major antigen presenting cells in the murine system, we sought to find out whether MΦ used as targets infected by *N1L* knock-in MVA could influence the antigen-specific CD4⁺ T cell activation. To answer this question, M-CSF derived MΦ were explored as the APC.

MΦ infected with MVA-GFP showed a nearly 88% infectious rate (data not shown). Compared to BMDCs, we observed similar activation levels of CD4⁺ T cells using cognate peptide pulsed MΦ. However, MΦ infected by MVA showed decreased but measurable T cell activation compared to the infected BMDCs (Fig.4.24 and Fig.4.25). Besides, consistent with what we found in BMDC, both MVA-N1L and MVA-OVA-N1L did not inhibit T cell activation using infected MΦ (Fig.4.25). MΦ induced very low levels of IL-2 which were indistinguishable from the background.

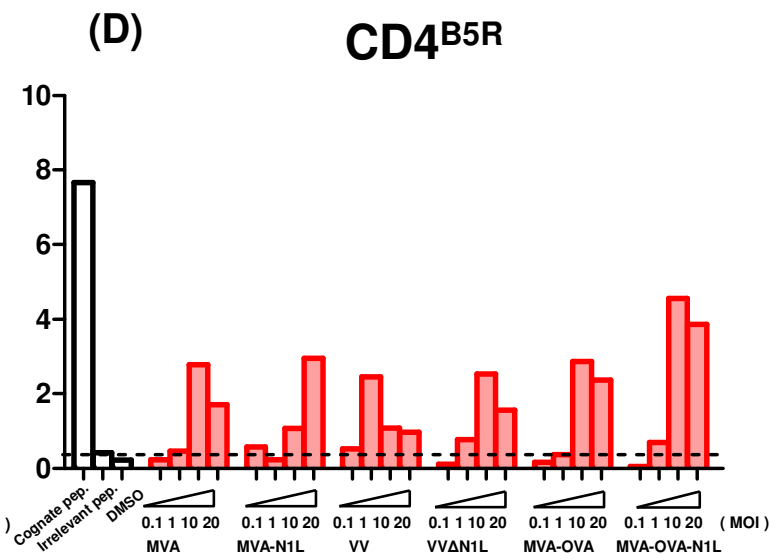
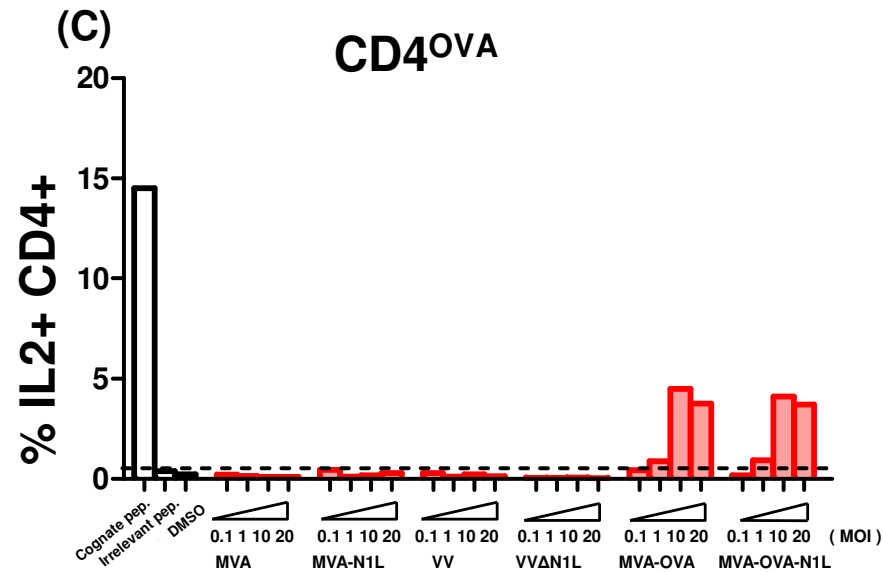
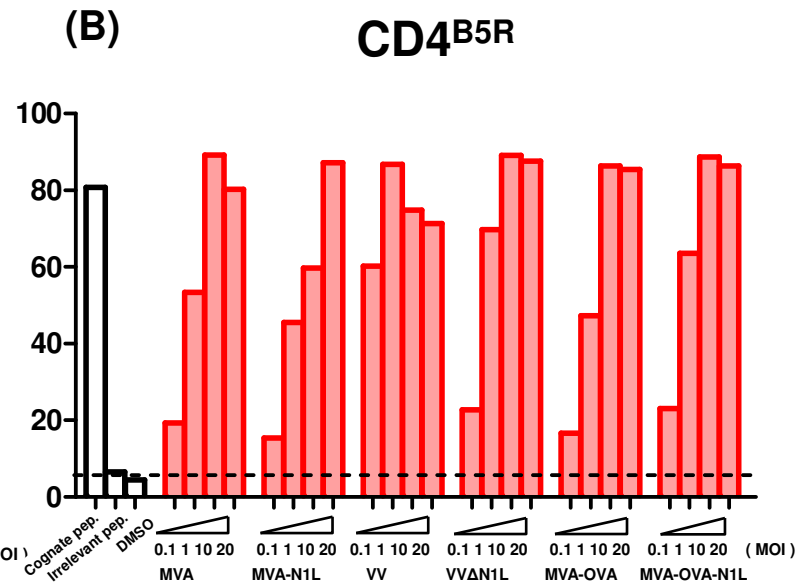
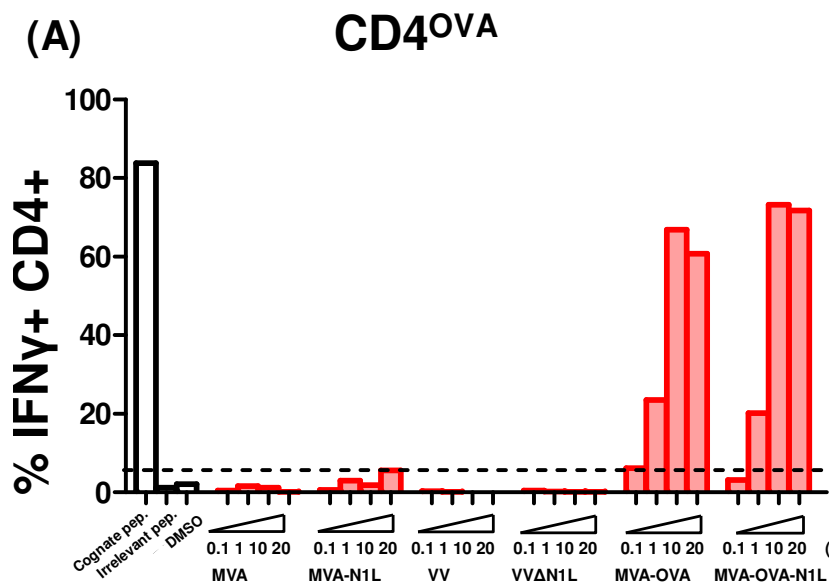


Figure.4.23. Virus-encoded N1 fails to inhibit antigen-specific CD4 T cell reactivation by infected BMDCs *in vitro*. Peptide-pulsed or virus-infected BMDCs from C57BL/6 mice were used as APCs for stimulation of CD4^{OVA} and CD4^{B5R} as indicated. Increased virus loads were used for infection (MOI 0.1, 1,10 and 20). The percentage of IFN γ (A,B) and IL-2 (C,D) producing CD4+ T-cells was determined by ICS and quantified by FACS analysis. Results for a representative experiment of two are shown.

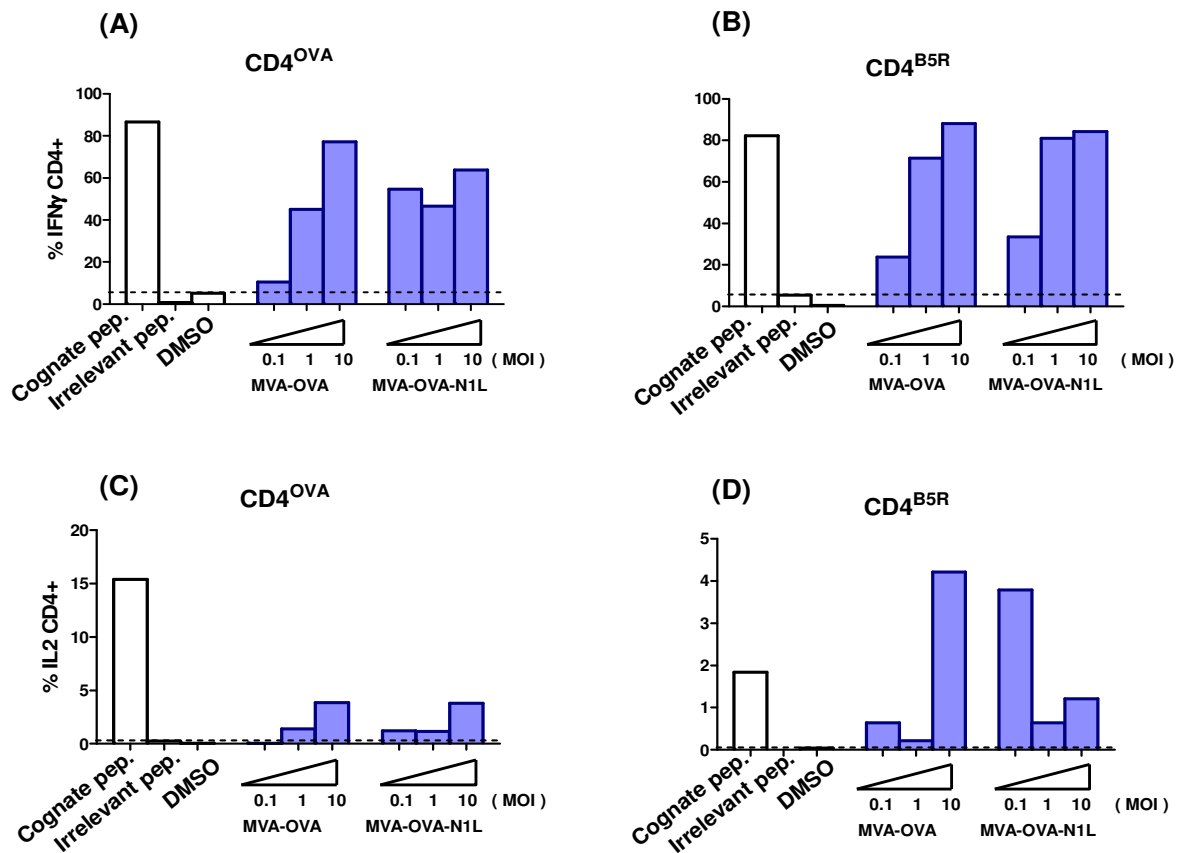


Figure.4.24. Impairment of IFN-I signaling in infected BMDCs from *IFNAR*^{-/-} mice as APC has no obvious effect on antigen-specific CD4+T cell activation for both MVA-OVA and MVA-OVA-N1L. BMDCs from *IFNAR*^{-/-} mice were peptide-pulsed or infected with indicated viruses for CD4^{OVA} and CD4^{B5R} stimulation. Increasing virus loads were used for infection (MOI 0.1, 1,10). The percentage of IFN γ (A,B) and IL-2 (C,D) producing CD4+ T-cells was determined by ICS and quantified by FACS analysis. Results for a representative experiment of one are shown.

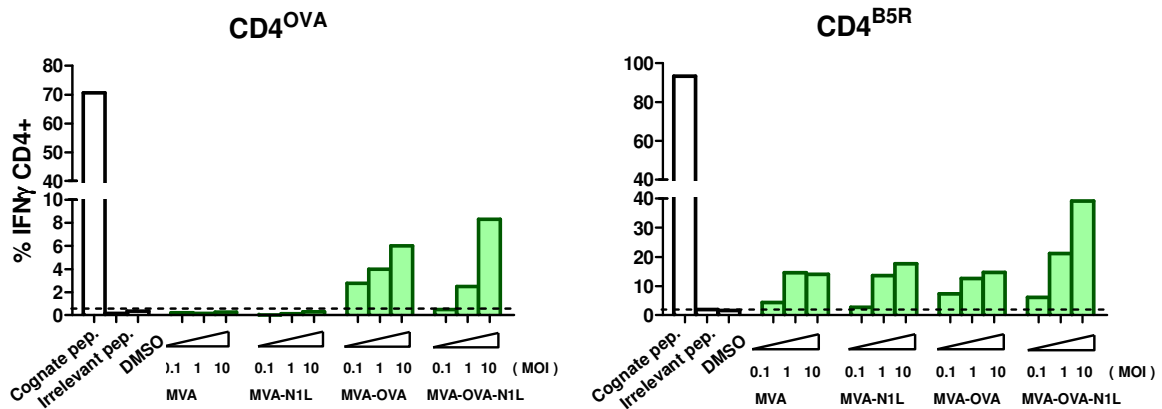


Figure.4.25. Virally encoded N1 does not inhibit antigen-specific CD4⁺ T cell activation by infected macrophages *in vitro*. Peptide-pulsed or virus-infected M Φ from C57BL/6 mice were used as APCs for stimulation of CD4^{OVA} and CD4^{B5R} as indicated. Increasing virus loads were used for infection (MOI 0.1, 1, 10). The percentage of IFN γ expressing CD4⁺ T-cells was determined by ICS and quantified by FACS analysis. Results for a representative experiment of two are shown.

4.14. MVA-N1L can not block STS- or infection-induced apoptosis

Vaccinia encoded N1 was reported to be anti-apoptotic and able to prevent both drug- and infection-induced apoptosis (Cooray *et al.*, 2007). However, a recent study revealed that N1 can not inhibit cell death, which made the anti-apoptotic function of N1 controversial (Postigo and Way, 2012). Compared to VV, MVA has lost a panel of anti-apoptotic viral genes and seems highly competent to trigger apoptosis of infected cells. Since T cell priming elicited by MVA *in vivo* is mainly executed by non-infected DCs through cross-presentation, a delayed apoptosis of infected cells may lead to reduced T cell induction (Alberts *et al.*, 1999). Therefore, if N1 could inhibit apoptosis in MVA-infected cells, it should impact the antigen presentation capability of the APC and subsequently reduce T cell priming by MVA vaccination. To address this question, we tested whether *N1L* knock-in MVA has the ability to inhibit drug- or infection-induced apoptosis. Here we expected MVA-N1L would be more sensitive for an anti-apoptotic analysis compared to VV. First of all, we titrated staurosporine (STS) for its ability to induce apoptosis in Hela cells to determine the optimal dose. Annexin V staining showed that STS treated Hela cells exerted a dose-dependent apoptosis and necrosis before reaching a saturation level (Fig.4.26). Then Hela cells were infected with MVA or MVA-N1L for 6 h and subsequently incubated with or without

1 μ M STS for 4 h. STS treatment of non-infected cells resulted in increased levels of apoptosis, as detected by cleavage of the apoptotic marker PARP and Caspase 3. Nevertheless, we found that cells infected with MVA or MVA-N1L showed similar protection against STS- and infection-

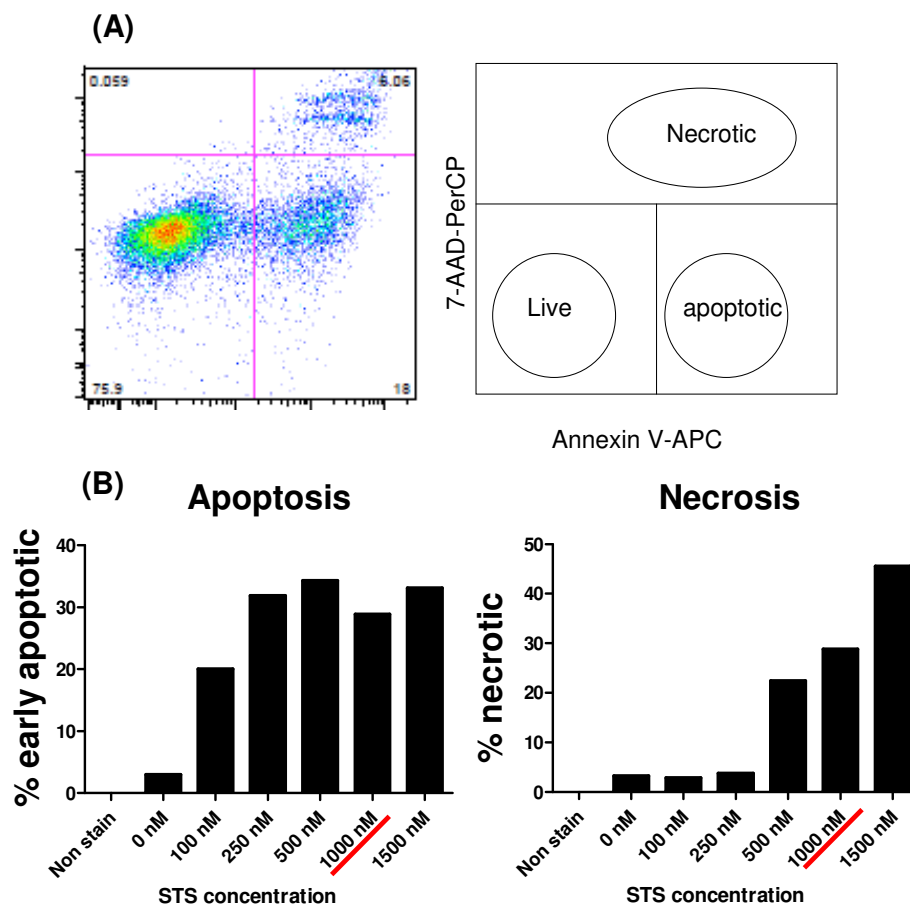


Figure.4.26. STS-induced apoptosis in HeLa cells. Gating strategy after annexin V staining for apoptosis. Living, early apoptotic or necrotic cells are indicated (upper right panel) (A). Annexin V staining of apoptotic or necrotic HeLa cells treated with STS at increasing concentrations as indicated (B).

induced apoptosis (Fig.4.27A). To check whether MVA-N1L could inhibit virus-induced cell death, we infected murine BMDCs with MVA, MVA-N1L or mock for 0 h, 6 h, 12 h, 24 h. In agreement with what we had found before, the virus infection induced increasing cell death compared with mock as determined by annexin V staining. In contrast, similar apoptotic levels were found between MVA- and MVA-

N1L- infected cells (Fig.4.27B). This was also confirmed when primary macrophages, HeLa cells, THP-1 cells or LCL were used (data not shown). Taken together, our results support the conclusion that N1 seems not to act as a viral anti-apoptotic protein (Postigo and Way, 2012).

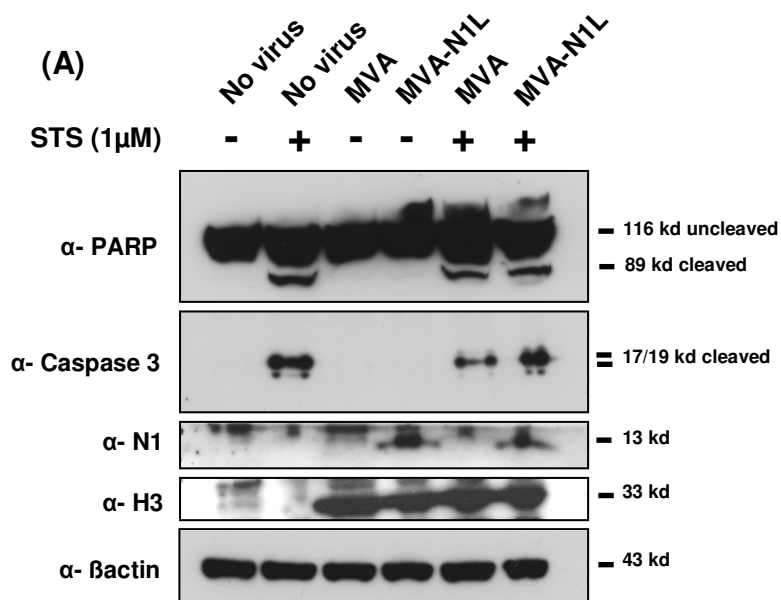
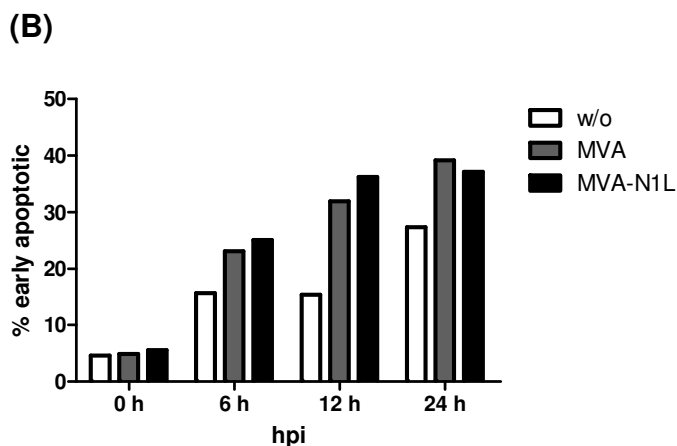


Figure.4.27. N1 does not protect from STS- and MVA infection-induced apoptosis. 2×10^6 HeLa cells were infected with MVA or MVA-N1L (MOI 20) or mock. Six h later, cells were treated with or without 1 μ M STS and cultured for 4 h. Western blot analysis of whole-cell lysates probed with antibodies against PARP, Caspase 3, N1, H3 and β -actin is shown (A). 1×10^6 BMDCs from C57BL/6 mice were infected with MVA or MVA-N1L (MOI 10) or mock. Annexin V staining of infected cells was carried out at 0, 6, 12 and 24 hpi. The percentage of apoptotic cells is shown (B).



5. Discussion

5.1. BAC-MVA mutagenesis platform for vector vaccine development and gene delivery

In the present work, we constructed a series of transfer plasmids targeting MVA deletion VI region and containing various VV specific promoters. Subsequently, we explored the fluorescent reporter gene mCherry driven by these promoters as the model to evaluate the BAC system for MVA mutagenesis. Since MVA naturally deletion III and VI locate in relatively conserved regions of the genome, the transgene expressed there is less affected by the sequence rearrangement. Targeting the exogene to deletion VI region revealed stability of target gene expression and viral growth. Moreover, the BAC cassette did not impact the replication of recMVA and transgene expression as well. Thus, the GFP in cassette can be valuably monitored as the viral infection and recombination marker. However, for clinical or pharmaceutical evaluation as a vaccine vector, MVA containing a BAC-GFP scar will bring some uncertainty for its usage even though the BAC cassette may not be putatively immunogenic. Therefore, the BAC self-excisable MVA_BAC strain showed a significant advantage. In addition, as an experimental tool, recMVA is indispensable because they would be compared with the viruses that naturally carry no BAC region. Furthermore, deleting the selective marker gene *aphAI* by *en passant* enables the repeatable mutagenesis of the MVA_BAC genome, however, *aphAI* gene could also be selectively maintained in the MVA_BAC genome to speed up the recMVA generation.

The concern still remained that genetical operation of the virus genome in *E.coli* might bring the viral genome mutations. Although in most cases these kinds of mutations are silent or insignificant for the properties of MVA as a vaccine vector, it will still be discomforting to predict their impact on the safety. To overcome this issue, a mandatory viral genomic sequencing would be of significant importance before entering preclinical studies.

5.2. The versatile usage of VV promoters for antigen expression in recMVA

The 5 VV specific promoters were chosen here, since they represent members of the distinct temporal classes that are commonly used for *in vitro* studies and (pre-) clinical trials. Promoter PK1L originated from vaccinia virus early gene *K1L*. We found it kept the early and rather weak activity of the *K1L* promoter when introduced into MVA dVI region (Fig.4.8, Fig.4.9). The early transcription machinery in poxviruses is contained in the viral particles (Broyles, 2003; Kates and McAuslan, 1967). When recMVA-PK1LmCherry was rescued by FPV, it was hardly detected by mCherry expression in the 1st passage of the rescue. This is likely due to the different localizations of the FPV early transcriptional machinery in the virion and the recMVA genome in the cytosol. P11 was reported as a strong late promoter driving the expression of a VV gene encoding for an 11-kDa structural protein (Alexander *et al.*, 1992). In our system, PK1L exerted mCherry gene expression mainly during the first 4 hpi, while P11 was activated and shows strong activity only after 4 hpi. This staggered temporal kinetics serve as a precise tool to investigate the requirements for antigen expression for immunotherapy. *G8R* was reported as an intermediate gene encoding essentially for a late gene transcription factor (Zhang *et al.*, 1992). We found that the promoter PG8R in deletion VI region obtained a similar promoter activity as expected in its authentic locus, and was activated for a period of time starting between early and late promoter (~1-2 hpi). Therefore, PG8R can serve as a good makeup for temporal regulation of transgene expression in MVA together with PK1L and P11. P7.5 and PmH5 are 2 classic promoters widely used for driving antigen expression in pre-clinical and clinical studies. PmH5 was reported as a strong early and moderate late promoter while P7.5 was defined as a weak early and moderate late promoter (Cochran *et al.*, 1985; Sumner *et al.*, 1991; Wyatt *et al.*, 1996). Consistent with literature, we found that PmH5 had a vigorous gene transcriptional activity during 3-4 hpi but a relatively attenuated activity at late time points after 8 hpi. The mCherry protein synthesis under control of PmH5 also showed a strong activity from 2 to 6 hpi (MFI from 1.6 to 24.5) and a moderate activity from 8 to 12 hpi (MFI from 24.2 to 42.2). For the P7.5 promoter a weak early protein expression activity was observed from 2 to 6 hpi (MFI from 0.6 to 2.3) and a moderate late activity from 8 to 12 hpi (MFI from 1.6 to 7.2) (Fig.4.9). Since PmH5 has a strong activity at the early phase, it may not only over-express the antigen, which is

sandwiched in the MVA vector vaccine, to enhance the immunogenicity, but might also build up an immunodominance during boost vaccination (Baur *et al.*, 2010; Kastenmuller *et al.*, 2007). It has been shown that antigen driven by PmH5 elicited dramatically a higher immunogenicity than those by P7.5 (Orubu *et al.*, 2012). Moreover, the strong activity of PmH5 may expand the strength and broadness of the cellular immune response since it may produce different transcriptional products e.g. defective ribosomal products (DRIPs) (Drexler *et al.*, unpublished). In addition, in a recent report, PmH5 used to express multi-antigens in MVA showed a remarkable stability during passages compared with some other strong and newly developed promoters such as pSyn I or II (Wang *et al.*, 2010). However sometimes over-expressing transgene(s) in recMVA may lead to genetic instability caused by selective growth disadvantage (Cottingham and Carroll, 2013). Therefore, the moderate promoter P7.5 could become a preferable alternative for MVA vaccine or gene delivery vectors for certain transgenes. P7.5 has been employed for all recMVA vaccine constructs for human use in the Jenner institute, which have not shown any detectable genetical instability during manufacturing (Cottingham and Carroll, 2013). Therefore, our data suggest a promising usage of the established promoter platform in research and vaccine development.

5.3. The benefit of the BAC- recombinant MVA system to investigate viral gene function

The efficient BAC-based manipulation of MVA genome rendered us a tool to rapidly analyse MVA gene functions. Since the anti-biotic resistant gene for selection has been removed during the 2nd Red Recombination, the recMVA genome can be employed for further genomic manipulations. This would be preferable when multi-genetic insertions, deletions or mutations in the same MVA are in need. In addition, repeated manipulations of the MVA genome can also be achieved by the system to re-insert or revertant delete a gene in MVA which are necessary for investigation of gene function. Theoretically, GS1783 *E.coli* harbouring the BAC-MVA genome always stored at -70°C and manipulated below 32°C, will be available for further genome mutagenesis. We applied this platform to generate recombinant MVA to study *N1L* gene functions. We found even after three subsequent BAC genome mutations, GS1783 *E.coli* still kept an accurate recombination quality without any

evidence of efficiency reduction of the *en passant* technology. Therefore, this platform is reliable to be used for accumulated genome mutagenesis.

In addition, when we analysed the gene expression with western blot, MVA-N1L and MVA-OVA-N1L was found to express lower amounts of detectable N1 protein than VV, whereas the viral *H3L* gene was equivalently expressed (Fig.4.13 and Fig.4.14), although *N1L* was expressed under the control of its own promoter in *N1L* knock-in MVA and was orthotopically located in the genome. We therefore suggest that the transcriptional machinery for *N1L* gene expression might somehow be impaired in MVA during CVA attenuation.

5.4. Other applications of the BAC-recombinant MVA system to generate recMVA

Based on the established BAC- recombinant MVA system, we also generated some other recMVA for further investigation.

OVA is a model antigen used for immunological studies. In order to trap the recMVA-encoded OVA intracellularly during infection, we constructed MVA-BAC transfer plasmids that express non-secreting OVA by a standard cloning strategy (method detail is described in Appendix 8.1). The newly reconstituted recMVA will be used as tools for further research purposes.

In addition, we also harnessed the BAC system to fuse the *ova* gene to the C terminus of viral gene *B5R*. Of note, we utilized a different strategy to insert the large *ova* gene into the authentic C-terminus of the B5R gene (method detail is described in Appendix 8.2). These newly generated viruses will be used for further investigation.

Taking advantage of the established BAC-based MVA mutagenesis system, we accomplished the generation of a battery of recombinant MVA as tools for different research purposes in our working group. The new insights into the immunomodulatory role of vaccinia N1 from innate to adaptive immunity.

5.4.1. Vaccinia virus N1 inhibits MVA- induced IFN β production

The vaccinia virulence gene *N1L* is highly conserved in all strains of vaccinia virus (see in section 1.7). Inactivation of the *N1L* gene in VV has been reported to result in

attenuation in the murine infection model (Bartlett *et al.*, 2002; Kotwal *et al.*, 1989). N1 belongs to a family of VV B-cell lymphoma (Bcl)-2 like proteins whose members inhibit apoptosis and activation of pro-inflammatory transcription factors. Previous studies found that N1 can inhibit the pro-inflammatory signaling of NF- κ B by interacting with the IKK complex and TBK1, and was able to inhibit the signaling via IRF3 stimulation by binding to TBK1 (DiPerna *et al.*, 2004). Therefore, N1 was indicated as an immunodominator to suppress the production of type I interferon during VV infection. Compared with VV, MVA lost a list of immunodomains that were attributed to achieve inhibition of the innate immune response, including IFN-I signalling (Table.1.1). Upon viral infection, MVA is potent to induce the production of IFN-I *in vivo* and *in vitro* (DCs), such as in Flt3-L pDCs and GM-CSF-derived BMDCs (Dai. *et al.*, 2014; Waibler *et al.*, 2009). Among the MVA ancestors which were generated during CVA attenuation, CVA and CVA₁₅₂ can't elicit the production of IFN α and IFN β in infected Flt3-L pDCs. Interestingly, however, after 386 passages of CVA attenuation CVA₃₈₆-infected Flt3-L pDCs were able to produce detectable IFN β but not IFN α . Subsequently, after 572 passages of CVA, the resulting MVA was competent to induce both IFN α and IFN β secretion in infected pDCs and cDCs (Waibler *et al.*, 2009). Therefore, we were interested in investigating MVA having lost immunomodulators that account for IFN-I inhibition during virus attenuation. Of note, the viral gene *B18R* encoding for an IFN-I decoy receptor has suffered functional inactivation between MVA ancestor CVA₁₅₂ and CVA₃₈₆ because of a gene fragmentation. Viral B18 is supposed to reduce IFN α in DCs as a soluble viral protein but it could not inhibit IFN β . Furthermore, IFN β was confirmed to be negated by the intracellular viral protein(s). Since the well-known strong IFN-I inhibitor *E3L* gene remained intact in MVA, other viral proteins should be involved in the suppression of IFN β in DCs. *N1L* encodes the protein that is capable to inhibit IRF3 activation, but in MVA, its ortholog contains a 27-aa fragmentation in its C terminus. MVA-N1L is able to dramatically suppress mRNA transcription of *IFNA4* and *IFNB* in infected BMDCs at 6 hpi. Moreover, VV could block the MVA-induced production of both IFN α and IFN β in BMDCs. In contrast, VV Δ N1L was only able to inhibit MVA-induced IFN α , but not IFN β in BMDCs. The findings above indicate that N1 is a key inhibition factor functioning within pathways of IFN β activation (Dai. *et al.*, 2014). It reduces the level of activation of p-TBK1 and p-IRF3, and finally blocks the cytosolic DNA-sensing pathway of STING/TBK1/IRF3 upon viral infection (Dai *et al.*, unpublished).

The knowledge gained from these investigations revealed that: out of 200 VV encoded viral proteins, a couple of them are involved in VV-mediated IFN-I inhibition, however, their functions are not redundant. They impair IFN-I activation at different stages of the signaling pathways. Moreover, VV *N1L* gene alone is strong enough to shut down IFN β production, and therefore able to suppress the IFN-I signaling feedback loop.

Based on that, it would be necessary to scrutinize N1 mediated inhibition of IFN-I *in vivo* and *in vitro*. To preclude that the reduced levels of IFNA4 and IFNB (mRNA and protein) in the infected BMDCs might be caused by unwanted mutations in the viral backbone during BAC mutagenesis for recombinant MVA-N1L generation (Dai. *et al.*, 2014), a revertant virus having deleted a functional N1L (rev Δ N1L MVA) would be useful as a control for real-time quantitative PCR and ELISA of IFNA4 and IFNB. Determination of serum levels of IFN-I will bring us more physiologically relevant information. Furthermore, it is also important to study how N1 impacts the expression profiles of interferon stimulated genes (ISGs), such as CXCL10, Mx protein, OAS etc, in the context of MVA infection *in vitro*.

Besides, it was been shown recently that VV can induce a vigorous IL-12 induction in DCs as compared to MVA (Frenz *et al.*, 2010). Therefore, It will be interesting to demonstrate, whether viral proteins such as N1 or B18 could mediate IL-12 secretion by inhibition of IFN-I pathways.

5.4.2. N1 is not an anti-apoptotic protein

N1 has a structure similarity to Bcl-2 family members and was reported to negate STS-induced apoptosis after transfection or VV infection (Cooray *et al.*, 2007). Cooray *et al* showed that N1 can co-precipitate with pro-apoptotic proteins Bid, Bad and Bax presumably via its BH3 binding domain. However, a recent report contradicted this conclusion (Postigo and Way, 2012). Their data showed that N1 did not associate with Bid, Bad and Bax from VV infected cell lysates, and could not reduce both STS- and UV- induced apoptosis after transfection or VV infection. Since MVA lost partly VV anti-apoptotic factors, it is competent to induce robust apoptosis in infected cells as compared with VV. Therefore, we anticipated MVA would be a more sensitive vector tool for exploring protein functions on anti-apoptosis in the context of viral infection. Taking advantage of the *N1L* knock-in MVA, we examined

protection from STS-induced or MVA infection-induced apoptosis by MVA-N1L. We infected the cells with MVA for 6 hours before STS treatment because N1 expression was first detectable after 2 hpi and with a maximum synthesized during 4-8 hpi (Fig.4.13). PARP and Caspase 3 are the classical cellular apoptotic markers which function in converged positions most downstream in apoptosis signaling pathways. Our finding supports Antonio Postigo and co-workers' conclusion that N1 cannot suppress STS- or MVA infection-induced apoptosis.

MVA-induced T cell priming is mainly through cross-presentation (Alberts *et al.*, 1999). Suppressed apoptosis of infected cells is therefore supposed to delay the antigen up-take by the by-stander APCs and consequently may impair T cell priming. Our data precludes the possibility that the diminished T cell response found for MVA-OVA-N1L was a result of an anti-apoptotic function of N1.

5.4.3. Immune modulatory role of N1 in MVA-induced T cell responses

Vaccinia virus N1 is a potent virulence factor in mice, however, the underlying mechanisms are not fully understood. The report from Postigo and Way (2012) and our work indicate that N1 does not function as an anti-apoptotic protein (Fig.4.27). Besides, N1 was also reported as an inhibitor for interleukin-1 α -induced NF- κ B activation, although there is still controversy over its ability to block TNF α - induced NF- κ B activation (Graham *et al.*, 2008). In addition, we observed that MVA- specific T cell responses were dramatically impaired after *N1L* gene knock-in in MVA in a murine model. Among innate inflammatory cytokines, type I IFNs are considered to play a critical role in linking innate to adaptive immunity. N1 is a potent inhibitor of IFN-I production in MVA-infected DCs (Dai. *et al.*, 2014), therefore our experimental data strongly support the hypothesis that N1 impairs MVA-induced T cell responses through inhibition of type I interferon production or signalling. Here we dissect the role of N1 for i) MVA-induced primary activation of naïve T cells, ii) reactivation of memory T cells and iii) re-stimulation of antigen-specific CD4+ T cell lines, respectively as follows:

1) Impairment of T cell priming

Our data show that T cell priming was dramatically reduced in mice immunized with MVA-OVA-N1L (*N1L* knock-in MVA). Both, IFN γ and IL-2- producing antigen-specific CD4+ T cells and immunodominant epitope-specific CD8+ T cells were diminished.

This impairment was IFN-I signaling dependent (Fig.4.18 and Fig.4.19). We speculate that the inhibition of IFN-I by N1 in APCs may have several consequences: 1) the up-regulation of IFN-I dependent co-stimulatory molecules could be affected. For instance, CD80/86 may be down-regulated in MVA-N1L infected APCs. Therefore the signal 2 required for naïve T cell activation would be impaired. Antigen recognition in the absence of sufficient co-stimulation will lead to functionally defective T cells. Especially, the expression of IL-2 (T cell growth factor) and the high-affinity IL-2 receptor are highly dependent on co-stimulation through CD28 signaling. When absent, activation of naïve T cells and proliferation of primed T cells will be diminished. 2) Since IFN-I inhibit apoptotic cell death of activated CD4+ T cells (Marrack *et al.*, 1999), suppression of IFN-I signaling would lead to increased apoptosis of activated CD4+ T cells. 3) Poor clonal expansion of CD4+ and CD8+ T cells may be caused by reduced IFN-I which effects T cells directly through their cognate IFN-I signaling (Frenz *et al.*, 2010; Garcia-Arriaza *et al.*, 2013).

2) Reduced expansion of IL2+ T cell populations

It is believed that CD80/CD86-CD28 co-stimulation is required for initiating the induction naïve T cells, but is not necessary for reactivating memory T cells (Boesteanu and Katsikis, 2009; Borowski *et al.*, 2007; Fang and Sigal, 2006; Fuse *et al.*, 2008). Recently, several reports show that in memory CD4+ T cells, blocking the co-stimulatory CD28 signaling led to non-discernable differences in the amount of IFN- γ production, while IL-2 production was significantly decreased (Boesteanu and Katsikis, 2009; Ndejemi *et al.*, 2006). In line with this, our data demonstrate that, in the memory response, amounts of IFN γ -producing CD4+ and CD8+ T cells were comparable in mice vaccinated with MVA-OVA or MVA-OVA-N1L. Nevertheless, IL-2-producing T cells were markedly decreased in MVA-OVA-N1L vaccinated mice. Since N1 could impair DC maturation by IFN-I inhibition, co-stimulatory molecules might be poorly expressed in DCs from boosted mice after MVA-OVA-N1L vaccination. Of note, since MVA was demonstrated to impair maturation of infected DCs, but promote maturation of non-infected bystander DCs, we speculate that co-stimulatory signaling in bystander DCs close to MVA-OVA-N1L infected DC will be hampered (Pascutti *et al.*, 2011). Thereby, this study supports the dogma that IL-2 rather than IFN γ production is more dependent on CD28-mediated co-stimulatory

signaling. Our data reveal specific requirements for memory T cell activation upon MVA boosting.

Besides, our previous data showed that, the priming of subdominant antigen-specific CD8⁺ T cells in vaccinated IFNAR^{-/-} mice was paradoxically higher compared to wt mice, although the immunodominant B8R-specific T cell response was significantly decreased (Fig.4.19). It has been described that interfering with the immunodominant B8R-specific CD8⁺ T cell response will subsequently promote the subdominant antigen-specific T cell response (Baur *et al.*, 2010). In line with this hypothesis the increase of the CD8⁺ T cell response against the subdominant A8R epitope in immunized IFNAR^{-/-} mice may be due to the weakened immunodominant B8R-specific CD8⁺ T cell response.

3) N1-independent re-activation of antigen-specific CD4⁺ T cell lines

Memory and effector T cells have a lower activation threshold since they have a higher TCR-pMHC binding affinity. Antigen-specific CD4⁺ T cell lines were generated by weekly re-stimulating with peptide-loaded splenocytes *in vitro*. It has been demonstrated that *in vitro* activation of memory T cells is independent of CD28 co-stimulatory signaling (Bachmann *et al.*, 1999; Flynn and Mullbacher, 1996). Consistent with these findings, we observed no difference for IFN γ or IL-2 secretion in antigen-specific CD4⁺ T cells stimulated by BMDCs infected by MVA-wt or MVA-N1L. Our data suggest a decreasing dependency on IFN-I induced co-stimulatory signaling from naïve T cells to memory T cells and then to antigen-specific CD4⁺ T cell lines based on a decreased activation threshold.

Based on our findings, we postulate that N1 inhibits MVA-induced T cell priming, and impairs MVA-mediated secondary immune responses for IL-2 production. This inhibition seems to be exerted by interrupting IFN-I signalling in the host. To this point, the orchestration of how virulence factor N1 induces suppression of innate immunity and thereby affecting adaptive immunity needs further investigation.

We have demonstrated that MVA-induced T cell priming is highly dependent on IFN-I signaling through the interferon-alpha receptor (IFNAR). Since MVA-OVA-N1L caused impairment of T cell priming through IFN-I suppression by inhibiting the activation of TBK1/IRF3/IFNB signaling pathway (Dai *et al.*, 2014), IFN-I could presumably up-regulate co-stimulatory molecules through the type I interferon

feedback loop in DCs, and hence mature DCs and enhance CD4 T cell immunity. (Schaefer *et al.*, 1999). Besides, IFN-I is also able to directly affect T cells in a bidirectional way: in the priming phase, IFN-I promote clonal expansion of effector T cells (Garcia-Arriaza *et al.*, 2013), however, during the memory phase, IFN-I is considered to induce apoptosis in effector T cells through the IFNAR on T cells (Bahl *et al.*, 2010; McNally *et al.*, 2001). Therefore, it would be interesting to dissect which IFN-I signaling pathway is important for MVA- induced T cell priming and is the target for the *N1L* knock-in MVA induced impairment of T cell priming. For this purpose, T cell depleted mice, which were reconstituted with adoptively transferred naïve T cells from *IFNAR*^{-/-} mice (IFNAR is deficient only in T cells), will serve as good model. Dendritic cells require IFN-I for maturation and can subsequently induce CD4⁺ Th1 immunity (Schaefer *et al.*, 1999). By measuring T cell priming in MVA-OVA-N1L or MVA-OVA vaccinated mice, which were adoptively transferred with WT or *IFNAR*^{-/-} T cells, we may be able to define the importance of IFN-I signaling in T cells for MVA-elicited T cell priming.

In addition, our work indicates that the suppression of IFN-I production may lead to severe impairment of T cell priming and partial impairment of T cell boosting. Based on the role that N1 plays in T cell responses, this impairment could be explained by inhibition of DC maturation upon *N1L* knock-in MVA infection. CD80/CD86-CD28 was reported to play a pivotal role for T cell priming and for IL-2 production in the recall (Boesteanu and Katsikis, 2009; Ndejemi *et al.*, 2006). Therefore, it will be interesting to investigate the expression level of maturation markers such as co-stimulatory molecules (CD80/CD86, CD40) or MHC-II on the surface of APC in the context of infection with MVA-OVA-N1L, MVA-OVA or MVA-OVA- Δ N1L *in vitro* and *in vivo*.

Moreover, as reported by Havenar-Daughton *et al.*, the direct action of IFN-I on CD4⁺ T cells is important for clonal expansion *in vivo* in the LCMV infection model (Havenar-Daughton *et al.*, 2006) To investigate whether the impaired CD4⁺ T cell priming in MVA-OVA-N1L immunized mice is due to the limited clonal expansion caused by restrained IFN-I production, we will assess CD4⁺ T cell proliferation profiles *in vitro* and *in vivo*. The determination of T cell proliferation rather than T cell priming will provide a more conclusive insight into the mechanisms of the impaired T cell activation caused by N1.

Furthermore, our investigations indicate that there were likely different requirements for T cell responses between priming and boosting upon MVA and N1L knock-in MVA vaccination. Both MVA-induced CD4⁺ T cell priming and secondary immune responses were impaired by N1, however with distinguished impact. A comparative analysis of the quality and quantity of naïve versus memory T cell responses in the same host may elucidate the different effects of N1 on naïve CD4⁺ and memory T responses.

5.4.4. Role of N1L in NF-κB activation in the context of MVA infection

N1 is a multi-functional protein that is also able to inhibit pro-inflammatory signaling (DiPerna *et al.*, 2004). DiPerna *et al.* reported that N1 could inhibit NF-κB activation by targeting the iKK complex. However, no obvious inhibition of the IL-1β and TNF-α induced NF-κB activation in the context of *N1L* knock-out VV infection was observed (Cooray *et al.*, 2007; Graham *et al.*, 2008). Their explanation was that there were some other NF-κB inhibitors encoded by VV which masked a possible N1 effect. Actually, as compared with VV, MVA lost several suppressors of NF-κB signaling, such as *A52R*, *K1L*, *M2L* (see Table 1.1). Therefore, it would be interesting to measure NF-κB activation in the context of MVA infection e.g. by using an NF-κB reporter system.

5.4.5. Implication for MVA vector vaccine optimization

Based on our data, IFN-I signaling is inferred as an important factor in mediating MVA-induced T cell responses for both priming and boosting. The viral virulence gene *N1L*, which encodes a protein inhibiting the IFN-I signaling pathway, results in a remarkable decrease in antigen-specific T cell responses. Therefore, to improve the immunogenicity elicited by MVA, deletion of other MVA genes targeting type I interferon signaling would be a promising approach. Some reports have shown the good efficacy of MVA-vector vaccines against HIV/AIDS by deleting viral genes *C6L* and *K7R* (Garcia-Arriaza *et al.*, 2013). Based on our BAC- mutagenesis platform, we could not only insert desired genes encoding for antigens, but also delete the existing viral immunomodulatory genes listed in Table 1.1. Since IFN-I could promote the antigen-specific T cell response, it might be useful to evaluate the MVA-induced immunogenicity by adding IFNα/β or its stimulators such as poly I:C as adjuvants.

6. Final conclusion

1) ***En passant*-BAC: A versatile platform for MVA mutagenesis**

The novel BAC system for MVA mutagenesis by the *en passant* method proved to be highly efficient. A battery of transfer vectors has been developed for target gene-insertion into the MVA deletion VI region. VV promoters with different strength (strong, moderate, weak) and temporal activity (early, intermediate, late, constitutive) were characterized for these vectors. The selective marker (resistance) can be removed from the recMVA generated by this method, which facilitates subsequent manipulations of recMVA genome using the same method. Besides, the BAC-GFP cassette may be optionally kept as a viral marker or alternatively, were efficiently deleted in self-excising MVA-BACs. There were no signs of genetic instability in this system. All antigens driven by the respective VV promoters in MVA deletion VI region were expressed with expected strength and kinetics as determined on the level of transcription and translation. We have exploited this versatile platform by using different strategies to generate recMVA. Generally, the foreign antigen gene can be inserted into the MVA deletion VI region by using pEP-MVA-dVI-VV promoter plasmids. Under these circumstances, the recMVA will be generated according to the standard method as described for the MVA-dVI-P11mCherry generation. To create deletions or insert or mutate short sequences, the optimal design of the primer sequences used for amplification of the marker cassette is critical. The *N1L* knock-in and respective revertant knock-out recMVA were generated following this strategy. For insertion of even larger sequences, such as promoters, genes or complete expression cassettes, a transfer plasmid construct optimized to harbour these sequences as an intermediate has to be created as demonstrated for MVA-B5R/OVA generation.

Taken together, our data suggest an efficient and reliable system for MVA mutagenesis and a promising platform for MVA-vector vaccine development.

2) **New role of vaccinia virulence gene *N1L* in adaptive immunity**

In order to investigate immunologically relevant functions of the vaccinia virulence gene *N1L*, we applied the newly-established MVA-BAC mutagenesis system for generating *N1L* knock-in as well as respective revertant MVA. Since a series of immunomodulators are lost in MVA during CVA attenuation, the investigation of *N1L*

functions in the context of MVA infection seems more sensitive than in the context of VV. Thereby, we could extend the functional repertoire of N1 from innate to adaptive immunity. *N1L* knock-in MVA was able to severely inhibit MVA-induced T cell priming. This inhibition was highly dependent on IFN-I signaling. Besides, for secondary immune responses, N1 knock-in MVA could significantly impair the expansion of IL-2-secreting T cells while IFN γ secretion was unchanged. Our data for the first time depict a mechanism that *N1L* impacts activation of naïve and memory T cells via IFN-I mediated co-stimulatory signaling, and demonstrate the function of *N1L* as the virus virulence gene interfering with adaptive immunity.

MVA has been proposed as a boosting vaccine in the heterologous prime/boost vaccination strategies. The elucidation of characteristic features of N1 as an important viral immunomodulator increases our understanding of host-pathogen interplay and provides relevant information for vaccine optimization.

7. Reference

- Alberts, B.M., Ayala, F.J., Botstein, D., Frank, E., Holmes, E.W., Lee, R.D., Macagno, E.R., Marrack, P., Oparil, S., Orkin, S.H., *et al.* (1999). Proposed changes for NIH's Center for Scientific Review. Panel on Scientific Boundaries for Review. Center for Scientific Review Advisory Committee, National Institutes of Health. *Science* *285*, 666-667.
- Alexander, W.A., Moss, B., and Fuerst, T.R. (1992). Regulated expression of foreign genes in vaccinia virus under the control of bacteriophage T7 RNA polymerase and the Escherichia coli lac repressor. *Journal of virology* *66*, 2934-2942.
- Alexopoulou, L., Holt, A.C., Medzhitov, R., and Flavell, R.A. (2001). Recognition of double-stranded RNA and activation of NF-kappaB by Toll-like receptor 3. *Nature* *413*, 732-738.
- Bachmann, M.F., Gallimore, A., Linkert, S., Cerundolo, V., Lanzavecchia, A., Kopf, M., and Viola, A. (1999). Developmental regulation of Lck targeting to the CD8 coreceptor controls signaling in naive and memory T cells. *The Journal of experimental medicine* *189*, 1521-1530.
- Bahl, K., Huebner, A., Davis, R.J., and Welsh, R.M. (2010). Analysis of apoptosis of memory T cells and dendritic cells during the early stages of viral infection or exposure to toll-like receptor agonists. *Journal of virology* *84*, 4866-4877.
- Barbalat, R., Lau, L., Locksley, R.M., and Barton, G.M. (2009). Toll-like receptor 2 on inflammatory monocytes induces type I interferon in response to viral but not bacterial ligands. *Nature immunology* *10*, 1200-1207.
- Bartlett, N., Symons, J.A., Tschärke, D.C., and Smith, G.L. (2002). The vaccinia virus N1L protein is an intracellular homodimer that promotes virulence. *The Journal of general virology* *83*, 1965-1976.
- Baur, K., Brinkmann, K., Schweneker, M., Patzold, J., Meisinger-Henschel, C., Hermann, J., Steigerwald, R., Chaplin, P., Suter, M., and Hausmann, J. (2010). Immediate-early expression of a recombinant antigen by modified vaccinia virus ankara breaks the immunodominance of strong vector-specific B8R antigen in acute and memory CD8 T-cell responses. *Journal of virology* *84*, 8743-8752.
- Beattie, E., Tartaglia, J., and Paoletti, E. (1991). Vaccinia virus-encoded eIF-2 alpha homolog abrogates the antiviral effect of interferon. *Virology* *183*, 419-422.
- Blanchard, T.J., Alcami, A., Andrea, P., and Smith, G.L. (1998). Modified vaccinia virus Ankara undergoes limited replication in human cells and lacks several immunomodulatory proteins: implications for use as a human vaccine. *The Journal of general virology* *79* (Pt 5), 1159-1167.
- Boesteanu, A.C., and Katsikis, P.D. (2009). Memory T cells need CD28 costimulation to remember. *Seminars in immunology* *21*, 69-77.
- Borowski, A.B., Boesteanu, A.C., Mueller, Y.M., Carafides, C., Topham, D.J., Altman, J.D., Jennings, S.R., and Katsikis, P.D. (2007). Memory CD8+ T cells require CD28 costimulation. *Journal of immunology* *179*, 6494-6503.
- Bowie, A., Kiss-Toth, E., Symons, J.A., Smith, G.L., Dower, S.K., and O'Neill, L.A. (2000). A46R and A52R from vaccinia virus are antagonists of host IL-1 and toll-like

receptor signaling. *Proceedings of the National Academy of Sciences of the United States of America* *97*, 10162-10167.

Brave, A., Ljungberg, K., Wahren, B., and Liu, M.A. (2007). Vaccine delivery methods using viral vectors. *Molecular pharmaceutics* *4*, 18-32.

Breathnach, C.C., Clark, H.J., Clark, R.C., Olsen, C.W., Townsend, H.G., and Lunn, D.P. (2006). Immunization with recombinant modified vaccinia Ankara (rMVA) constructs encoding the HA or NP gene protects ponies from equine influenza virus challenge. *Vaccine* *24*, 1180-1190.

Brinkmann, V., Geiger, T., Alkan, S., and Heusser, C.H. (1993). Interferon alpha increases the frequency of interferon gamma-producing human CD4+ T cells. *The Journal of experimental medicine* *178*, 1655-1663.

Broyles, S.S. (2003). Vaccinia virus transcription. *The Journal of general virology* *84*, 2293-2303.

Carreno, B.M., Bennett, F., Chau, T.A., Ling, V., Luxenberg, D., Jussif, J., Baroja, M.L., and Madrenas, J. (2000). CTLA-4 (CD152) can inhibit T cell activation by two different mechanisms depending on its level of cell surface expression. *Journal of immunology* *165*, 1352-1356.

Carroll, M.W., and Moss, B. (1997). Host range and cytopathogenicity of the highly attenuated MVA strain of vaccinia virus: propagation and generation of recombinant viruses in a nonhuman mammalian cell line. *Virology* *238*, 198-211.

Chang, H.W., Watson, J.C., and Jacobs, B.L. (1992). The E3L gene of vaccinia virus encodes an inhibitor of the interferon-induced, double-stranded RNA-dependent protein kinase. *Proceedings of the National Academy of Sciences of the United States of America* *89*, 4825-4829.

Cheltsov, A.V., Aoyagi, M., Aleshin, A., Yu, E.C., Gilliland, T., Zhai, D., Bobkov, A.A., Reed, J.C., Liddington, R.C., and Abagyan, R. (2010). Vaccinia virus virulence factor N1L is a novel promising target for antiviral therapeutic intervention. *Journal of medicinal chemistry* *53*, 3899-3906.

Chen, R.A., Ryzhakov, G., Cooray, S., Randow, F., and Smith, G.L. (2008). Inhibition of IkkappaB kinase by vaccinia virus virulence factor B14. *PLoS pathogens* *4*, e22.

Cochran, M.A., Puckett, C., and Moss, B. (1985). In vitro mutagenesis of the promoter region for a vaccinia virus gene: evidence for tandem early and late regulatory signals. *Journal of virology* *54*, 30-37.

Condit, R.C., and Niles, E.G. (2002). Regulation of viral transcription elongation and termination during vaccinia virus infection. *Biochimica et biophysica acta* *1577*, 325-336.

Cooray, S., Bahar, M.W., Abrescia, N.G., McVey, C.E., Bartlett, N.W., Chen, R.A., Stuart, D.I., Grimes, J.M., and Smith, G.L. (2007). Functional and structural studies of the vaccinia virus virulence factor N1 reveal a Bcl-2-like anti-apoptotic protein. *The Journal of general virology* *88*, 1656-1666.

Corona Gutierrez, C.M., Tinoco, A., Lopez Contreras, M., Navarro, T., Calzado, P., Vargas, L., Reyes, L., Posternak, R., and Rosales, R. (2002). Clinical protocol. A phase II study: efficacy of the gene therapy of the MVA E2 recombinant virus in the treatment of precancerous lesions (NIC I and NIC II) associated with infection of oncogenic human papillomavirus. *Human gene therapy* *13*, 1127-1140.

- Cosma, A., Nagaraj, R., Buhler, S., Hinkula, J., Busch, D.H., Sutter, G., Goebel, F.D., and Erfle, V. (2003). Therapeutic vaccination with MVA-HIV-1 nef elicits Nef-specific T-helper cell responses in chronically HIV-1 infected individuals. *Vaccine* 22, 21-29.
- Cottingham, M.G., Andersen, R.F., Spencer, A.J., Saurya, S., Furze, J., Hill, A.V., and Gilbert, S.C. (2008). Recombination-mediated genetic engineering of a bacterial artificial chromosome clone of modified vaccinia virus Ankara (MVA). *PloS one* 3, e1638.
- Cottingham, M.G., and Carroll, M.W. (2013). Recombinant MVA vaccines: dispelling the myths. *Vaccine* 31, 4247-4251.
- Cottingham, M.G., and Gilbert, S.C. (2010). Rapid generation of markerless recombinant MVA vaccines by en passant recombineering of a self-excising bacterial artificial chromosome. *Journal of virological methods* 168, 233-236.
- Dai, P., Wang, W., Cao, H., Avogadri, F., Dai, L., Drexler, I., Joyce, J.A., Li, X.D., Chen, Z., Merghoub, T., *et al.* (2014). Modified Vaccinia Virus Ankara Triggers Type I IFN Production in Murine Conventional Dendritic Cells via a cGAS/STING-Mediated DNA-Sensing Pathway. *PLoS pathogens* *In press*.
- Delaloye, J., Roger, T., Steiner-Tardivel, Q.G., Le Roy, D., Knaup Reymond, M., Akira, S., Petrilli, V., Gomez, C.E., Perdiguero, B., Tschopp, J., *et al.* (2009). Innate immune sensing of modified vaccinia virus Ankara (MVA) is mediated by TLR2-TLR6, MDA-5 and the NALP3 inflammasome. *PLoS pathogens* 5, e1000480.
- Di Nicola, M., Carlo-Stella, C., Anichini, A., Mortarini, R., Guidetti, A., Tragni, G., Gallino, F., Del Vecchio, M., Ravagnani, F., Morelli, D., *et al.* (2003). Clinical protocol. Immunization of patients with malignant melanoma with autologous CD34(+) cell-derived dendritic cells transduced ex vivo with a recombinant replication-deficient vaccinia vector encoding the human tyrosinase gene: a phase I trial. *Human gene therapy* 14, 1347-1360.
- Di Nicola, M., Carlo-Stella, C., Mortarini, R., Baldassari, P., Guidetti, A., Gallino, G.F., Del Vecchio, M., Ravagnani, F., Magni, M., Chaplin, P., *et al.* (2004). Boosting T cell-mediated immunity to tyrosinase by vaccinia virus-transduced, CD34(+)-derived dendritic cell vaccination: a phase I trial in metastatic melanoma. *Clinical cancer research : an official journal of the American Association for Cancer Research* 10, 5381-5390.
- DiPerna, G., Stack, J., Bowie, A.G., Boyd, A., Kotwal, G., Zhang, Z., Arvikar, S., Latz, E., Fitzgerald, K.A., and Marshall, W.L. (2004). Poxvirus protein N1L targets the I-kappaB kinase complex, inhibits signaling to NF-kappaB by the tumor necrosis factor superfamily of receptors, and inhibits NF-kappaB and IRF3 signaling by toll-like receptors. *The Journal of biological chemistry* 279, 36570-36578.
- Drexler, I., Staib, C., and Sutter, G. (2004). Modified vaccinia virus Ankara as antigen delivery system: how can we best use its potential? *Current opinion in biotechnology* 15, 506-512.
- Earl, P.L., Americo, J.L., Wyatt, L.S., Eller, L.A., Whitbeck, J.C., Cohen, G.H., Eisenberg, R.J., Hartmann, C.J., Jackson, D.L., Kulesh, D.A., *et al.* (2004). Immunogenicity of a highly attenuated MVA smallpox vaccine and protection against monkeypox. *Nature* 428, 182-185.

- Fang, M., and Sigal, L.J. (2006). Direct CD28 costimulation is required for CD8+ T cell-mediated resistance to an acute viral disease in a natural host. *Journal of immunology* *177*, 8027-8036.
- Ferguson, B.J., Benfield, C.T., Ren, H., Lee, V.H., Frazer, G.L., Strnadova, P., Sumner, R.P., and Smith, G.L. (2013). Vaccinia virus protein N2 is a nuclear IRF3 inhibitor that promotes virulence. *The Journal of general virology* *94*, 2070-2081.
- Flynn, K., and Mullbacher, A. (1996). Memory alloreactive cytotoxic T cells do not require costimulation for activation in vitro. *Immunology and cell biology* *74*, 413-420.
- Frenz, T., Waibler, Z., Hofmann, J., Hamdorf, M., Lantermann, M., Reizis, B., Tovey, M.G., Aichele, P., Sutter, G., and Kalinke, U. (2010). Concomitant type I IFN receptor-triggering of T cells and of DC is required to promote maximal modified vaccinia virus Ankara-induced T-cell expansion. *European journal of immunology* *40*, 2769-2777.
- Fuse, S., Zhang, W., and Usherwood, E.J. (2008). Control of memory CD8+ T cell differentiation by CD80/CD86-CD28 costimulation and restoration by IL-2 during the recall response. *Journal of immunology* *180*, 1148-1157.
- Galindo, I., Lorenzo, M.M., and Blasco, R. (2001). Set of vectors for the expression of histidine-tagged proteins in vaccinia virus recombinants. *BioTechniques* *30*, 524-526, 528-529.
- Garcia-Arriaza, J., Arnaez, P., Gomez, C.E., Sorzano, C.O., and Esteban, M. (2013). Improving Adaptive and Memory Immune Responses of an HIV/AIDS Vaccine Candidate MVA-B by Deletion of Vaccinia Virus Genes (C6L and K7R) Blocking Interferon Signaling Pathways. *PloS one* *8*, e66894.
- Gedey, R., Jin, X.L., Hinthong, O., and Shisler, J.L. (2006). Poxviral regulation of the host NF-kappaB response: the vaccinia virus M2L protein inhibits induction of NF-kappaB activation via an ERK2 pathway in virus-infected human embryonic kidney cells. *Journal of virology* *80*, 8676-8685.
- Goet, P., Robert, X., and Courcelle, E. (2003). ESPript/ENDscript: Extracting and rendering sequence and 3D information from atomic structures of proteins. *Nucleic acids research* *31*, 3320-3323.
- Graham, S.C., Bahar, M.W., Cooray, S., Chen, R.A., Whalen, D.M., Abrescia, N.G., Alderton, D., Owens, R.J., Stuart, D.I., Smith, G.L., *et al.* (2008). Vaccinia virus proteins A52 and B14 Share a Bcl-2-like fold but have evolved to inhibit NF-kappaB rather than apoptosis. *PLoS pathogens* *4*, e1000128.
- Guerra, S., Caceres, A., Knobloch, K.P., Horak, I., and Esteban, M. (2008). Vaccinia virus E3 protein prevents the antiviral action of ISG15. *PLoS pathogens* *4*, e1000096.
- Harte, M.T., Haga, I.R., Maloney, G., Gray, P., Reading, P.C., Bartlett, N.W., Smith, G.L., Bowie, A., and O'Neill, L.A. (2003). The poxvirus protein A52R targets Toll-like receptor signaling complexes to suppress host defense. *The Journal of experimental medicine* *197*, 343-351.
- Havenar-Daughton, C., Kolumam, G.A., and Murali-Krishna, K. (2006). Cutting Edge: The direct action of type I IFN on CD4 T cells is critical for sustaining clonal expansion in response to a viral but not a bacterial infection. *Journal of immunology* *176*, 3315-3319.

- Hinthong, O., Jin, X.L., and Shisler, J.L. (2008). Characterization of wild-type and mutant vaccinia virus M2L proteins' abilities to localize to the endoplasmic reticulum and to inhibit NF-kappaB activation during infection. *Virology* 373, 248-262.
- Hogquist, K.A., Jameson, S.C., Heath, W.R., Howard, J.L., Bevan, M.J., and Carbone, F.R. (1994). T cell receptor antagonist peptides induce positive selection. *Cell* 76, 17-27.
- Honda, K., Takaoka, A., and Taniguchi, T. (2006). Type I interferon [corrected] gene induction by the interferon regulatory factor family of transcription factors. *Immunity* 25, 349-360.
- Hwang, S.Y., Hertzog, P.J., Holland, K.A., Sumarsono, S.H., Tymms, M.J., Hamilton, J.A., Whitty, G., Bertoncello, I., and Kola, I. (1995). A null mutation in the gene encoding a type I interferon receptor component eliminates antiproliferative and antiviral responses to interferons alpha and beta and alters macrophage responses. *Proceedings of the National Academy of Sciences of the United States of America* 92, 11284-11288.
- Ishii, K.J., Coban, C., Kato, H., Takahashi, K., Torii, Y., Takeshita, F., Ludwig, H., Sutter, G., Suzuki, K., Hemmi, H., *et al.* (2006). A Toll-like receptor-independent antiviral response induced by double-stranded B-form DNA. *Nature immunology* 7, 40-48.
- Jacobs, N., Bartlett, N.W., Clark, R.H., and Smith, G.L. (2008). Vaccinia virus lacking the Bcl-2-like protein N1 induces a stronger natural killer cell response to infection. *The Journal of general virology* 89, 2877-2881.
- Kastenmuller, W., Gasteiger, G., Gronau, J.H., Baier, R., Ljapoci, R., Busch, D.H., and Drexler, I. (2007). Cross-competition of CD8+ T cells shapes the immunodominance hierarchy during boost vaccination. *The Journal of experimental medicine* 204, 2187-2198.
- Kates, J.R., and McAuslan, B.R. (1967). Poxvirus DNA-dependent RNA polymerase. *Proceedings of the National Academy of Sciences of the United States of America* 58, 134-141.
- Keating, S.E., Maloney, G.M., Moran, E.M., and Bowie, A.G. (2007). IRAK-2 participates in multiple toll-like receptor signaling pathways to NFkappaB via activation of TRAF6 ubiquitination. *The Journal of biological chemistry* 282, 33435-33443.
- Koksal, A.C., and Cingolani, G. (2011). Dimerization of Vaccinia virus VH1 is essential for dephosphorylation of STAT1 at tyrosine 701. *The Journal of biological chemistry* 286, 14373-14382.
- Kotwal, G.J., Hugin, A.W., and Moss, B. (1989). Mapping and insertional mutagenesis of a vaccinia virus gene encoding a 13,800-Da secreted protein. *Virology* 171, 579-587.
- Lin, R., Heylbroeck, C., Pitha, P.M., and Hiscott, J. (1998). Virus-dependent phosphorylation of the IRF-3 transcription factor regulates nuclear translocation, transactivation potential, and proteasome-mediated degradation. *Molecular and cellular biology* 18, 2986-2996.
- Maluquer de Motes, C., Cooray, S., Ren, H., Almeida, G.M., McGourty, K., Bahar, M.W., Stuart, D.I., Grimes, J.M., Graham, S.C., and Smith, G.L. (2011). Inhibition of

apoptosis and NF-kappaB activation by vaccinia protein N1 occur via distinct binding surfaces and make different contributions to virulence. *PLoS pathogens* 7, e1002430.

Marrack, P., Kappler, J., and Mitchell, T. (1999). Type I interferons keep activated T cells alive. *The Journal of experimental medicine* 189, 521-530.

Mathew, A., O'Bryan, J., Marshall, W., Kotwal, G.J., Terajima, M., Green, S., Rothman, A.L., and Ennis, F.A. (2008). Robust intrapulmonary CD8 T cell responses and protection with an attenuated N1L deleted vaccinia virus. *PloS one* 3, e3323.

Mayr, A., Stickl, H., Muller, H.K., Danner, K., and Singer, H. (1978). [The smallpox vaccination strain MVA: marker, genetic structure, experience gained with the parenteral vaccination and behavior in organisms with a debilitated defence mechanism (author's transl)]. *Zentralblatt fur Bakteriologie, Parasitenkunde, Infektionskrankheiten und Hygiene Erste Abteilung Originale Reihe B: Hygiene, Betriebshygiene, praventive Medizin* 167, 375-390.

McConkey, S.J., Reece, W.H., Moorthy, V.S., Webster, D., Dunachie, S., Butcher, G., Vuola, J.M., Blanchard, T.J., Gothard, P., Watkins, K., *et al.* (2003). Enhanced T-cell immunogenicity of plasmid DNA vaccines boosted by recombinant modified vaccinia virus Ankara in humans. *Nature medicine* 9, 729-735.

McNally, J.M., Zarozinski, C.C., Lin, M.Y., Brehm, M.A., Chen, H.D., and Welsh, R.M. (2001). Attrition of bystander CD8 T cells during virus-induced T-cell and interferon responses. *Journal of virology* 75, 5965-5976.

McShane, H., Pathan, A.A., Sander, C.R., Keating, S.M., Gilbert, S.C., Huygen, K., Fletcher, H.A., and Hill, A.V. (2004). Recombinant modified vaccinia virus Ankara expressing antigen 85A boosts BCG-primed and naturally acquired antimycobacterial immunity in humans. *Nature medicine* 10, 1240-1244.

Meisinger-Henschel, C., Schmidt, M., Lukassen, S., Linke, B., Krause, L., Konietzny, S., Goesmann, A., Howley, P., Chaplin, P., Suter, M., *et al.* (2007). Genomic sequence of chorioallantois vaccinia virus Ankara, the ancestor of modified vaccinia virus Ankara. *The Journal of general virology* 88, 3249-3259.

Meisinger-Henschel, C., Spath, M., Lukassen, S., Wolferstatter, M., Kachelriess, H., Baur, K., Dirmeier, U., Wagner, M., Chaplin, P., Suter, M., *et al.* (2010). Introduction of the six major genomic deletions of modified vaccinia virus Ankara (MVA) into the parental vaccinia virus is not sufficient to reproduce an MVA-like phenotype in cell culture and in mice. *Journal of virology* 84, 9907-9919.

Merzlyak, E.M., Goedhart, J., Shcherbo, D., Bulina, M.E., Shcheglov, A.S., Fradkov, A.F., Gaintzeva, A., Lukyanov, K.A., Lukyanov, S., Gadella, T.W., *et al.* (2007). Bright monomeric red fluorescent protein with an extended fluorescence lifetime. *Nature methods* 4, 555-557.

Montoya, M., Schiavoni, G., Mattei, F., Gresser, I., Belardelli, F., Borrow, P., and Tough, D.F. (2002). Type I interferons produced by dendritic cells promote their phenotypic and functional activation. *Blood* 99, 3263-3271.

Moorthy, V.S., Pinder, M., Reece, W.H., Watkins, K., Atabani, S., Hannan, C., Bojang, K., McAdam, K.P., Schneider, J., Gilbert, S., *et al.* (2003). Safety and immunogenicity of DNA/modified vaccinia virus ankara malaria vaccination in African adults. *The Journal of infectious diseases* 188, 1239-1244.

- Moss, B. (1996). Genetically engineered poxviruses for recombinant gene expression, vaccination, and safety. *Proceedings of the National Academy of Sciences of the United States of America* *93*, 11341-11348.
- Mulryan, K., Ryan, M.G., Myers, K.A., Shaw, D., Wang, W., Kingsman, S.M., Stern, P.L., and Carroll, M.W. (2002). Attenuated recombinant vaccinia virus expressing oncofetal antigen (tumor-associated antigen) 5T4 induces active therapy of established tumors. *Molecular cancer therapeutics* *1*, 1129-1137.
- Murphy, K. (2007). *Janeway's Immunobiology*.
- Mwau, M., Ceber, I., Sutton, J., Chikoti, P., Winstone, N., Wee, E.G., Beattie, T., Chen, Y.H., Dorrell, L., McShane, H., *et al.* (2004). A human immunodeficiency virus 1 (HIV-1) clade A vaccine in clinical trials: stimulation of HIV-specific T-cell responses by DNA and recombinant modified vaccinia virus Ankara (MVA) vaccines in humans. *The Journal of general virology* *85*, 911-919.
- Nam, J.H., Cha, S.L., and Cho, H.W. (2002). Immunogenicity of a recombinant MVA and a DNA vaccine for Japanese encephalitis virus in swine. *Microbiology and immunology* *46*, 23-28.
- Ndejemi, M.P., Teijaro, J.R., Patke, D.S., Bingaman, A.W., Chandok, M.R., Azimzadeh, A., Nadler, S.G., and Farber, D.L. (2006). Control of memory CD4 T cell recall by the CD28/B7 costimulatory pathway. *Journal of immunology* *177*, 7698-7706.
- Nguyen, K.B., Watford, W.T., Salomon, R., Hofmann, S.R., Pien, G.C., Morinobu, A., Gadina, M., O'Shea, J.J., and Biron, C.A. (2002). Critical role for STAT4 activation by type 1 interferons in the interferon-gamma response to viral infection. *Science* *297*, 2063-2066.
- Pascutti, M.F., Rodriguez, A.M., Falivene, J., Giavedoni, L., Drexler, I., and Gherardi, M.M. (2011). Interplay between modified vaccinia virus Ankara and dendritic cells: phenotypic and functional maturation of bystander dendritic cells. *Journal of virology* *85*, 5532-5545.
- Perdiguerro, B., and Esteban, M. (2009). The interferon system and vaccinia virus evasion mechanisms. *Journal of interferon & cytokine research : the official journal of the International Society for Interferon and Cytokine Research* *29*, 581-598.
- Postigo, A., and Way, M. (2012). The vaccinia virus-encoded Bcl-2 homologues do not act as direct Bax inhibitors. *Journal of virology* *86*, 203-213.
- Prieur, E., Gilbert, S.C., Schneider, J., Moore, A.C., Sheu, E.G., Goonetilleke, N., Robson, K.J., and Hill, A.V. (2004). A *Plasmodium falciparum* candidate vaccine based on a six-antigen polyprotein encoded by recombinant poxviruses. *Proceedings of the National Academy of Sciences of the United States of America* *101*, 290-295.
- Quigley, M., Huang, X., and Yang, Y. (2008). STAT1 signaling in CD8 T cells is required for their clonal expansion and memory formation following viral infection in vivo. *Journal of immunology* *180*, 2158-2164.
- Ramos, I., Alonso, A., Marcen, J.M., Peris, A., Castillo, J.A., Colmenares, M., and Larraga, V. (2008). Heterologous prime-boost vaccination with a non-replicative vaccinia recombinant vector expressing LACK confers protection against canine visceral leishmaniasis with a predominant Th1-specific immune response. *Vaccine* *26*, 333-344.

- Ricci, P.S., Schafer, B., Kreil, T.R., Falkner, F.G., and Holzer, G.W. (2011). Selection of recombinant MVA by rescue of the essential D4R gene. *Virology journal* 8, 529.
- Robinson, H.L., Sharma, S., Zhao, J., Kannanganat, S., Lai, L., Chennareddi, L., Yu, T., Montefiori, D.C., Amara, R.R., Wyatt, L.S., *et al.* (2007). Immunogenicity in macaques of the clinical product for a clade B DNA/MVA HIV vaccine: elicitation of IFN-gamma, IL-2, and TNF-alpha coproducing CD4 and CD8 T cells. *AIDS research and human retroviruses* 23, 1555-1562.
- Rochlitz, C., Figlin, R., Squiban, P., Salzberg, M., Pless, M., Herrmann, R., Tartour, E., Zhao, Y., Bizouarne, N., Baudin, M., *et al.* (2003). Phase I immunotherapy with a modified vaccinia virus (MVA) expressing human MUC1 as antigen-specific immunotherapy in patients with MUC1-positive advanced cancer. *The journal of gene medicine* 5, 690-699.
- Romano, P.R., Zhang, F., Tan, S.L., Garcia-Barrio, M.T., Katze, M.G., Dever, T.E., and Hinnebusch, A.G. (1998). Inhibition of double-stranded RNA-dependent protein kinase PKR by vaccinia virus E3: role of complex formation and the E3 N-terminal domain. *Molecular and cellular biology* 18, 7304-7316.
- Sadler, A.J., and Williams, B.R. (2008). Interferon-inducible antiviral effectors. *Nature reviews Immunology* 8, 559-568.
- Schaefer, B.C., Ware, M.F., Marrack, P., Fanger, G.R., Kappler, J.W., Johnson, G.L., and Monks, C.R. (1999). Live cell fluorescence imaging of T cell MEKK2: redistribution and activation in response to antigen stimulation of the T cell receptor. *Immunity* 11, 411-421.
- Scheiflinger, F., Dorner, F., and Falkner, F.G. (1998). Transient marker stabilisation: a general procedure to construct marker-free recombinant vaccinia virus. *Archives of virology* 143, 467-474.
- Schroder, M., Baran, M., and Bowie, A.G. (2008). Viral targeting of DEAD box protein 3 reveals its role in TBK1/IKKepsilon-mediated IRF activation. *The EMBO journal* 27, 2147-2157.
- Shisler, J.L., and Jin, X.L. (2004). The vaccinia virus K1L gene product inhibits host NF-kappaB activation by preventing IkappaBalpha degradation. *Journal of virology* 78, 3553-3560.
- Smith, E.J., Marie, I., Prakash, A., Garcia-Sastre, A., and Levy, D.E. (2001). IRF3 and IRF7 phosphorylation in virus-infected cells does not require double-stranded RNA-dependent protein kinase R or Ikappa B kinase but is blocked by Vaccinia virus E3L protein. *The Journal of biological chemistry* 276, 8951-8957.
- Stack, J., Haga, I.R., Schroder, M., Bartlett, N.W., Maloney, G., Reading, P.C., Fitzgerald, K.A., Smith, G.L., and Bowie, A.G. (2005). Vaccinia virus protein A46R targets multiple Toll-like-interleukin-1 receptor adaptors and contributes to virulence. *The Journal of experimental medicine* 201, 1007-1018.
- Staib, C., Drexler, I., and Sutter, G. (2004). Construction and isolation of recombinant MVA. *Methods Mol Biol* 269, 77-100.
- Staib, C., Lowel, M., Erfle, V., and Sutter, G. (2003). Improved host range selection for recombinant modified vaccinia virus Ankara. *BioTechniques* 34, 694-696, 698, 700.
- Stickl, H., Hochstein-Mintzel, V., Mayr, A., Huber, H.C., Schafer, H., and Holzner, A. (1974). [MVA vaccination against smallpox: clinical tests with an attenuated live

vaccinia virus strain (MVA) (author's transl)]. *Deutsche medizinische Wochenschrift* 99, 2386-2392.

Stittelaar, K.J., van Amerongen, G., Kondova, I., Kuiken, T., van Lavieren, R.F., Pistor, F.H., Niesters, H.G., van Doornum, G., van der Zeijst, B.A., Mateo, L., *et al.* (2005). Modified vaccinia virus Ankara protects macaques against respiratory challenge with monkeypox virus. *Journal of virology* 79, 7845-7851.

Sumner, J.W., Fekadu, M., Shaddock, J.H., Esposito, J.J., and Bellini, W.J. (1991). Protection of mice with vaccinia virus recombinants that express the rabies nucleoprotein. *Virology* 183, 703-710.

Sutter, G., and Staib, C. (2003). Vaccinia vectors as candidate vaccines: the development of modified vaccinia virus Ankara for antigen delivery. *Current drug targets Infectious disorders* 3, 263-271.

Taracha, E.L., Bishop, R., Musoke, A.J., Hill, A.V., and Gilbert, S.C. (2003). Heterologous priming-boosting immunization of cattle with *Mycobacterium tuberculosis* 85A induces antigen-specific T-cell responses. *Infection and immunity* 71, 6906-6914.

Teijaro, J.R., Ng, C., Lee, A.M., Sullivan, B.M., Sheehan, K.C., Welch, M., Schreiber, R.D., de la Torre, J.C., and Oldstone, M.B. (2013). Persistent LCMV infection is controlled by blockade of type I interferon signaling. *Science* 340, 207-211.

Thompson, J.D., Gibson, T.J., Plewniak, F., Jeanmougin, F., and Higgins, D.G. (1997). The CLUSTAL_X windows interface: flexible strategies for multiple sequence alignment aided by quality analysis tools. *Nucleic acids research* 25, 4876-4882.

Tischer, B.K., Kaufer, B.B., Sommer, M., Wussow, F., Arvin, A.M., and Osterrieder, N. (2007). A self-excisable infectious bacterial artificial chromosome clone of varicella-zoster virus allows analysis of the essential tegument protein encoded by ORF9. *Journal of virology* 81, 13200-13208.

Tischer, B.K., Smith, G.A., and Osterrieder, N. (2010). En passant mutagenesis: a two step markerless red recombination system. *Methods in molecular biology* 634, 421-430.

Tischer, B.K., von Einem, J., Kaufer, B., and Osterrieder, N. (2006). Two-step red-mediated recombination for versatile high-efficiency markerless DNA manipulation in *Escherichia coli*. *BioTechniques* 40, 191-197.

Tscharke, D.C., Karupiah, G., Zhou, J., Palmore, T., Irvine, K.R., Haeryfar, S.M., Williams, S., Sidney, J., Sette, A., Bennink, J.R., *et al.* (2005). Identification of poxvirus CD8+ T cell determinants to enable rational design and characterization of smallpox vaccines. *The Journal of experimental medicine* 201, 95-104.

Unterholzner, L., Sumner, R.P., Baran, M., Ren, H., Mansur, D.S., Bourke, N.M., Randow, F., Smith, G.L., and Bowie, A.G. (2011). Vaccinia virus protein C6 is a virulence factor that binds TBK-1 adaptor proteins and inhibits activation of IRF3 and IRF7. *PLoS pathogens* 7, e1002247.

van Boxel-Dezaire, A.H., Rani, M.R., and Stark, G.R. (2006). Complex modulation of cell type-specific signaling in response to type I interferons. *Immunity* 25, 361-372.

Wagner, M., Jonjic, S., Koszinowski, U.H., and Messerle, M. (1999). Systematic excision of vector sequences from the BAC-cloned herpesvirus genome during virus reconstitution. *Journal of virology* 73, 7056-7060.

- Waibler, Z., Anzaghe, M., Frenz, T., Schwantes, A., Pohlmann, C., Ludwig, H., Palomo-Otero, M., Alcami, A., Sutter, G., and Kalinke, U. (2009). Vaccinia virus-mediated inhibition of type I interferon responses is a multifactorial process involving the soluble type I interferon receptor B18 and intracellular components. *Journal of virology* *83*, 1563-1571.
- Wang, Z., Choi, M.K., Ban, T., Yanai, H., Negishi, H., Lu, Y., Tamura, T., Takaoka, A., Nishikura, K., and Taniguchi, T. (2008). Regulation of innate immune responses by DAI (DLM-1/ZBP1) and other DNA-sensing molecules. *Proceedings of the National Academy of Sciences of the United States of America* *105*, 5477-5482.
- Wang, Z., Martinez, J., Zhou, W., La Rosa, C., Srivastava, T., Dasgupta, A., Rawal, R., Li, Z., Britt, W.J., and Diamond, D. (2010). Modified H5 promoter improves stability of insert genes while maintaining immunogenicity during extended passage of genetically engineered MVA vaccines. *Vaccine* *28*, 1547-1557.
- Wathelet, M.G., Lin, C.H., Parekh, B.S., Ronco, L.V., Howley, P.M., and Maniatis, T. (1998). Virus infection induces the assembly of coordinately activated transcription factors on the IFN-beta enhancer in vivo. *Molecular cell* *1*, 507-518.
- Welsh, R.M., Bahl, K., Marshall, H.D., and Urban, S.L. (2012). Type 1 interferons and antiviral CD8 T-cell responses. *PLoS pathogens* *8*, e1002352.
- Willis, K.L., Langland, J.O., and Shisler, J.L. (2011). Viral double-stranded RNAs from vaccinia virus early or intermediate gene transcripts possess PKR activating function, resulting in NF-kappaB activation, when the K1 protein is absent or mutated. *The Journal of biological chemistry* *286*, 7765-7778.
- Wilson, E.B., Yamada, D.H., Elsaesser, H., Herskovitz, J., Deng, J., Cheng, G., Aronow, B.J., Karp, C.L., and Brooks, D.G. (2013). Blockade of chronic type I interferon signaling to control persistent LCMV infection. *Science* *340*, 202-207.
- Wyatt, L.S., Belyakov, I.M., Earl, P.L., Berzofsky, J.A., and Moss, B. (2008). Enhanced cell surface expression, immunogenicity and genetic stability resulting from a spontaneous truncation of HIV Env expressed by a recombinant MVA. *Virology* *372*, 260-272.
- Wyatt, L.S., Earl, P.L., Xiao, W., Americo, J.L., Cotter, C.A., Vogt, J., and Moss, B. (2009). Elucidating and minimizing the loss by recombinant vaccinia virus of human immunodeficiency virus gene expression resulting from spontaneous mutations and positive selection. *Journal of virology* *83*, 7176-7184.
- Wyatt, L.S., Shors, S.T., Murphy, B.R., and Moss, B. (1996). Development of a replication-deficient recombinant vaccinia virus vaccine effective against parainfluenza virus 3 infection in an animal model. *Vaccine* *14*, 1451-1458.
- Zagursky, R.J., and Hays, J.B. (1983). Expression of the phage lambda recombination genes *exo* and *bet* under *lacPO* control on a multi-copy plasmid. *Gene* *23*, 277-292.
- Zhang, Y., Keck, J.G., and Moss, B. (1992). Transcription of viral late genes is dependent on expression of the viral intermediate gene G8R in cells infected with an inducible conditional-lethal mutant vaccinia virus. *Journal of virology* *66*, 6470-6479.

List of Publication:

1 Dai, L., Thiele, F., Baier, R., Muschaweckh, A., Tischer, K., and Drexler, I. Generation and Characterization of a Novel Bacterial Artificial Chromosome Based Recombinant MVA System. in preparation

2 Dai, P., Wang, W., Cao, H., Avogadri, F., Dai, L., Drexler, I., Joyce, J.A., Li, X., Chen, Z., Merghoub, T., Shuman, S., and Deng, L. (2014) Modified Vaccinia Virus Ankara Triggers Type I IFN Production in Murine Conventional Dendritic Cells via a cGAS/STING-Mediated DNA-Sensing Pathway. PLoS Pathogens. In press

8. Appendix

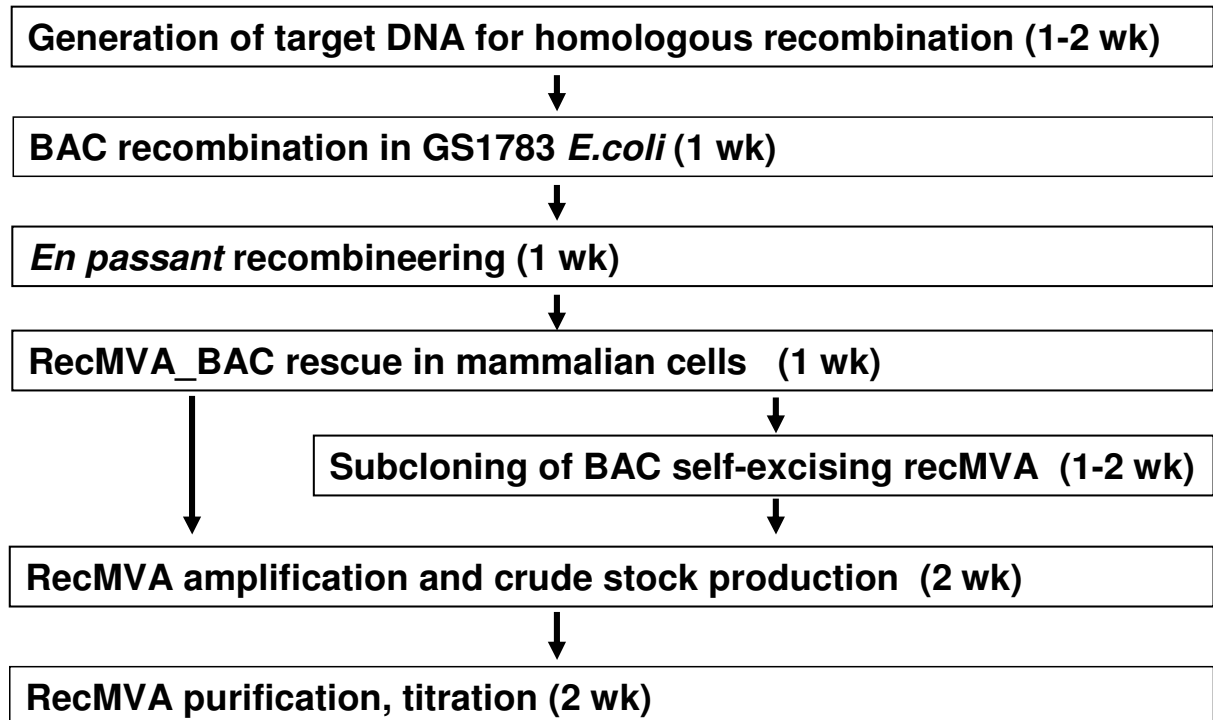


Fig.8.1. Schematic workflow for the generation of recMVA using the MVA-BAC *en passant* technology.

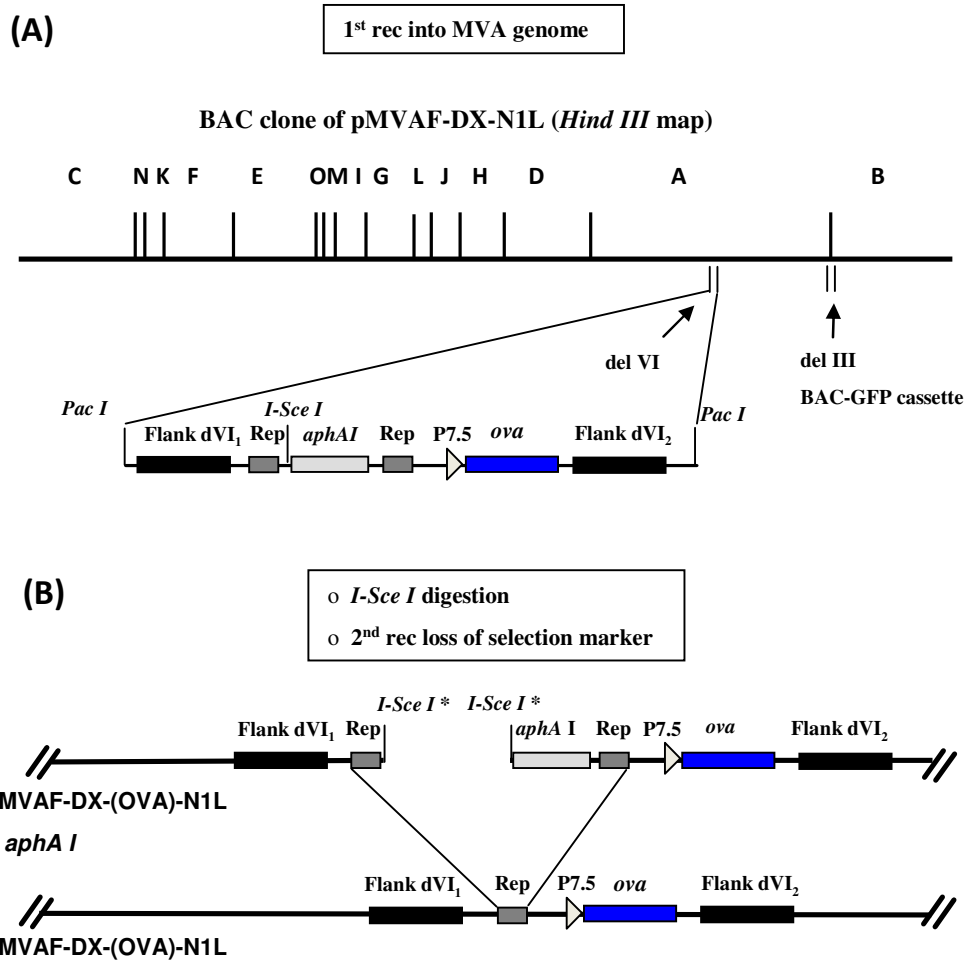


Figure.8.2. Construction of BAC clone MVA-OVA-N1L by the *en passant* technology. Schematic map of the *Pac I* linearized P7.5-OVA containing expression cassette which was transfected into GS1783 *E.coli* harbouring pMVAF-DX-N1L. The 1st Red Recombination inserted the cassette into the MVA deletion VI (A). Schematic map of 2nd red recombination showing *I-Sce I* cleavage and selective marker *aphAI* deletion, yielding the BAC clone of pMVAF-DX-(OVA)-N1L (B).

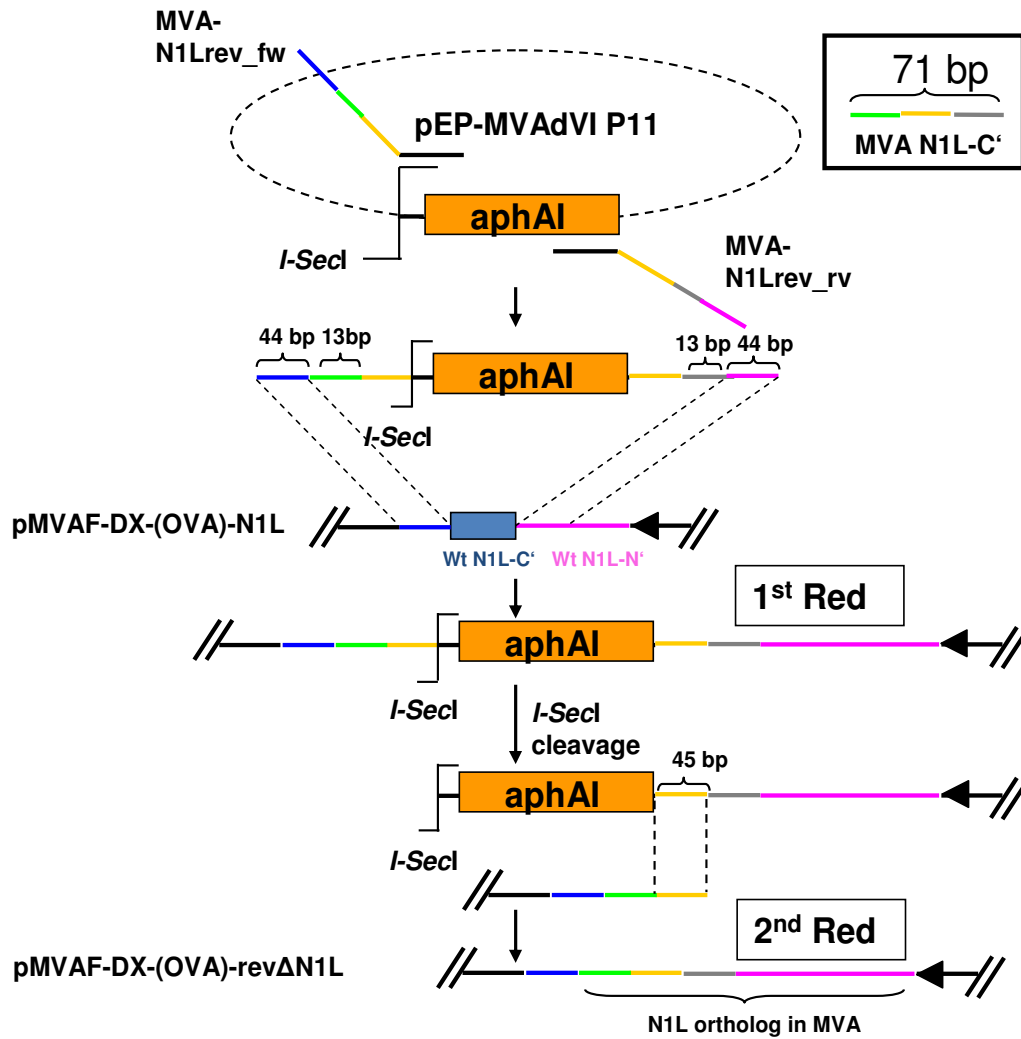


Figure.8.3. Construction of BAC clone MVA-OVA-revΔN1L by the *en passant* technology. Schematic map of the cloning strategy is depicted. Sequence colour blue indicates MVA backbone; Green and grey indicate *N1L* C' terminal sequences; Yellow indicates *N1L* sequences identical for both primers; Pink indicates *N1L* N' terminal sequences.

8.1. Generation of recMVA expressing non-secreted OVA

pIIIDHR-P11-OVA was taken as the template for PCR amplification of a truncated *ova* ORF using primers Pfw-non-Secret-OVA and Prw-Secret-OVA. The PCR product and plasmid pEPMVAdVI-P11 (or pEPMVAdVI-PK1L) were digested with *Sac*II and *Xba*I. After electrophoresis and gel extraction, the DNA fragments were ligated, resulting plasmid pEPMVAdVI-P11-nsOVA or pEPMVAdVI-PK1L-nsOVA, in which the N-terminal 47 aa of the putative leading sequence of OVA was truncated. Transient Western blot experiments using pEP-MVA-dVI-P11-nsOVA showed expression of OVA in lysates, but not in the supernatant (data not shown). The subsequent recMVA rescue and virus amplification was carried out as previously described (see section 1.21).

8.2. Generation of recMVA expressing fusion protein B5-OVA

pEP-MVAdVI-P11-OVA and pEP-MVAdVI-P11-nsOVA plasmids were digested at an intrinsic and unique *Bmg*BI recognition site within the *ova* gene. Then the I-SceI-aphAI cassette was amplified by PCR flanked with a duplication sequence and *Bmg*BI recognition sites. The resulting PCR product and pEP-MVAdVI-P11-OVA plasmid were digested with *Bmg*BI endonuclease and ligated. The OVA-I-SceI-aphAI cassette was then amplified by PCR from the resulting plasmid, and simultaneously homologous B5R-specific sequences were introduced at the flanks for subsequent insertion into the B5R C-terminus. The selection marker was removed by the 2nd Red Recombination. By BAC-mutagenesis in GS1783 *E.coli*, we generated the recombinant MVA genome of MVA-B5R/OVA and MVA-B5R/nsOVA. The corresponding viruses were then reconstituted in BHK-21 and CEFs.

9. Acknowledgement

First of all, I would like to thank my supervisor, Prof. Ingo Drexler. He not only inspired me for every progress of science, but also gave a hand and encouragement to help me move on when I faced difficulties. Without his guide, this thesis cannot be accomplished.

I would also give my deep gratitude to Prof. Volker Bruß and Prof. Heiko Adler for their kindness to be advisors in my thesis committee and the valuable suggestions they provided.

I also thank my colleagues, Andreas Muschaweckh, Frank Thiele, Robert Baier and Borja Hanhsen for their specific help through this working period.

I am grateful to Prof. Klaus Pfeffer, Dr. Philipp Lang, Prof. Jürgen Schrader and Dr. Albert Zimmermann for their endorsement to my lab rotation.

I would like to thank Dr. Karsten Tischer (Freie Universität Berlin), Dr. Liang Deng (MSKCC, NewYork), Dr. Weiyi Wang (MSKCC, NewYork), Dr. Eric Keil for the wonderful cooperative work.

I will also appreciate Dr. Matthew Cottingham (University of Oxford, UK) for generously providing us GS1783 BAC_MVA strain, Greg Smith (Northwestern University, USA) for allowing us to use this materials, Prof. Michael Way (Cancer Research UK) for kindly sending us N1 antibody and Prof. Stefanie Scheu for giving us IFNAR^{-/-} mice.

Besides, I wish to thank the following people for the technical advices: Ms. Katharina Raba, Dr. Daniela Friebe and Chris Haifeng Xu.

I would like to thank Zhang Yang to share the experiences and encouragement of each other for the struggle. I would also thank Liu Zhiqiang, Kim and Erkelenz Steffen for their advice for thesis language improvement.

Finally, I dedicate this work to my family and darling for their love and support. Particularly, I would like to thank my esteemed grandfather Difan Liu (1926 - 2012), and I hope he could feel it at this moment.